

Ministry of Higher Education
And Scientific Research
University of Kerbala
College of Education for pure Science
Department of Chemistry



Removal of Water-Polluting Dyes Using a New Nano co-polymer

A Thesis

Submitted to the Council of College of Education for pure Science University of
Kerbala/ In Partial Fulfillment of the Requirements for the Degree of Master in
Chemistry Science

By

Ali Fadhil Abdullah Al -Ameri

(B.Sc. in Chemistry / Al-Qadisiyah University of – 2014)

Supervisor

Prof. Dr. Mohammed Nadhum Bahjat

2022A.D

1443A.H

بِسْمِ اللَّهِ الرَّحْمَنِ الرَّحِيمِ

بِسْمِ اللَّهِ الرَّحْمَنِ الرَّحِيمِ

وجعلنا من الماء كل شيء حي

صدق الله العلي العظيم

(سورة الأنبياء آية 30)

بِسْمِ اللَّهِ الرَّحْمَنِ الرَّحِيمِ

Supervisor Certification

I certify that this thesis (**Removal of Water-Polluting Dyes Using a New Nano -co-polymer**) was papered under my supervision in the Chemistry Department-College of Education for Pure Sciences-University of Kerbala, in partial Fulfillment of the requirements for the degree of Master in Chemistry Sciences by the student (**Ali Fadhil Abdullah Al Ameri**).

Signature: 

Prof. Dr. Mohammad N. Al-Baiati

Supervisor

Date: 26/ 6 /2022

Supervisor Certification

I certify that this thesis (**Removal Of Water-Polluting Dyes Using A New Composite Nano polymer**) was papered under my supervision in the Chemistry Department-College of Education for Pure Sciences-University of Kerbala, in partial Fulfillment of the requirements for the degree of Master in Chemistry Sciences by the student (**Ali Fadhil Abdullah Al Ameri**).

Signature: 


Prof. Dr. Mohammad N. Al-Baiati

Supervisor

Date: 26/ 6 /2022

Committee Certification


We certify that, we read this thesis (**Removal of Water-Polluting Dyes Using a New Nano co-Polymer**) and as examining committee examined the student (**Ali Fadhil Abdullah Al-Ameri**) in its content, and that in our opinion it is adequate () with standing as a thesis for degree of master in chemistry sciences.

Signature: 

Name: Prof. Dr. **Hamieda Idan Salman**

Date: 11/8 /2022

(Chairman)

Signature: 

Name: Prof. Dr. **Dhafir T. A. Al-Heetimi**

Date: / /2022

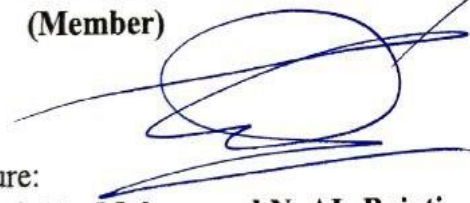
(Member)

Signature: 

Name: Asst. prof. **Dr. Sana Hitur Awad**

Date: / /2022

(Member)


Signature: 

Name: Prof. Dr. **Mohammad N. AL-Baiati**

Date: / /2022

(Supervisor & member)

Approved for the College Council.....

Signature: 

Name: Prof. Dr. **Hamieda Idan Salman**

Dean of the College of Education for Pure Sciences

Date: 17/8 /2022

Amendment Report

This is to certify that I have read the thesis entitled (**Removal Of Water-Polluting Dyes Using A New Nano polymer**) and corrected the grammatical mistakes I found. The thesis is, therefore, qualified for debate .

Signature : 

Name: ASSE-Prof. Dr. Reith Z Unair

Date: / / 2022

Dedication

To the owner of the heavenly message, the symbol of knowledge and the illuminating lamp, the Prophet Mohammed, may God's prayers and peace be upon him and his family

In front of us and our example, Imam Al-Mahdi, may God hasten his relief, and may God facilitate the way out

To whom we proudly bear his name, teach me to give without waiting, my dear father

To the symbol of love and healing balm

To the white heart (my beloved mother), may God protect her

To the one who was my support and help in thick and thin

My wife... with love and appreciation

To those whose soul I embraced with my soul

My children...Hussain...Rehana...Zainab

For those whom I am proud to have around me and my strength is stronger for them

To all my brothers, sisters and friends



Student Ali Fadel

Acknowledgements

Praise be to God, Lord of the Worlds, and peace and blessings be upon our master Muhammad al-Hadi al-Amin, and upon his good family and companions

I am pleased to extend my sincere thanks and gratitude to Prof. Dr. **Mohammed Nadhum Bahjat (God made his way for good)**

I would like to thank the Deanship of the College of Education for Pure Sciences and the Presidency of the Department of Chemistry at the College, especially **Prof. Dr. Hamida Idan Salman** and Assistant **Professor Dr. Sajid Hassan** and all the teachers and employees of the College of Education for Pure Sciences

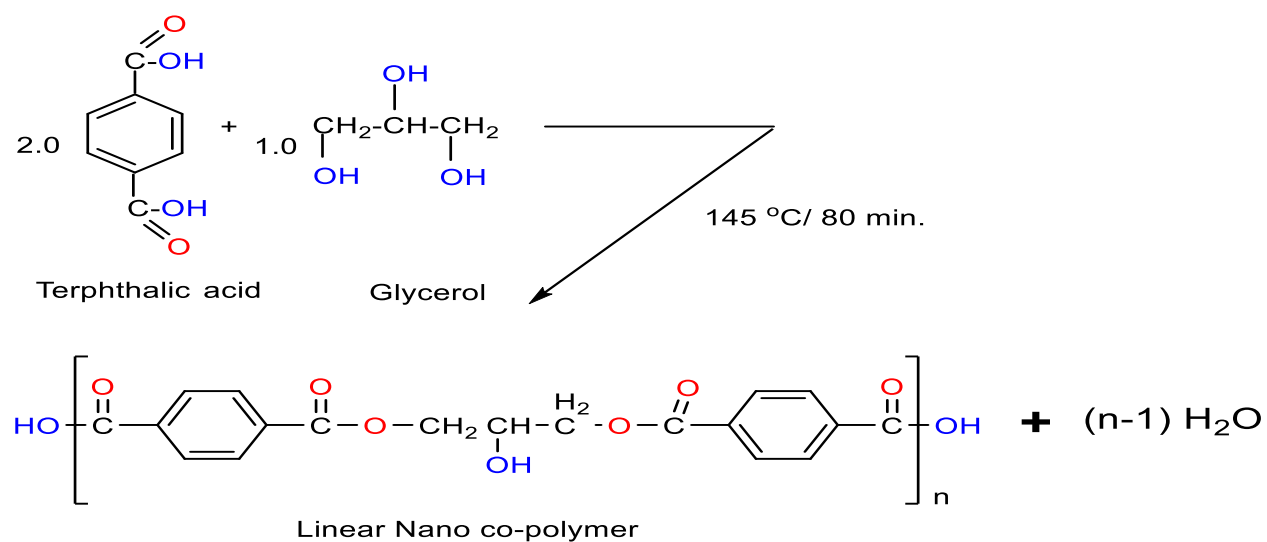
I have their continuous support and assistance during the preparatory year and the research year. Finally, I extend my thanks and appreciation to all the assistants for facilitating work, facing difficulties and expressing opinion.

In particular, **M. M. Amir Salem Al-Mayali**

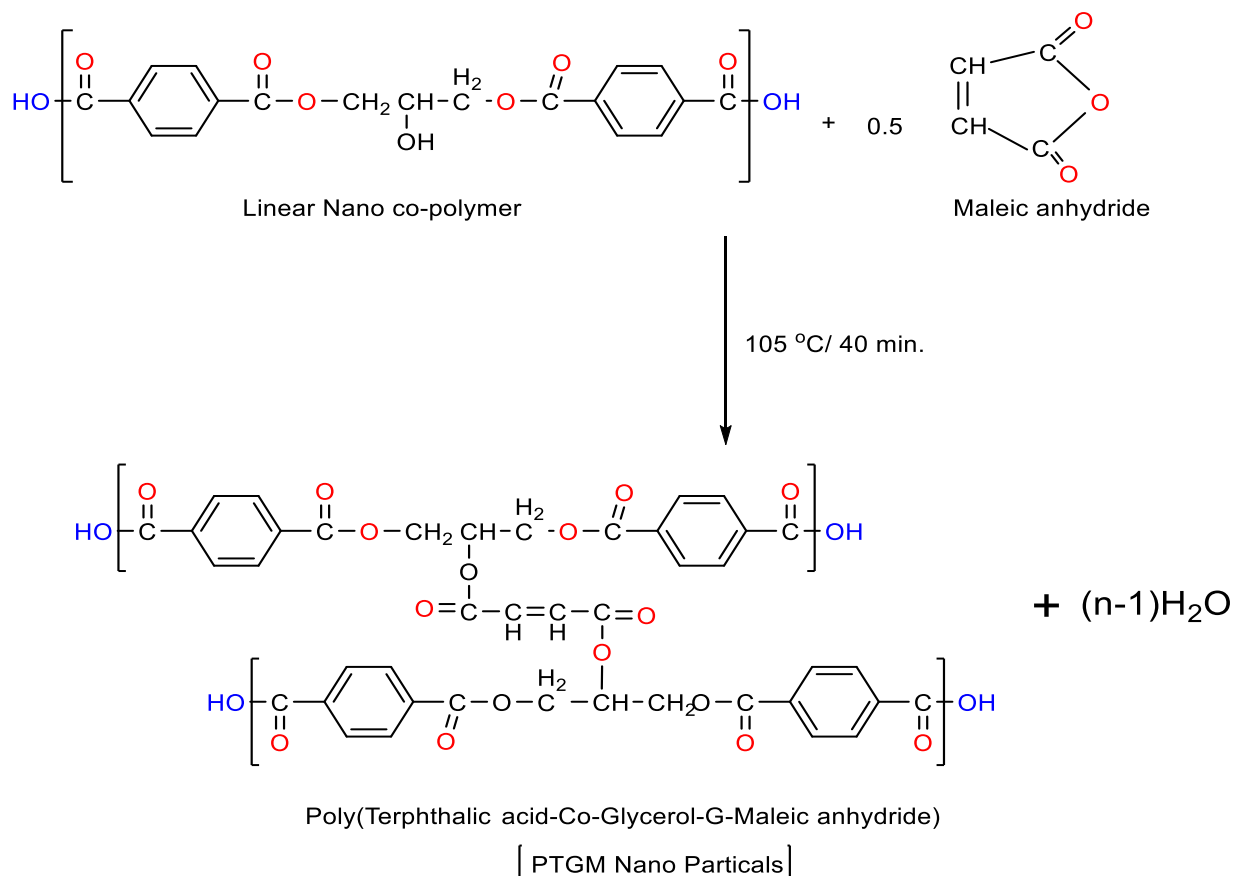
Abstract

ABSTRACT

The grafted nano-copolymer was synthesized by esterification process, by dissolving method to preparing a linear co-polymer as a first step from the reaction of (2.0 mole) Terphthalic acid with (1.0 mole) Glycerol. About (0.5 mole) of Maleic anhydride was added to the resulting linear co-polymer solution to get the graft nano co-polymer, as shown in the below equations:



The first step; Synthesis linear nano-copolymer



Second step Synthesis of nano graft PTGM particles.

This nano co-polymer was characterized by several techniques (FT-IR, ¹H-NMR and AFM). The AFM results showed that the average particle size of the nano co-polymer is 74.39 nm, this proves that the prepared co-polymer is nano scale.

The decontamination of three types of dyes (Reactive Yellow145 , Orange-G and Disperse Red 1) from their aqueous solutions was studied.

The effect of three temperatures (298, 308 and 318 K) and four different concentrations (1, 3, 5 and 7 ppm) of nano co-polymer has been studied and it is clear that they play a very important role in the adsorption process, and the experimental results showed that the adsorption of dyes (Reactive Yellow145) on the surface of this nano

polymer decreases with increasing temperature, which means that the process is an exothermic process, while the experimental results showed that the adsorption of dyes (Orange-G and Disperse Red 1) on the surface of this nano co-polymer increases with increasing temperature, which means that the process is an endothermic process.

showed a high effectiveness of nano co-polymer in the disposal of pollutants (Reactive Yellow145, Orange-G and Disperse Red 1) dyes.

List of Contents

Pages	Contents	
I	Abstract	
V	Contents	
VIII	List of Tables	
XI	List of Figures	
XIII	List of Equations	
XIV	List of Abbreviations	
Pages	CHAPTER ONE	Serial No.
1	Introduction	1
1	Nanotechnology	1.1
2	History of Nanotechnology	1.2
4	Preparation Techniques	1.3
5	Preparation Technology (descending path)	1.3.1
5	Preparation Technology(ascending path)	1.3.2
6	Nanomaterials	1.4
7	Polymer Nanocomposites	1.5
9	Fields Nanotechnology using	1.6
10	Field of Nutrition	1.6.1

10	field of optics and Electronics	1.6.2
11	Field of Treating Salty and Contaminated Waterfield	1.6.3
12	Water Pollution	1.7
12	Heavy metals	1.7.1
13	Nitrates and Phosphate	1.7.2
14	Pollution by petroleum derivatives and halogens	1.7.3
14	Alkaline and acidic compounds	1.7.4
15	Water pollution by industrial waste	1.7.5
15	The textile industry and its environmental impact	1.7.6
19	The Pollution by Dyes	1.7.7
21	Reactive Yellow145 dye	2.7.1
23	Orange-G Dye	2.7.2
24	Dispersed Red1 dye	2.7.3
26	Aim of the work	1.8
Pages	CHAPTER TWO	Serial No.
27	Experimental	2
27	Chemical and Techniques	2.1
27	Chemicals	2.1.1
27	Instruments used	2.1.2
28	synthesis of nanoparticles co-polymers	2.2
30	Preparation of dye solutions	2.3
31	Determination of Calibration Curve	2.4

34	Determination of Equilibrium Factors	2.5
35	Determination of adsorption isotherms	2.6
36	The effect of temperature on adsorption	2.7
Pages	CHAPTER THREE	Serial No.
37	Results and discussion	3
37	Synthesis of nano co-polymers	3.1
48	Removal of pollutants	3.2
48	Adsorption isotherm on the surface of the nano co-polymer	3.3
69	The effect of temperature on adsorption on the surface of the nanocomposite.	3.4
76	Calculate the thermodynamic values of $\Delta H, \Delta S, \Delta G$	3.5
86	Conclusion	
87	Future Work	
88	References	

List of Tables		
Pages	Description	Serial NO.
20	Classification of dyes	1-1
22	Properties of Reactive Yellow 145 dye	1-2
23	Properties of Orange-G dye	1-3
25	Properties of Disperse Red 1 dye	1-4
27	Chemical material, purity and companies supply	2-1

35	the weight and equilibrium time for each dye	2-2
44	The total rate of the particle sizes of the linear co-polymer nanoparticle and the different proportions of these volumes	3-1
47	The total rate of the particle sizes of the graft co-polymer nanoparticle and the different proportions of these volumes	3-2
49	Adsorption of Reactive Yellow145 on the surface of the nanocomposite at a temperature of 298K.	3-3
50	Adsorption of Orange-G dye on the surface of nano co-polymers at 298K	3-4
51	Adsorption of Disperse Red 1 dye on the surface of nano co-polymers at 298K	3-5
52	Adsorption of Reactive Yellow145 dye on the surface of nano co-polymers at 298K,308k and 318k (by applying Freundlich equation).	3-6
54	Adsorption of Orange-G dye on the surface of nano co-polymers at 298K,308k and 318k (by applying Freundlich equation).	3-7
54	Adsorption of Disperse Red 1 dye on the surface of nano co-polymers at 298K,308k and 318k (by applying Freundlich equation).	3-8
57	Adsorption of Reactive Yellow145 dye on the surface of nano co-polymers at 298K,308k and 318k (by applying Langmuir equation).	3-9
59	Adsorption of Orange-G dye on the surface of nano co-polymers at 298K,308k and 318k (by applying Langmuir equation).	3-10
59	Adsorption of Disperse Red 1 dye on the surface of nano co-polymers at 298K,308k and 318k (by applying	3-11

	Langmuir equation).	
62	Adsorption of Reactive Yellow145 dye on the surface of nano co-polymers at 298K,308K and 318K (by applying Temkin equation).	3-12
64	Adsorption of Orange-G dye on the surface of nano co-polymers at 298K,308K and 318K (by applying Temkin equation).	3-13
64	Adsorption of Disperse Red 1 dye on the surface of nano co-polymers at 298K,308K and 318K (by applying Temkin equation).	3-14
68	the values of the Friendelsh and Langmeier constants, and the correlation coefficients enable the adsorption of Reactive Yellow145, Orange-G and Disperse Red 1 dyes on the surface of the nanocomposite	3-15
69	Effect of temperature on adsorption of Reactive Yellow145 dye.	3-16
70	Effect of temperature on adsorption of Orange-G dye.	3-17
71	Effect of temperature on adsorption of Disperse Red 1 dye	3-18
73	The percentage of Orange-G removal due to the effect of temperature.	3-19
74	The percentage of Disperse Red 1 removal due to the effect of temperature.	3-20
75	The percentage of Reactive Yellow145 removal due to the effect of temperature.	3-21
75	The values of $1 / T$, $\text{Log } X_m$ of Reactive Yellow145 on	3-22

	the surface of the nanocomposite within the experimental heat range (298,308,318 K).	
78	The values of $1/T$, $\log X_m$ of Orange-G on the surface of the nanocomposite within the experimental heat range (298,308,318 K).	2-23
79	Shows the values of $1/T$, $\log X_m$ of Disperse Red 1 on the surface of the nanocomposite within the experimental heat range (298,308,318K)	3-24
80	Shows the values of the thermodynamic functions $\Delta H, \Delta G$, and ΔS to remove Reactive Yellow145, Orange-G and Disperse Red 1 dyes on the surface of the nanocomposite at different temperature	3-25

Pages	List of Figures	Serial No.
2	shows some materials and their comparison with nano scale	1-1
5	Shows techniques for preparing nano materials	1-2
9	Applications of nano technology	1-3
21	Structural formula of Reactive Yellow145 dye	1-4
23	Structural formula of Orange-G dye	1-5
25	Structural formula of Disperse Red 1	1-6
31	The maximum wavelength (λ_{max}) for the Reactive Yellow145 dye.	2-1a
32	The Calibration Curve between absorption and concentration of Reactive Yellow145 dye	2-1b
32	The maximum wavelength (λ_{max}) for the Orange-G dye	2-2a

33	The Calibration Curve between absorption and concentration of Orange-G dye	2-2b
33	The maximum wavelength (λ_{\max}) for the Disperse Red 1 dye	2-3a
34	The Calibration Curve between absorption and concentration of Disperse Red 1 dye	2-3b
37	FT-IR linear copolymer spectrum.	3-1
38	$^1\text{HNMR}$ spectrum of linear co-polymer	3-2
39	FT-IR spectrum of graft co-polymer	3-3
40	The $^1\text{HNMR}$ spectrum of graft co-polymer	3-4
41	Image of Atomic Force Microscope for 3D Image.	3-5a
42	Image of Atomic Force Mic linear co-polymer shows roscope for co-polymer shows 2D Image	3-5b
43	Image of Atomic Force Microscope for linear co-polymer shows 2D Image and showing all details of particles	3-5c
45	Image of Atomic Force Microscope for graft co-polymer shows 3D Image	3-7a
45	Image of Atomic Force Microscope for graft co-polymer shows 2D Image	3-7b
46	Image of Atomic Force Microscope for graft co-polymer shows 2D Image and showing all details of particles	3-7c
44	Distribution of the different proportions of particle sizes of the nano co-polymer	3-6
47	Figure Distribution of the different proportions of particle sizes of the graft co-polymer nanoparticle.	3.8

50	Adsorption isotherm Reactive Yellow145 dye on the surface of graft co-polymer	3-9
51	Adsorption isotherm Orange-G dye on the surface of graft co-polymer	3-10
52	Adsorption isotherm dispersion red dye on the surface of graft co-polymer.	3-11
53	Apply Freundlich equation on adsorption of Reactive Yellow145 dye on the surface of graft co-polymer at 298K,308K and318K.	3-12
55	Apply Freundlich equation on adsorption of Orange-G dyeon the surface of graft co-polymer at 298K,308K and 318K.	3-13
56	Apply Freundlich equation on adsorption of dispersion red dye on the surface of graft co-polymer at 298K,308K and 318K.	3-14
58	Apply Langmuir equation on adsorption of Reactive Yellow145 dye on the surface of graft co-polymer at298k,308k and 318K	3-15
60	Apply Langmuir equation on adsorption of Orange-G dye on the surface of graft co-polymer at298K,308K and 318K.	3-16
61	Apply Langmuir equation on adsorption of Disperse Red 1 dye on the surface of graft co-polymer at298K,308K and 318K	3-17
63	Apply Temkin equation on adsorption of Reactive Yellow145 dye on the surface of graft co-polymer at 298K,308K and 318K.	3-18
65): Apply Temkin equation on adsorption of Orange-G dye on the surface of graft co-polymer at 298K,308K and 318K.	3-19
66	Apply Temkin equation on adsorption of Disperse Red	3-20

	1 dye on the surface of graft co-polymer at 298K,308 K and 318K.	
70	Effect of temperature on adsorption of graft co-polymer at (1, 3 ,5and 7ppm) of Reactive Yellow145 dye.	3-21
71	Effect of temperature on adsorption of graft co-polymer at (1, 3 ,5and 7ppm) of Orange-G.dye .	3-22
72	Effect of temperature on adsorption of graft co-polymer at (1, 3 ,5 and 7ppm) of Disperse Red 1 dye.	3-23
77	shows a graph between the logarithm of the highest value in the reciprocal of the temperature of the Reactive Yellow145 dye.	3-24
78	shows a graph between the logarithm of the highest value in the reciprocal of the temperature of the Orange-G dye.	3-25
79	shows a graph between the logarithm of the highest value in the reciprocal of the temperature of the Disperse Red 1 dye.	3-26
Pages	List of Equations	Serial No.
29	Reaction of synthesis of nano co-polymer	2-1
30	Reaction of synthesis of of graft PTGM nanoparticles	2-2

List of Abbreviations

Symbol	Description
DMSO	Di methyl sulfoxide
UV-Vis	Ultra violet-visible
pH	Acid value
<u>IUPAC</u>	International Union of Pure and Applied Chemistry
Qe	The amount of adsorbate substance
Ce	The concentration at equilibrium
C.I.No	Colour Index number
mg/g	Milligram per gram
mg/L	<u>Milligram per liter</u>
d_{hkl}	Inter planer spacing between atoms
Nm	Nanometer
K	Kelvin
$^1\text{H-NMR}$	Proton nuclear magnetic resonance
FT-IR	Fourier transform infrared
Mw	Average weight of molecular weight
AFM	Atomic Force Microscope
Mn	Average number of molecular weight
ppm	Parts per million
K_f	The adsorption amplitude
N	The adsorption intensity

INTRODUCTION

1. Introduction

1.1 Nano Technology

Nano technology is a set of tools, techniques, and applications related to the fabrication and synthesis of a particular structure on a very small scale called nano structures. The word nano takes its meaning from the Greek word “nanos” which means dwarf. Nanoparticles can be defined as materials with a size of between 1 and 100 nanometers and nanoparticles, i.e. one billionth of a meter (1 nano meter = 10^{-9} meters). The nano size is about 80,000 times smaller than the diameter of a hair. Where about eight carbon atoms can be arranged next to each other in one nano meter ^[1]. The basis of nanotechnology is to build materials precisely from small parts of nano sizes (things are fragmented in nanotechnology from 1 to 100 nanometers) resulting in a material that is free of impurities and a higher level of quality . The properties of materials change dramatically when they are broken into very small nano-sized parts in terms of electrical conductivity, color. They can be fabricated using a bottom-up or top-down approach, and with recent developments, it is possible to better control the size, shape and structure by adopting an appropriate synthesis approach and dealing with installation conditions ^[2] . Thus, Nanoscience is concerned with the manufacture of machines, tools and materials at a nanoscale that is infinitesimally small and cannot be observed with the naked eye. The word nanotechnology is also used in the sense of nano materials technology or micro technology ^[3], as is shown in Figure (1-1). The nano scientist is the boundary between the world of atoms and molecules and the world of the macro ^[4].

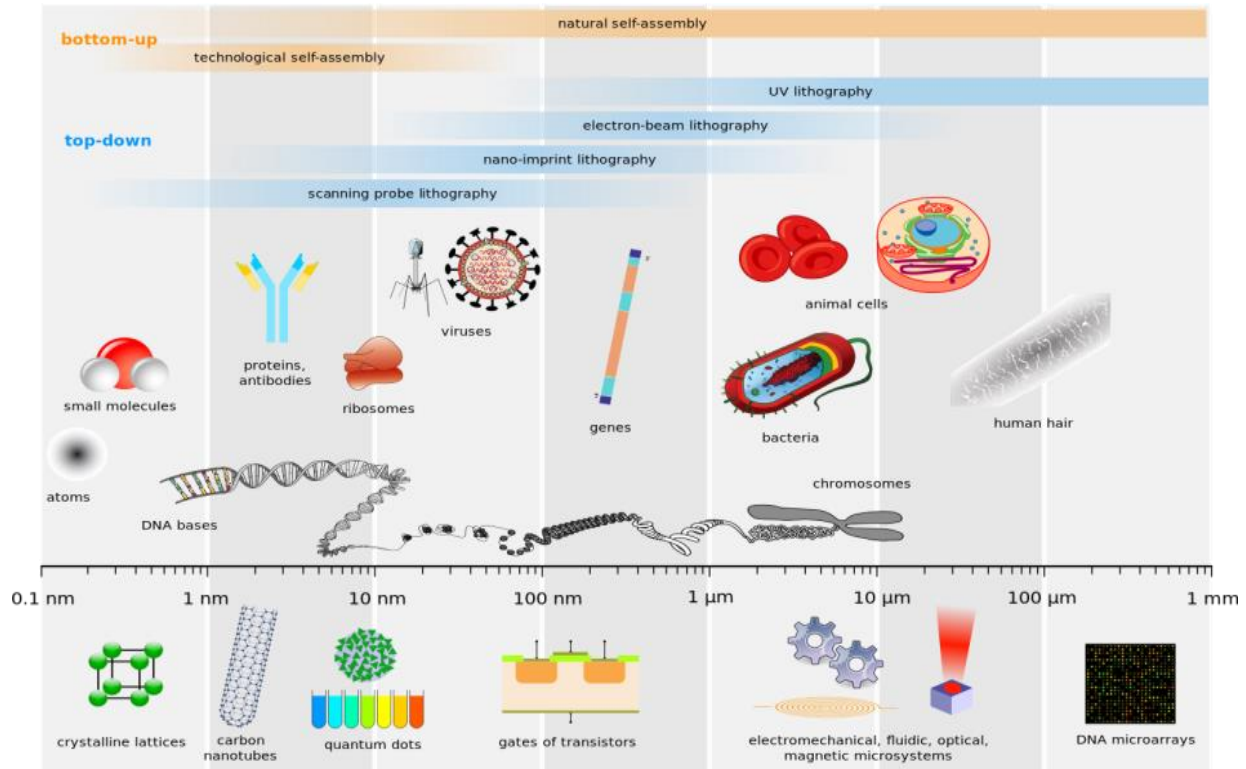


Figure (1-1): shows some materials and their comparison at the nano scale.

1.2 History of Nanotechnology

It is not possible to pinpoint a specific age or era for the emergence of nanotechnology, but it is clear that one of the first people to use this technology (without realizing what it is) were medieval glass makers who were using colloidal gold nanoparticles for coloring^[5]. The use of nanoparticles and structures in the fourth century AD, by the Romans, which showed one of the most interesting examples of nanotechnology in the ancient world a cup that shows glass green in direct light, and red and purple when light shines through glass ^[6]. Feiman is considered one of the pioneers in the field of nanotechnology. American Nobel Prize-winning physicist Richard Feynman introduced the concept of nanotechnology in 1959. During the annual meeting of the American Physics

Association, Feynman gave a lecture entitled "There is plenty of room at the bottom" at Caltech. In this lecture, Feynman put forward the hypothesis "why not write the entire 24 volumes of Encyclopedia Britannica on a pin head? Where he introduced the concept of manipulating matter at the atomic level, this new idea made it clear that Feynman's hypotheses proved true, and for these reasons he is considered the father of modern nanotechnology^[7]. Fifteen years later, the Japanese scientist Norio Tanigo-chi was the first to use the term "nanotechnology" in 1974 inspired by Feynman's concepts, as follows Nanotechnology mainly consists of processing, fusion separation, and reshaping of materials by a single atom or single molecule · K. Eric Drexler used the so-called "nanotechnology" in his 1986 book "Drivers of Creativity and Considers the Next Age of Nanotechnology," which proposed the idea of a "nanoscale" that would be able to build a copy of itself and other elements of arbitrary complexity with atomic control. And in 1986, Drexler co-founded the Foresight Institute (which he no longer belongs to) help increase public awareness and understanding of the concepts and effects of nanotechnology. Thus, the emergence of nanotechnology in the 1980s through a convergence of theoretical and practical work drew Drexler, who developed and designed an experimental framework High Precision and Nanotechnology, Attention to Prospects for Atomic Control Since the great rise of the 1980s, most nanotechnology has involved the study of several methods for fabricating mechanical devices from a few atoms ^[8,9]. With the invention of the scanning tunneling microscope, scientists Gerd Bing and Henrik Rohr in 1981, nano-growth is considered in the modern era, a device that images nano-sized objects and because of this invention, the two scientists won the Nobel Prize in Physics in 1986 ^[10]. Where Fluorines were discovered by Harold Kroto, Richard Smalley and Robert Curl, they are molecules consisting of 60 carbon atoms gathered in the form of a football (they were awarded the Nobel Prize in Chemistry in 1996 AD, the

experimental progress since the eighties and the recognition of the potential of nano materials led to a real breakthrough In the field of nano science, it is interdisciplinary in nature ^[11]. New technologies that work at the nano scale, they have already brought about changes in society, and will also surely mean a huge impact on developed and developing societies and the planet we live in. Health as a federal government program to promote nano science-related research and development ^[12]. This is reflected in the way in which public investment in research and development in nanotechnology has risen over the past decade ^[13]. In a large number of different scientific fields because of their great benefits in terms of improving performance in the fields; Various types of nanostructures and nano-strategies have been developed including nano rods, nanowires, nano tissues, nano fibers, nanoparticles, quantum dots, and spheroids, As well as in tissue engineering and strategies for regenerative medicine ^[14]. Nanotechnology has found important applications in our daily lives and there is a lot to come. Scientists are still working for new breakthroughs in nano science and nanotechnology in order to make human life easier and more convenient ^[15].

1.3 Preparation Techniques

The reason for the quality of the technology used in constructing the nanoparticles is the size of the particles involved. In addition, the nature of the use is a critical act in the nature of the technology used, particularly in the field of optical technologies and the medical field. There are a variety of technologies that have the potential to produce nanostructures with varying degrees of quality, speed, and cost ^[16]. The methods for preparing nano materials can be categorized into two main methods that include different methods. The first is from the bottom up. The second method is up –down.

1.3.1 Preparation Technology (bottom - top)

Where this method begins with individual molecules as the smallest unit and assembled into a larger structure, these methods are often chemical, and are characterized by small size of products (1 nm), less waste than the original material and to obtain the bonding strength between the resulting nanoparticles, there are many different methods Used in this technique, such as chemical vapor deposition, sol-gel, electro deposition method [17].

1.3.2 Preparation Technique (top-down)

This method begins with a large amount of the material under study and is reduced little by little until it reaches the nano scale. Techniques used in this include light photo catalysis, cutting, scraping and milling. As shown in Figure (1-2).These techniques have been used to access microelectronic compounds such as computer chips etc, and the smallest size can be reached within 100 nm [18].

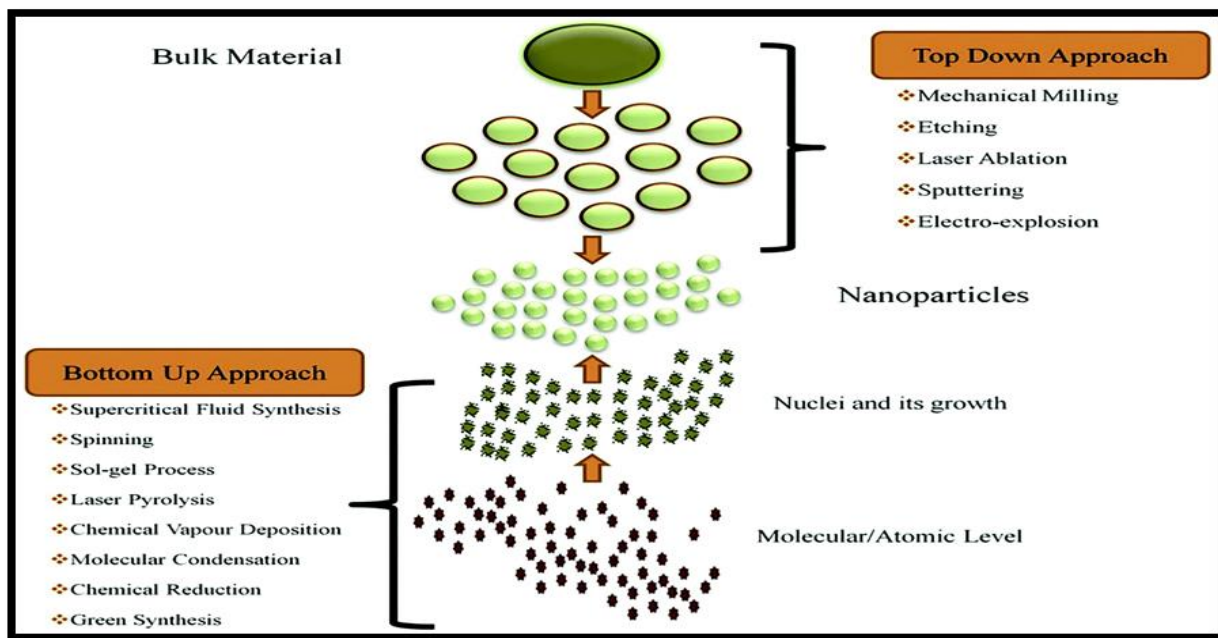


Figure (1-2): Techniques for preparing nano materials.

1.4 Nano Materials

Nanotechnology is defined as the union of two or more materials within the microscopic scale, where the lengths of their molecules are in the order of (100 nanometers), through which the materials show new behavior and properties because the particles on the nano scale interact in a way that differs from their natural size, Nanocomposites are defined as the union of two or more substances within the microscopic scale, where the lengths of its molecules are within the limits: (1-100 nanometers) ^[19]. The chemical and physical concentration of raw elements employed in nanoscale production affects the characteristics of the final nano materials, and nano composites materials are distinguished by significant improvements in thermal, optical, electrical, mechanical, and conductivity properties. Nanomaterials are often made up of a cluster of grains containing a number of atoms that may be seen via a microscope and range in size from 1 to 100 nanometers, but are invisible to the human eye ^[20-25]. Because of their unique properties, these compounds are used in a variety of applications, the most important of which are medical ones, due to their ability to enter the human body and monitor disease sites, such as using gold nanoparticles as a material to destroy cancer cells through a process known as chemoradiation. Vehicles are used to solve water and soil pollution problems using a variety of methods. Nano materials that show very small amounts of organic and inorganic dyes are known as nano-enhancers. Nano filtration membranes, which include nano-zeolite, are used to remove micro-organic pollutants from brine that are difficult to remove using conventional procedures. Nano-catalysts are materials that reduce pollution levels and remove heavy metals such as arsenic from water. They can also get rid of magnetic nanoparticle salts ^[26-29].

1.5 Nano polymer Compounds

They are the compounds resulting from the union of two or more materials within the microscopic range, where the lengths of their molecules are in the range (1-100 nm) to form new nano composites with properties and characteristics different from the original compounds. One of the now known nano composites is polymeric nano composites ^[30]. Innovative synthesis pathways have led to new polymer and nano composites with improved properties, which have been successfully integrated into fields as diverse as aerospace, automotive, construction, petroleum, biomedicine, and wastewater treatment ^[31]. When manufacturing nano-sized materials, the physical composition and chemical concentration of the raw materials used in manufacturing play an important role in the properties of the resulting nano-material, unlike what happens when manufacturing ordinary materials. The materials are usually composed of a group of granules that contain a number of atoms and these granules may be visible or invisible to the naked eye depending on its size ^[32]. The main compound classes include matrix organic compounds (OMC S), matrix metal compounds (MMC S) and matrix ceramic compounds (CMC S). It is generally assumed that the term organic matrix compounds includes two classes of compounds: polymer matrix compounds (PMCS) and carbon matrix compounds ^[33]. In the simplest case, when nanoparticles are appropriately added to a polymer matrix they can enhance their performance, often significantly, by simply taking advantage of the nature and properties of nano scale fillers (these materials are best described by the term nano-filled polymer composites . Nano materials can be one-dimensional nanotubes or nano fibers, two-dimensional clay sheets, or three-dimensional spherical particles ^[34]. Nanoparticles such as graphene, carbon nanotubes, molybdenum disulfide and tungsten disulfide are used as strengthening agents for the fabrication

of strong, mechanically biodegradable polymeric nano composites for bone tissue engineering applications ^[35] . Compounds or (composites material) means the group of engineering materials produced by adding certain weight or volume ratios of one or more materials (reinforcement material) to the matrix material (mold material) which well combines and mixes the supporting material with the mold material, ensuring that the a homogeneous compound in which the particles of the support material are optimally distributed, which is required for the selection of the supports to obtain complete neutrality so that they do not react with each other or with the base material to retain their members. Identity within the mold material.^[36] Scientists where improving the properties of composites are examining compounds with a minimum volume and fewer fillers, leading to the development of micro composites A recent trend in composite research is nano composites. Nano composites refer to compounds in which a single phase has a nano scale form such as nanoparticles, nanotubes, or lamellar nanostructures. The properties can be improved by adding particles when.

1. Good enough interaction between nanoparticles and matrix
2. Good dispersion of particles within the matrix.

The bonds in nano composites are covalent bonds, ionic bonds and Van der Waals forces, hydrogen bonding can exist between matrix and filler components ^[37] . The advantage of nanoparticles is that due to their large surface area and small size, significant effects on properties can be obtained. Over the past years, polymer nano composites have attracted great interest in both academia and industry, but one prominent problem is the control of the dispersion state of nanoparticles, which is largely determined by the method of preparation, therefore, different preparation methods for polymer nano composites ^[38] . Some nano composites may

show properties that are dominated by interfacial interactions and others show effects associated with nano scale structures. Efficient nanoparticle diffusion combined with good polymer and particle adhesion between the face and dispersion layers allows an exciting possibility to develop strong, transparent, layers and films [39].

1.6 Fields Nano Technology Using

The applications of nanotechnology are broad in scope and are included in many industrial, military, medical, agricultural, nutrition, water treatment, optics, electronics, household appliances, sports field and others. Figure (1-3), shows some applications of nano technology and they are used in every field as follows [40, 42,43,44,45,46,47].

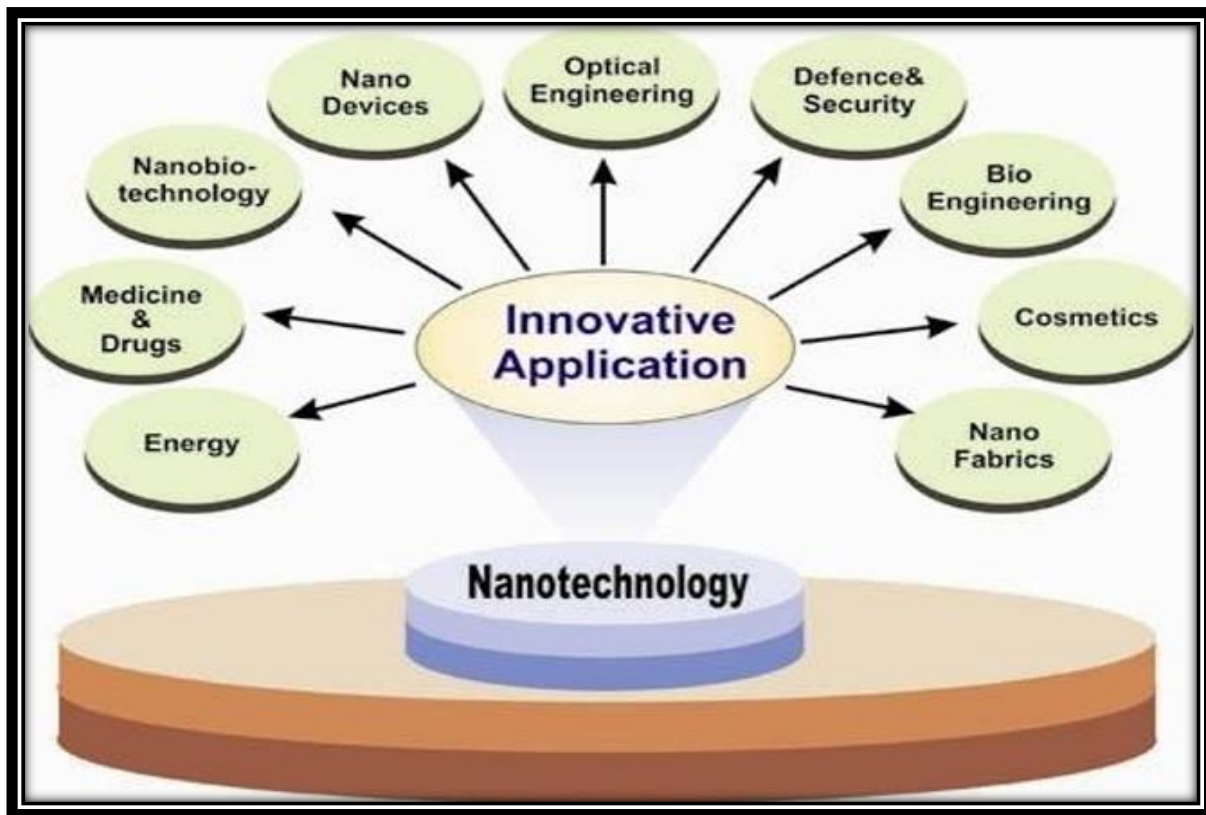


Figure (1-3): Applications of nano technology

1.6.1 Nutrition field

The term “Nano-food” is given to the food that was used in its production or at any stage of its production using nanotechnology, in other words it is the food that is used nanotechnology in cultivation, processing or packaging, and packaging is currently considered one of the most practical applications of nano technology, where nanoparticles are used to make strong, light and heat-resistant plastic covers ^[48] and most importantly, it is able to prevent oxygen and carbon dioxide from entering and spoiling foods, and it also has the advantage that it is resistant to microbes and bacteria, and this helps foods stay fresh for a longer period without spoiling as the packaging is equipped with nano-particles that are anti-microbial and anti-fungal from the minerals silver, magnesium and zinc ^[49]. Nanoparticles are often used as food additives to protect food from contamination and thus improve shelf life texture, and flavor ^[50, 51]. Forming nano capsules from, food ingredients (nano-sized), nutritional supplements (e.g proteins, antioxidants) and additives (eg. flavor color) nano capsules that can be combined in functional foods and improved bioavailability of many vitamins and their precursors, in addition to the addition of nano-sized nutritional supplements such as: iron-free zinc and minerals, as well as nano-capsules containing high concentrations of the famous fish oils (omega 3) enzyme materials ^[52].

1.6.2 The field of optics and Electronics

The first sunglasses are now available with a protective, anti-reflective ultra-thin polymer coating. Scratch-resistant surface coatings using nanotechnology can also be used in optics. Nano-optics can also be used to create the cornea of the eye, enabling better accuracy in pupillary correction and other types of laser eye

surgery ^[53]. In the world of electronics, tablets and phones with touch screens have increasingly in recent years, as is the case with multi-core processors with four to eight cores, which facilitates and speeds up their work, as well as encapsulating them with nano materials that make them waterproof. the speed and efficiency of computers increased thanks to the shrinkage of transistor components The speed and efficiency of computers increased, and their capacity increased thanks to the contraction of transistor components. it also led to their smaller sizes and lower prices, as we see today ^[54,55,56,57].

1.6.3 Field of Treating Salty and Contaminated Water

Some nanoparticles can be used to make filters that clean and desalinate water more efficiently in homes and villages than other types of filters to remove bacterial pollutants, nitrates, arsenic, pesticides, fluorine and viruses are removed by nano filtration ^[58, 59]. Nano filtration also needs low pressure and provides high quality water with minimal investment costs ^[60] . Nano filters are designed to isolate most nitrates ^[61] . Nano-membrane filtration technology is used to separate sugars, organic compounds, polyvalent and monovalent ions, as well as water ^[62]. The main role of NF is to selectively remove ions and organic debris, and it is used in some brine desalination applications. Nano-membranes can be used to reduce salinity and eliminate hardness before it enters processing units. British scientist Michael Pritchard has developed a filter that can be loaded with polluted water and extract only clean, dust-free water. Viruses and bacteria are avoided, as well as water change and turbidity over a period of time, ensuring that humans have access to clean water at all times. The filter is easily replaced. ^[63, 64].

1.7 Water pollution

Any physical or chemical change in water quality, direct or indirect, that has a detrimental effect on living organisms or renders the water unfit for its intended purpose. Water pollution has a tremendous impact on the life of the individual, family and society if the water is such. Pollutants, a major cause of end-of-life on civic pollutants on Earth, industrial pollutants, agricultural pollutants, thermal pollutants, and radioactive pollutants are all examples of water pollution ^[65]. When hazardous substances, such as chemicals or microbes, contaminate a stream, river, lake, ocean, aquifer or other body of water reducing its quality and making it harmful to humans and the environment; Water is very sensitive to pollution. Water is known as the “universal solvent” because it can dissolve more chemicals than any other liquid on the planet ^[66]. There are two main types of water pollution. The first is the natural pollution that appears in the form of an increase in water temperature, an increase in salinity, or a rise in suspended matter ^[67]. The second category of chemical pollution includes (sewage pollution, oil spills, pollution from industrial and agricultural waste and others. Pesticides and agricultural fertilizers, for example, and among the most important sources of water pollution is the discharge of chemicals and heavy metals through companies ^[68, 69]. Chemical water pollution can be dangerous to the environment and human health. The most important chemicals that pollute water can be summarized as follows ^[70].

1.7.1 Heavy metals

The body needs small amounts of heavy metals when ingesting heavy metals from water, air or food than normal concentrations, they can pose a real danger to the health of the individual, causing health disorders that can lead to the death of the person ^[71]. The most important of them is lead, and if this percentage increases,

lead poisoning will occur, and drinking water is caused by lead contamination from home delivery pipes . Spasms of the nervous system may lead to limb paralysis. As for cadmium, and it seeps into drinking water from plastic pipes. Cadmium in excess of the permissible limit affects the amount of calcium and human osteomalacia ^[72]. Cadmium is a very toxic heavy metal. Cadmium poisoning occurs as a result of ingesting foods or drinks contaminated with high concentrations of the metal. Poisoning diseases appear after several years and after the accumulation of large amounts in the body. The main symptoms of poisoning are nausea, vomiting and abdominal pain Cadmium (Cd) is one of the most toxic elements encountered by industry and polluted environments ^[73]. Arsenic enters drinking water from pesticides or factory waste, and leads to human liver or lung cancer and rapid death, various methods have been applied to provide treatment for pollution, including adsorption ^[75].

1.7.2 Compounds phosphates and nitrates

When large doses of phosphate compounds reach people, they can cause sore throats, breathing difficulties, pain in the eyes, nose, ears, and tongue, vision problems, and severe abdominal pain that leads to vomiting, loss of appetite, and nausea^[76].Nitrates are one of the world's biggest and most serious pollution concerns. The reduction of nitrate in the body to nitrite, a chemical that converts to nitrosamines and promotes cancer, poses a threat to human health. Bacteria in the gut cause these transformations, while saliva in the mouth can lower Nitrates, which are contained in food and subsequently enter the blood stream, when entering the circulatory system, nitrite oxidizes hemoglobin in the blood, turning it into "dead hemoglobin", which the physiology of the infant cannot convert again. To produce hemoglobin, causing it to suffocate internally ^[77] .

1.7.3 Pollution by Petroleum Derivatives and Halogens

Fluoride is used to purify and sterilize drinking water. . This chemical is beneficial for human teeth because it prevents cavities. However, if the excess amount exceeds the permissible, it causes the appearance of spots. Brown teeth or their collapse ^[78]; As for chlorine chemical also used to disinfect drinking water, high levels of chlorine in water cause organic molecules in the water to react with chlorine, creating additional chemicals that increase the risk of cancer. Drinking chlorinated water increases the chances of developing bladder cancer ^[79]. Oil pollutants are also considered one of the largest sources of water pollution in terms of prevalence and influence, despite their recent history, and oil pollution occurs when oil materials seep into water bodies, especially marine ones, which are not limited to coastal areas only, but extend to reach the surface of ocean waters and deep water layers when oil is swallowed by marine species. And its derivatives, the hydrocarbons that make up the oil accumulate in the fatty tissues, liver and pancreas of fish, eventually killing people through cancer while ingesting them ^[80].

1.7.4 Alkaline and acidic compounds

Alkaline pollution leads to the formation of carbonate and bicarbonate salts, hydroxides and chlorides, which are important causes of water hardness, such as magnesium carbonate, calcium, bicarbonate, chloride compounds and sulfates that cause salinity in the earth ^[81]. Alkaline rain, whose pH may reach more than 8, is one of the main causes of water pollution, as it is rich in calcite and other dissolved alkaline substances such as carbonates ^[82]. The increase in the acidity of water is due to the transfer of sulfuric acid and nitric acid (nitrogen) to it with the waters of torrents and rivers after acid rain ^[83].

1.7.5 Water Pollution by Industrial Waste

All waste remaining from industrial activity, in particular the chemical, mining and food processing sectors, is referred to as industrial waste. Water pollutants, such as heavy metals, chemicals and detergents, are mostly produced by mining and manufacturing industries. Water is used in industry for several purposes, including washing and cooling machines, processing raw materials or foodstuffs, other washing and cooling machines, processing raw materials or foodstuffs, and other production processes. Large amounts of industrial water are released every day, which leads to different levels of water pollution. Mining industries produce heavy metals such as lily, lead and cadmium that pollute the environment. Zinc is considered a major problem due to its accumulation in living tissues ^[84]. Especially mercury, which is the most prevalent and toxic and has the ability to accumulate in tissues, as well as its role in consuming a large amount of oxygen, four times that; Sewage waste is consumed, killing more organisms in the water as it is disposed of Many other manufacturing companies, such as chemicals, oil refining, pharmaceuticals, and food processing, contribute to water pollution in the same way that heavy metals do the iron steel industry ^[85].

1.7.6 The Textile Industry and Its Environmental Impact

Textile industries are widespread, in developed countries and even poor countries, and the steps of the industrial textile production process include pretreatment, dyeing, printing and finishing. Production processes rely on water to a large extent, especially in the processes of washing raw materials to impart desired characteristics to fabrics. The textile industry uses a variety of dyes, chemicals and other materials. These procedures generate a large amount of waste, and if improperly disposed of and without treatment of the different tissue stages, it

may cause environmental difficulties and threaten many organisms with toxic, mutagenic and carcinogenic effects through the accumulation in aquatic organisms, which leads to a decrease in the percentage of dissolved oxygen in these Water in addition to toxic effects and in the textile industry ^[86] .reactive, dispersion and direct dyes are the most commonly used dyes. During the installation and treatment procedures, a large part of it (20%) is lost and ends up in wastewater ^[87] .(Wool in particular, which raises the concentration of plankton significantly, as well as dyeing and coloring processes in which pigments from salts of heavy metals or toxic organic materials are used, and , and cotton industries lead to similar pollution, but to a lesser degree ^[88] . Solid wastes should be removed from wastewater, such as fibers, yarns, textiles, exhaust coils (empty spools and cartons), empty containers of dyes, chemicals and impurities of wax materials, to avoid exposure of personnel to the toxic effects of its high toxicity, which poses a great threat to living organisms and ecological balance. These systems include adsorption, filtration, precipitation, ion exchange, and other methods for removing organic pollutants in water, such as dyes and heavy metals from their aqueous solutions, while continuing to develop new technological systems for removing organic pollutants in water, such as dyes ^[89] .

Many researchers have been interested in nanotechnology and the preparation of nano polymers, and these polymers have been used in many applications as in some of the following studies: -

Several nano particle co-polymers (1,2,3,4 and 5) were prepared by condensation polymerization from the reaction of one mole of glycerol with (1.0, 1.5, 2.0, 2.5and 3.0) moles of phthalic anhydride at specific temperatures and times with the release of water as a byproduct was studied, and the effect of three temperatures (298, 308 and 318 K), and three different concentrations (1, 3 and 5

ppm) of nano composite copolymers were studied and it is clear that they play a very important role in the adsorption process, the experimental results showed that. The adsorption of of dyes (methylene blue and eosin yellow) on the surface of these nano composite co-polymers decreases with increasing temperature, which means that the process is a heat-emitting process, and the results obtained showed a high efficacy of the co-polymers in removing contaminants (methylene blue and eosin yellow dyes) ^[90].

In another study conducted by the researcher Al-Mayali ^[91], the study was conducted the nano particle co-polymer was synthesized using solubilization process by condensation polymerization from the reaction of 1.0 mole of Pentaerythrytol with 2.0 moles of Phthalic anhydride at constant temperature and time with releasing of water as by-product, the synthesis nano co-polymer was characterized by infrared spectroscopy (FT-IR), Proton nuclear magnetic resonance (¹H-NMR) and Carbone nuclear magnetic resonance (¹³CNMR); On other hand, the size of the particles of the nano co-polymer was measured by atomic force microscopy technique (AFM) and X-ray diffraction analysis (XRD); the results of AFM, showed that, the particle sizes of the nano co-polymer were (97. 23nm) respectively, the results of XRD, showed that, the total average crystallites sizes were (92.63) nm; Which proved that the synthesis co-polymer is a nano-polymer. The synthesis nano-polymer was used as an absorber surface, so as to adsorb pollutants from water resulting from the process of dyeing tissues.

Three types of dyes (Malachite green and Disperse Blue and Reactive Red(dyes, which are used in dyeing tissues and are pollutants water from textile and dyeing factories, have been used to study the effectiveness of nano polymers in purifying water from industrial pollutants

The effect of three temperatures (298, 308 and 318 K) and three different concentrations (1, 3 and 5 ppm) of nano co-polymer were studied and it is apparent they play a very important role in the adsorption operation; the experimental results showed that the adsorption of (Malachite green and Reactive Red) dyes on the surface of these nano co-polymer increasing with increasing of temperature, meaning that the process is endothermic process, while the (Disperse Blue) dye the results obtained showed the adsorption decreases with increasing of temperature, meaning that the process is exothermic process, and the results obtained showed a high effectiveness of nano co-polymer in the disposal of pollutants (Malachite green, Reactive Red and Disperse Blue) dye.

The researcher Zahraa^[92], conducted an adsorption study of three types of different dyes (Orange-G), ((Reactive Yellow145)) and (Fuchsin acid), on the surface of a nano-copolymer (Nano polymer). The Nanoparticle Co-polymer was synthesized using the solubilization process by condensation polymerization from the reaction of one mole of glycerol with 1.5 mole of phthalic anhydride at 52min and 117oC with releasing water as a by-product, and then diagnosed using several techniques including (FT-IR, XRD, AFM, TEM, DSC and 1H-NMR), a series of experiments were conducted and several experimental variables were studied, including : Surface mass, pH, Temperature effect and Adsorption Isotherms.

The values of thermodynamic functions were calculated ΔG , ΔH , ΔS , through which it was shown that the adsorption process of dyes (Orange-G, Reactive Yellow 145 and Acid Fuchsin) on the surface Nano Co-Polymer is a spontaneous and exothermic process through the negative values of ΔG and ΔH , and an increase in randomness through the positive values of entropy ΔS .

The removal of dyes (Orange-G, Reactive Yellow 145 and Acid Fuchsin) on the surface Nano Co-Polymer as an adsorbent surface at different temperatures (298K, 308K and 318K) was studied to determine the Adsorption isotherms and Thermodynamic functions.

The hypotheses isotherms of Freundlich, Temkin and Langmuir were used, in order to describe the experimental isotherms and isotherms constants, and data showed for dyes (Orange-G, Reactive Yellow 145 and Acid Fuchsin) on surface Nano Co-Polymer agrees with hypothesis isotherm the Freundlich, Temkin and Langmuir in the form of good.

1.7.7 Pollution by Dyes

Dyes are that can somehow associate with the material to be dyed and get vivid colors. In general, dyes are used to dye fabrics and to dye cell and tissue types to become more visible. Also, dyes are considered a type of common water pollutant and can be removed from their aqueous solutions in several ways. One of the most important of these methods is the adsorption method ^[93].

Dyes are widely used in the textile, paper, plastic, food and cosmetic industries. Waste from these industries can affect our atmosphere causing pollution. The level of pollutants even at low concentration is very visible and affects aquatic life. Hence, pollution from pigments is not only a serious public health concern, but also many serious environmental problems due to its persistence in nature and insoluble propertie ^[94]. Chemists found a relationship between the color of a substance and its composition. In the year (1868 AD), the scientist (Eraeb) and his colleagues explained that the presence of unsaturated groups in the molecule is a major factor in the emergence of color, Witt, explained about the presence of certain functional groups in the molecule. The compound that makes it colored.

They are called chromophores, they mean color bearing groups, they include $-C=C-$, $-C=S$, $-C=O$, $-N=O$, $-NO_2$, $-N=N-$. There are groups that increase the intensity of the color carried by the chromophore group, and these groups are called auxiliary groups or auxochromes, that is, color tonics ^[95]. In our study, dyes can be classified into several types according to their chemical composition. As shown in Table (1-1) ^[96].

Table (1-1): Classification of dyes

Applications	Example	The type of dye
Wool, silk, polyurethane fiber, nylon.	Methyl orange, Methyl red , RBB and Congo red	Acidic dyes
Pharmaceutical polyesters, cotton, paper.	Aniline yellow, Butter yellow, ,Azure C and Malachite green	Basil dyes
Cotton, wool, silk, nylon	Martius yellow and Congo red	Direct dyes
Cotton, wool, silk	Procion dye (2,4,6-trichloro 1,3,5-triazine), Reactive Red dye.	Reactive dyes
Wool, a coloring agent in food	Indigo ,Benzanthro and Tyrian purple	Oily dyes
Polyesters and Polyamides	Disperse Blue Dye	Disperse Dye

2.7.1 Dye 145 Reactive Yellow145.

It is a kind of dye that contains active groups that interact directly with the fibers, forming covalent bonds with the fabric that contains a hydroxyl or amine group present in the fibers (cotton, wool, silk, nylon), and these active groups frequently form a heterogeneous aromatic ring, Alternatively, chlorine or fluorine can be used to replace them ^[97]. This dye is used in the dyeing of cotton, rayon, and polyester, as well as in the production of industrial textiles and printing ^[98] and it causes cancer in both humans and aquatic organisms. They are the most widely used azo dyes. This group is generally identified by one or more azo bonds (-N-N-) and aromatic rings, both of which are toxic to living organisms in addition to the sulfate group related to ethyl sulfone and mono chloro thiazine (MCT)^[99].

Azo dyes are difficult to disassemble due to their complex composition and synthetic nature, they represent about 70% of all colors used^[100]. Some properties of the Reactive Yellow145 dye are shown in Figure (1-4) and Table (1-2) ^[101].

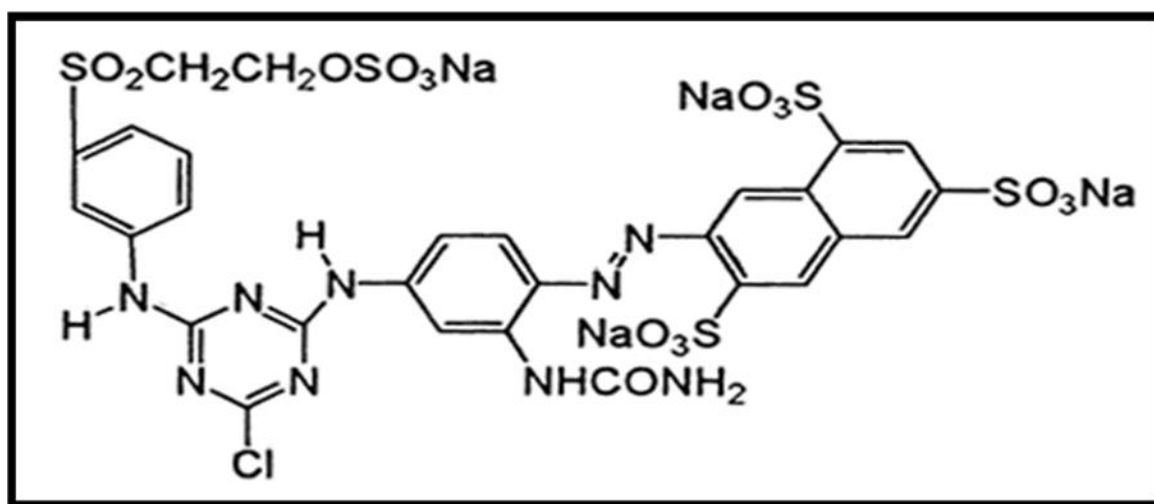


Figure (1-4): Structural formula of Reactive Yellow145 dye

Table (1-2): Properties of Reactive Yellow145 dye.

Properties	Description
Molecular formula	$C_{28}H_{20}ClN_9Na_4O_{16}S_5$
Class	Reactive dye
Solubility	Soluble in water
Molecular Weight (g/mole)	1026.3
Melting Point	237
λ_{max} (nm)	418
CINo	18159
IUPAC Name	tetrasodium;7-[[3-[[amino(oxido)methylidene]amino]-4-[[4-chloro-6-[4-(2-sulfooxyethylsulfonyl)anilino]-1,3,5-triazin-2-yl]amino]phenyl]diazenyl]naphthalene-1,3,6-trisulfonate

1.7.2. Orange-G Dye

It is one of the dyes containing one or more acidic groups, mostly a sulfonic acid group (SO₃H). which include brightly colored dyes and have a wide range of fastness properties and are used to dye textiles containing basic groups such as wool, silk and polyamide. The structural formula of the dye is shown in Figure (1-5), and Table (1-3) shows some properties of the dye^[102]. It is a typical anionic water-soluble dye. It is often used in the paper industry and has toxic effects on living organisms^[103]. It is a negatively charged monochromatic pigment widely used in the printing and textile industries. The dye has been reported to be highly toxic to humans due to its carcinogenic and pathogenic nature and it is also considered a typical azo dye in textile wastewater^[104].

Table (1-3): Properties of acid orange dye

Properties	Description
Molecular formula	$C_{16}H_{10}N_2Na_2O_7S_2$
Class	DyeAcid Orange
Solubility	Water Solubility 5 g/100 mL (20 °C)
Molecular Weight g / mole	452.38 g/mol
λ_{max} (nm)	422
Melting Point	141 °C
Density	0.80 g/mL at 20 °C
CINo	16230
IUPAC Name	1,8-dihydroxy-4-[4-(2-hydroxyethyl)anilino]-5-nitroanthracene-9,10-dione

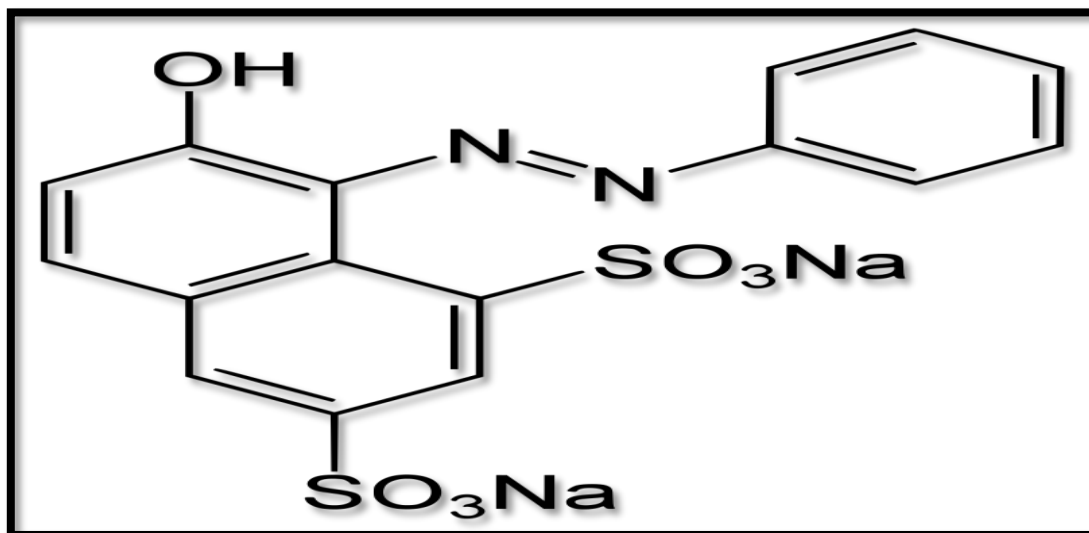


Figure (1-5): The structural formula of the orange dye.

1.7.3. Dispersed Red1 dye

It is a non-ionic compound poorly soluble in water and is one of the most common dyes invented in 1923, these dyes were developed. disperse dyes which are small polar compounds ^[105]. They often include anthraquinone, azo, or nitro groups but do not contain charged captions or anionic groups within the structure. The disperse dyes are slightly soluble in water ^[106]. However, dyes dissolve in aqueous medium in water and individual particles are dispersed throughout the fibers during dyeing, as mentioned later. The amino groups, hydroxyethylamine, azo, carbonyl, and other groups in disperse dyes are responsible for their solubility. These groups contain an electron (nitrogen, oxygen, and sometimes sulfur) that may interact with water molecules vigorously. Even if the aromatic rings are devoid of these atoms, they can affect how the dye interacts with water molecules and change the solubility of the dye ^[107]. The presence of amino groups associated with larger aromatic structures characterizes the basic (cationic) dyes. Positively charged amino groups are present in these colors. This provides them with water solubility and affinity for fibers with a lot of negatively charged groups, including nylon and acrylic. Water-resistant thermoplastic fibers such as nylon, polyester, acrylic and other synthetics can now be dyed using dispersion dyes, which have been developed and commercialized^[108]. These colors are available in powder or liquid form For some synthetic fibers, currently the most common dye class Azo dyes are among the most popular commercial azo dyes Synthetic fiber dispersion 1 in red. While this dye is known to exist as a complex mixture, the overall composition of the dyes is very small, flat and non-ionic, with attached polar functional groups (NO₂ hydroxyalkyl and -CN) as shown in Figure (6. 1). They are characterized by the low molecular weight of these colors. The dispersed dye

particles should be as small as possible and have a low molecular weight in the range of 400-600 for effective diffusion into the fabrics. The disperse dyes must be able to withstand dyeing conditions of varying pH and temperatures ^[109]. The properties of the dispersed red pigment are shown in Tables (1-4) ^[110]

Table (1-4): Properties of Disperse Red 1 dye

Properties	Description
Molecular formula	C ₁₆ H ₁₈ N ₄ O ₃
Class	Disperse Dye
Solubility	Soluble in water
Molecular Weight g / mole	314.34
Melting Point	160-162 °C
λ_{max} (nm)	536
CINo	11110
IUPAC Name	2-[N-ethyl-4-[(4-nitrophenyl)diazenyl]anilino]ethanol

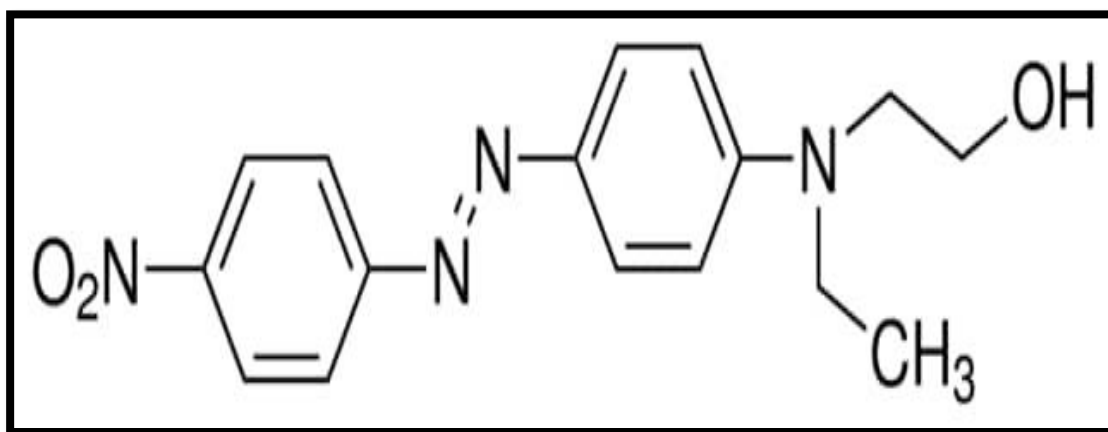


Figure (1-6): The structural formula of the dispersed Red1 dye

1.8 Aim of the Work

The work can be summarized as follows:

- 1- Synthesis of a novel nano co-polymer and its characterization using spectra FT-IR, ¹HNMR and AFM.
- 2- The use of the prepared nano co-polymer in removing pollution from aqueous solutions of some types of dyes

Experimental

Experimental Part

2.1 Chemical and Techniques

2.1.1 Chemicals

The following Table (2-1) shows all solid and liquid chemical materials used in this study

Table (2-1): Chemical material, purity and companies supply

Materials	Purities	Company
Terphthalic acid	99.5%	BHD
Glycerol	99%	ALPHA
Maleic anhydride	98%	MERCK
Dimethylsulfoxide (DMSO)	99.5%	CDH
para-Xylene	99%	MERCK
Reactive Yellow145	99%	MERCK
Orange-G	98%	MERCK
Disperse Red 1	98%	MERCK

2.1.2 Techniques and Instruments

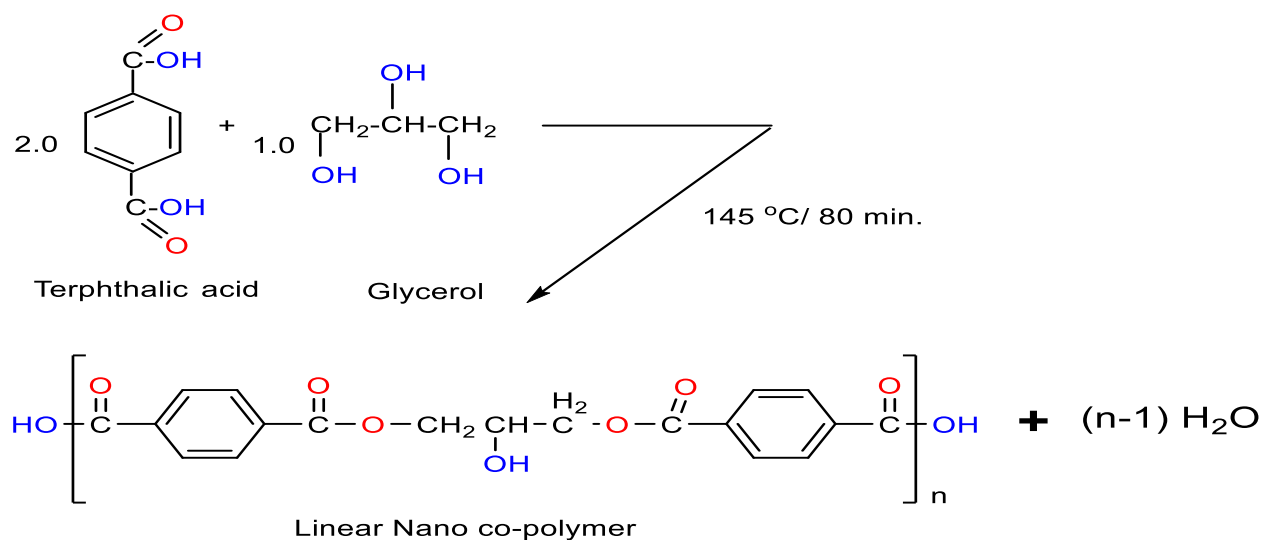
1. Fourier Transformer Infra-Red Spectroscopy (FT-IR) spectra in range 400-4000 cm^{-1} were used by using potassium bromide disc on FT-IR instrument Bruker spectrophotometer /USA, Department of Chemistry/ College of Sciences / University of Babylon.
2. $^1\text{H-NMR}$ Spectroscopy, Bruker Bio Spin 400 MHz spectrometer Ghazi Osman Pasha University / Turkey
3. Atomic Force Microscope (AFM), Oxford, USA / Department of Chemistry/ College of Sciences / Baghdad University
4. UV.-Vis. Spectrometer, Jenway, Genova Plus, Department of Chemistry/College of Education for Pure Sciences/ University of Kerbala
5. Thermostatic Shaker, GFL (D-3006)- Germany, Department of Chemistry/College of Education for Pure Sciences/ University of Kerbala
6. Electric Sensitive Balance, Lab.BL210, Sartorius median- Germany, Department of Chemistry/College of Education for Pure Sciences/ University of Kerbala

2.2 Synthesis of graft PTGM nanoparticles

Poly (Terphthalic acid-co-Glycerol-G-Maleic anhydride) nano particle was synthesis by esterification process, by dissolving method by two steps; the esterification technique was used to synthesis the nano co-polymer, and the preparation method is shown below:

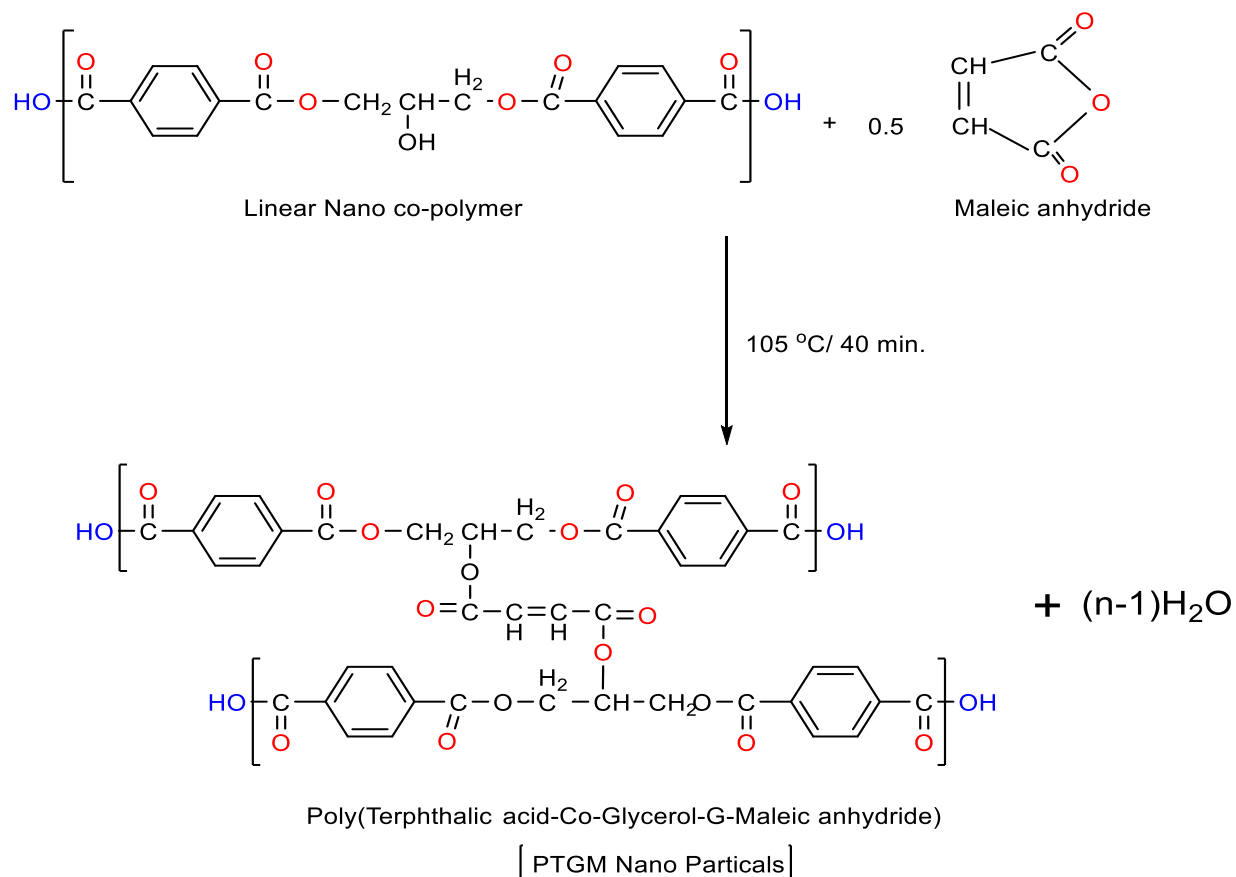
The first stage is: In a 200 ml two-necked round bottom flask, (2.0 mole, 332gm) of Terphthalic acid and (50 ml) of DMSO, were mixed together, this flask was equipped with a thermometer. The mixture warmed carefully with a hot plate magnetic stirrer to 40°C until clear liquor is formed and added (1.0 mole, 92gm) of

Glycerol to the solution. The mixture warmed carefully to 120°C, then about 25 ml of xylene was added carefully to the reaction flask, in the form of batch (two drops in each batch), withdrawal of water formed by the esterification process, and the flask was gently heated. Heating was stopped after 80 min. at 145°C, until no more water came off. Leave the reaction flask to cool to about 50°C, as shown in Equation (2-1).



Equation (2-1): Reaction of step 1

In the second stage; about (0.5mole, 58gm) of Maleic anhydride, was dissolved in 10 ml of DMSO at 40°C, and added to the mixture (which prepared in the first step above). The flask was gently rise heated to 90°C, added the drops of xylene in the form of batch (two drops in each batch), and until no more water came off at 105°C after 40 min. to prepared of nano graft PTGM particles. Leave the reaction flask to cool to room temperature, and then add the cold distilled water, where the suspension solution is form after 6.0 hr., then leave the suspension solution to precipitate overnight and then filtered and washed with distilled water and leaves to dry, as shown in Equation (2-2).



Equation (2-2): Reaction of step 2 Synthesis of graft PTGM nanoparticles

2.3 Preparation of Dyes Solutions^[111]

Dye solutions (Reactive Yellow145, Orange-G and Disperse Red 1 dyes) were prepared using the following general method:

The standard solution of the dye prepared by dissolving (0.5 g) of the dye in a certain amount of distilled water and then completes it to (1000 mL) to prepare a concentration (500 ppm) of this solution. From this concentrated solution, the diluted solutions were prepared in concentrations (1, 3, 5 and 7 ppm) by taking the appropriate volume of the concentrated solution and then dilute with (100 mL) distilled water.

2.4 Determination of Calibration Curve ^[112]

The Calibration curve that represented the relationship between absorbance and concentration was determined by prepared four concentrations (1, 3,5 and 7ppm) of the three types of dyes (Reactive Yellow145, Orange-G and dispersion red) for solutions used in the study, the absorbance of these concentrations was measured at the maximum wavelength ($\lambda_{\max} = 418 \text{ nm}$) for the Reactive Yellow145 dye as shown in Figure (2-1 a), after which the calibration curve between absorption and concentration is drawn as in Figure (2-1 b) and at the maximum wavelength ($\lambda_{\max} = 480 \text{ nm}$) for the Orange-G dye as shown in Figure (2-2 a), after which the calibration curve between absorption and concentration is drawn as in Figure (2-2b) and at the maximum wavelength ($\lambda_{\max} = 536 \text{ nm}$) for the dispersion red dye as shown in Figure (2-3a), after which the calibration curve between absorption and concentration is drawn as in Figure (2-3b).

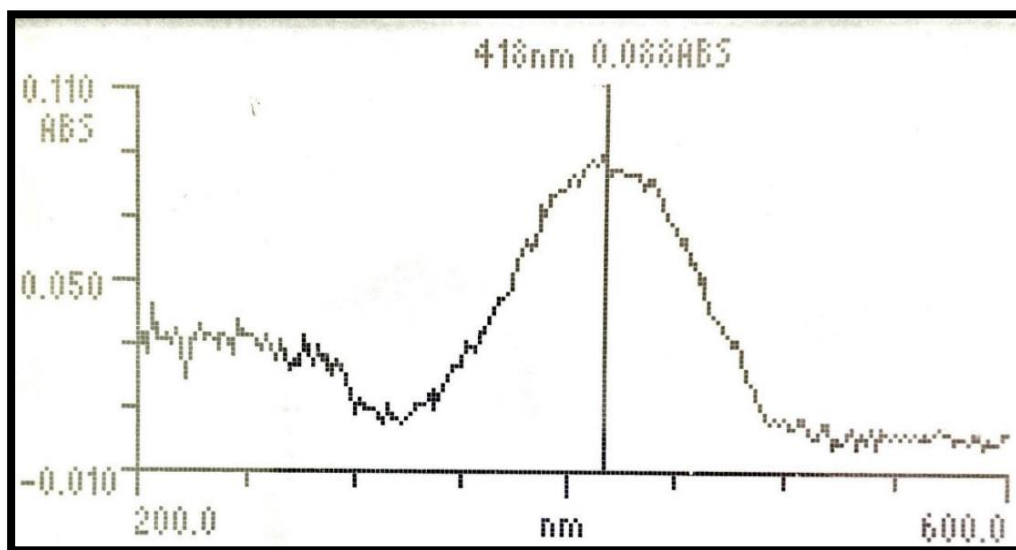


Figure (2-1 a): The maximum wavelength (λ_{\max}) for the (Reactive Yellow145).

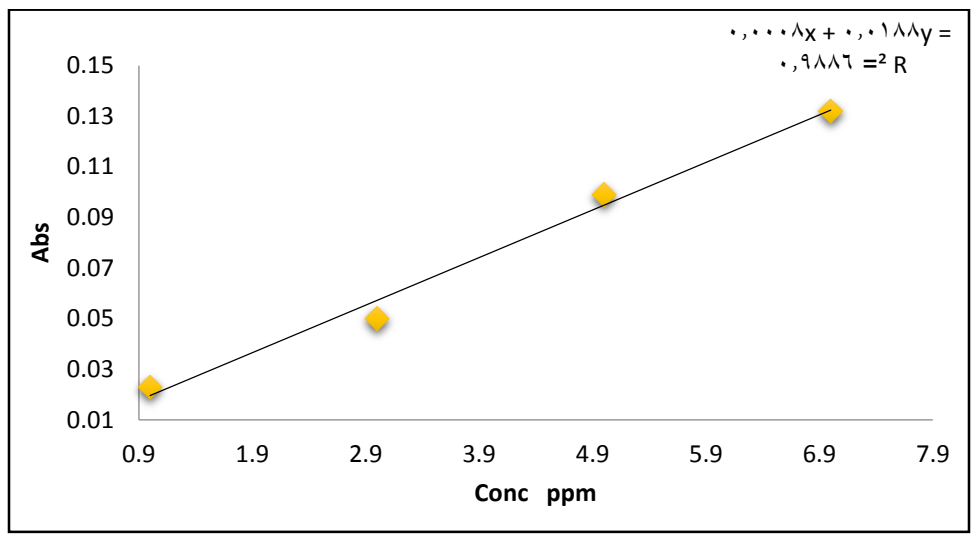


Figure (2-1 b): The calibration curve between absorption and concentration of Reactive Yellow145.

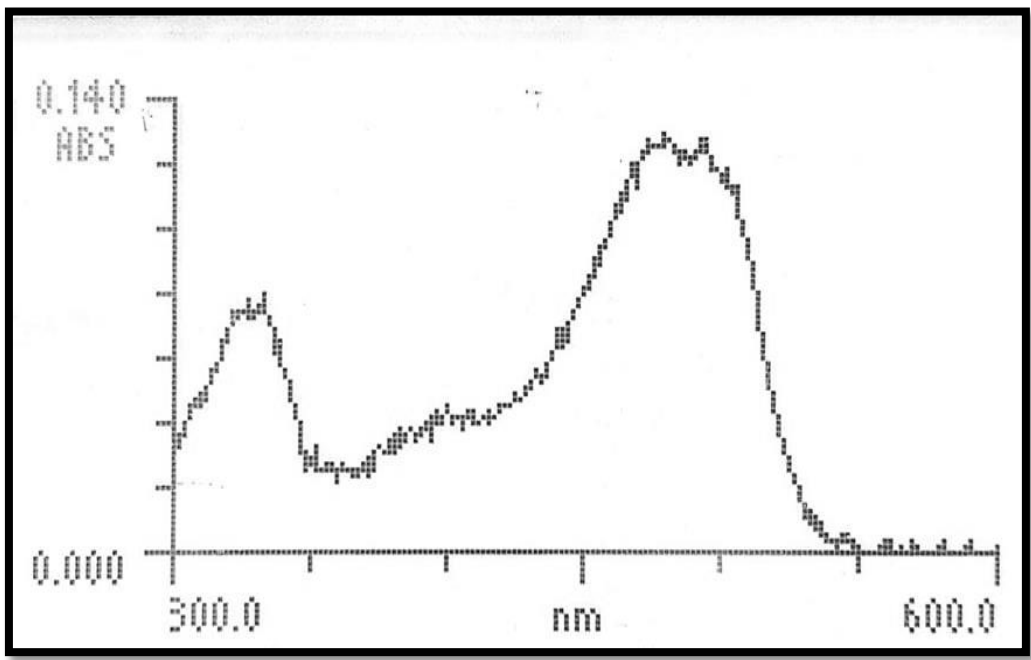


Figure (2-2 a): The maximum wavelength (λ_{max}) for the Orange-G dye.

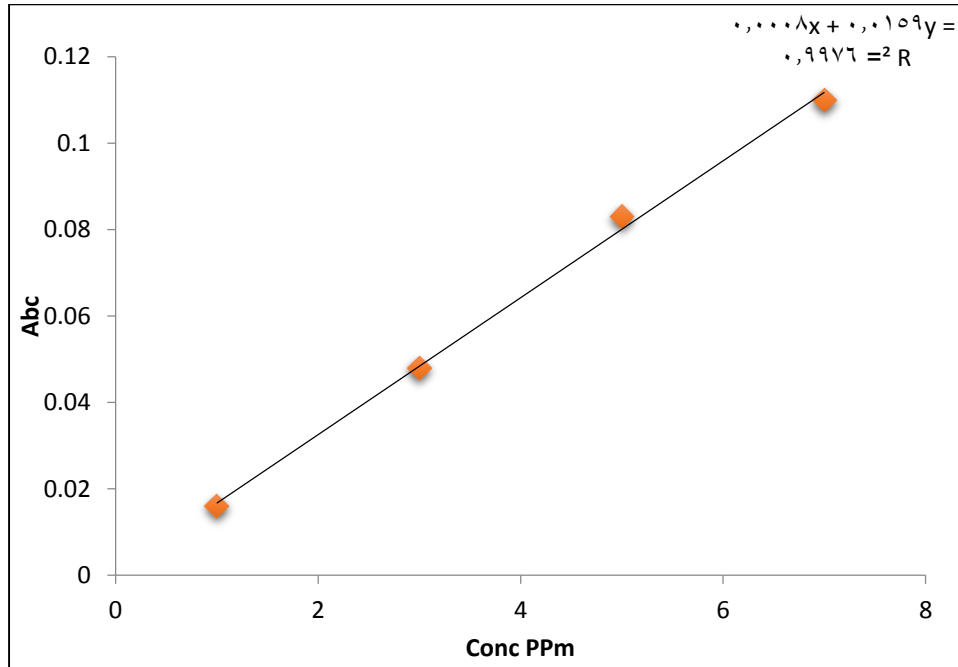


Figure (2-2 b): The calibration curve between absorption and concentration of Orange-G dye.

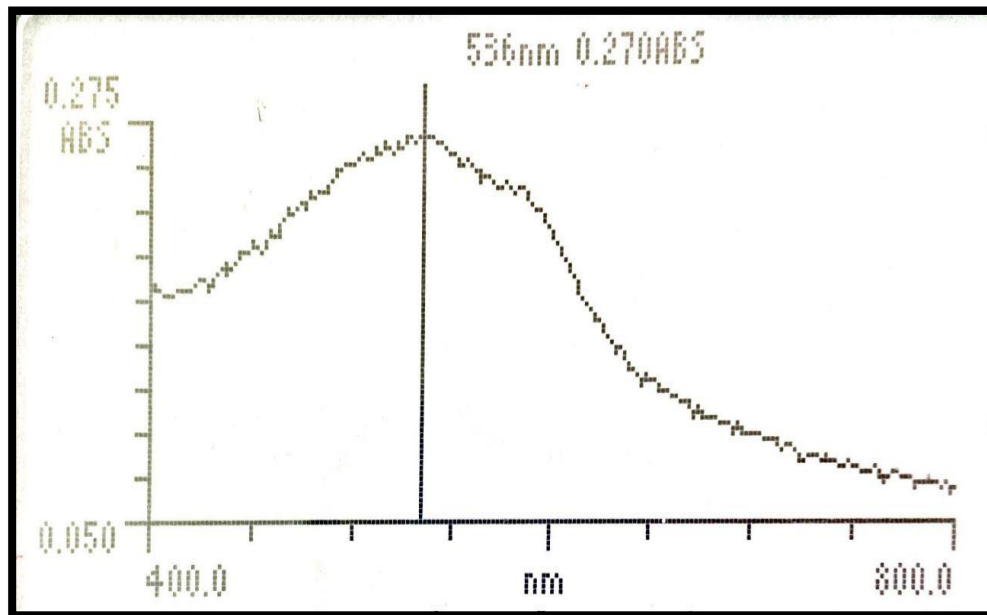


Figure (2-3 a): The maximum wavelength (λ_{max}) for the Disperse Red 1 dye.

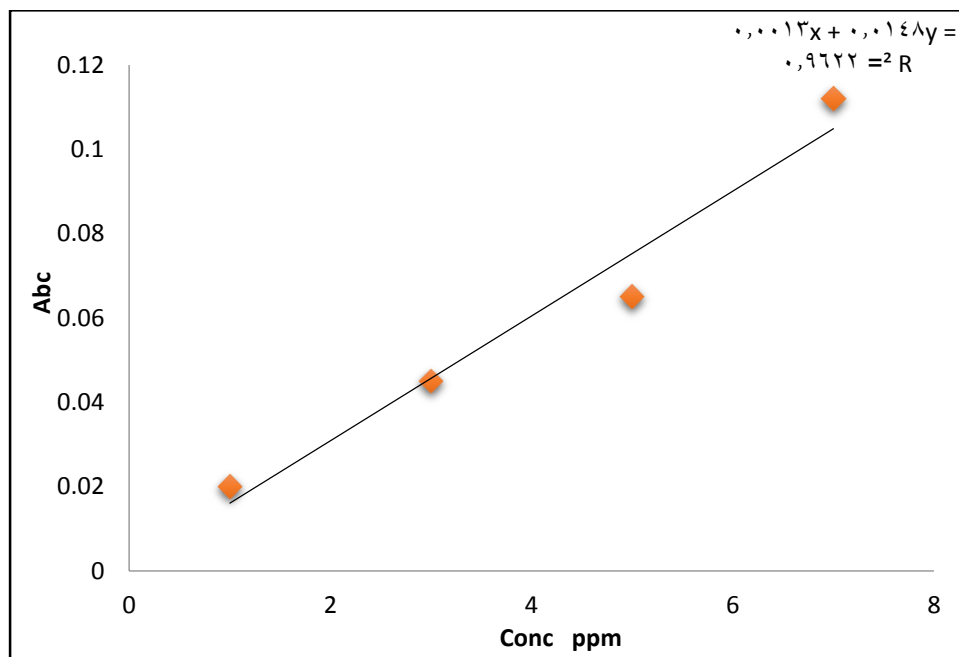


Figure (2-3b): The calibration curve between absorption and concentration of Disperse Red 1 dye.

2.5 Determination of Equilibrium Factors

To determine the weight of the adsorbent material that is given the highest amount of adsorption, different weights were taken from the adsorption surface graft co-polymer within the range (0.01,0.012,0.013,0.014,0.015 and 0.016g) and placed in contact with 15ml from the solution of the adsorbent (Reactive Yellow145, Orange-G and Disperse Red 1) dyes and by concentrating 7ppm of volumetric flask and the absorbance of it was measured after the of 60 min, from placing in the vibrator has a temperature 298k and the surface weight was chosen, which gave the lowest absorbency.

As for determining the time required for the equilibrium to occur between the adsorbent surface nano co-polymer and the adsorbent material (Reactive Yellow145, Orange-G and dispersion red) dyes. 12 volumetric flask were taken

according to the time in minutes (5,10,15,20,25,30,35,40,45,50,55,60) , First volumetric flask Time (5 min) second volumetric flask Time (10 min) third volumetric flask Time (15min) etc. up to the 12th volumetric flask Time (60 min) then and placed in it 15ml of 7ppm concentrations of each dye in contact with the predetermined weight (nano graft co-polymer) was placed in the water bath shaker at constant temperature of 298K , then samples were drawn from it at successive times and the absorbance was measured for as in the Table (2-2).

Table (2-2): shows the weight and equilibrium time for each dye

Dye	Wt (g)	Time(min)
Reactive Yellow145	0.012	20
Orange-G	0.01	30
Disperse Red 1	0.015	25

2.6 Determination of Adsorption Isotherms

For the purpose of finding adsorption isotherms, four solutions were prepared from each polymer and with concentrations of (1, 3, 5 and 7 ppm) of same dyes, then 15 ml of each concentration of dye was taken and placed in volumetric flasks in contact with the specified predetermined weight of the adsorbent surface (nano co-polymer), after these flasks were placed in shaking device with a temperature of 298K and after reaching the specified and the predetermined equilibrium time for each dye ,then the solutions were filtered and the samples were analyzed using UV.-Vis. spectroscopy, and determined the concentration of each solution at equilibrium C_e (mg/L) of the calibration curves and then determined the amount of the adsorbate substance Q_e (mg/g) under the following relationship ^[113].

$$Q_e = (C_o - C_e) \cdot V_{sol} / Wt \dots \dots \dots (2-1)$$

Were as:

Q_e: the amount of adsorbate (mg/g).

C_o: the initial concentration of the adsorbate (mg/L).

C_e: the residual concentration of the adsorbate at equilibrium (mg/L).

V_{sol}: the total volume of the adsorbate solution (L).

wt: weight of the adsorbent (g).

2.7 Effect of Temperature on Adsorption

For the purpose of studying the effect of temperature on adsorption, the adsorption isotherm was studied for each dye [Reactive Yellow145, Orange-G and dispersion red] at a temperature (298, 308 and 318 K).

RESULTS

&

DISCUSSION

Results and Discussions

3.1 Synthesis Graft Nano co-polymers

The nano co-polymer was synthesis through the esterification process by dissolving method, and characterized using (FT-IR, $^1\text{H-NMR}$ and AFM) technology. The FT-IR spectra of a linear nano co-polymer are depicted in Figure (3-1), showed the appearance of a strong broad band at about 3423 cm^{-1} for stretching alcoholic -OH with stretching (H-bond), and also showed a weak band at about 2902 cm^{-1} due to the -OH for Carboxylic acid, the C-H sp^3 and sp^2 hybridization absorption at about 2544 cm^{-1} , 2654 cm^{-1} respectively, and the spectrum also showed a strong band at about 1726 cm^{-1} assigned to a stretching band C=O for ester group. The spectrum appearance a weak sharp bands at about 1597 cm^{-1} , 1581 cm^{-1} due to C=C for conjugated system of benzene ring and also showed a bands at about $1284\text{--}1259\text{ cm}^{-1}$ assigned to C-O absorption band.

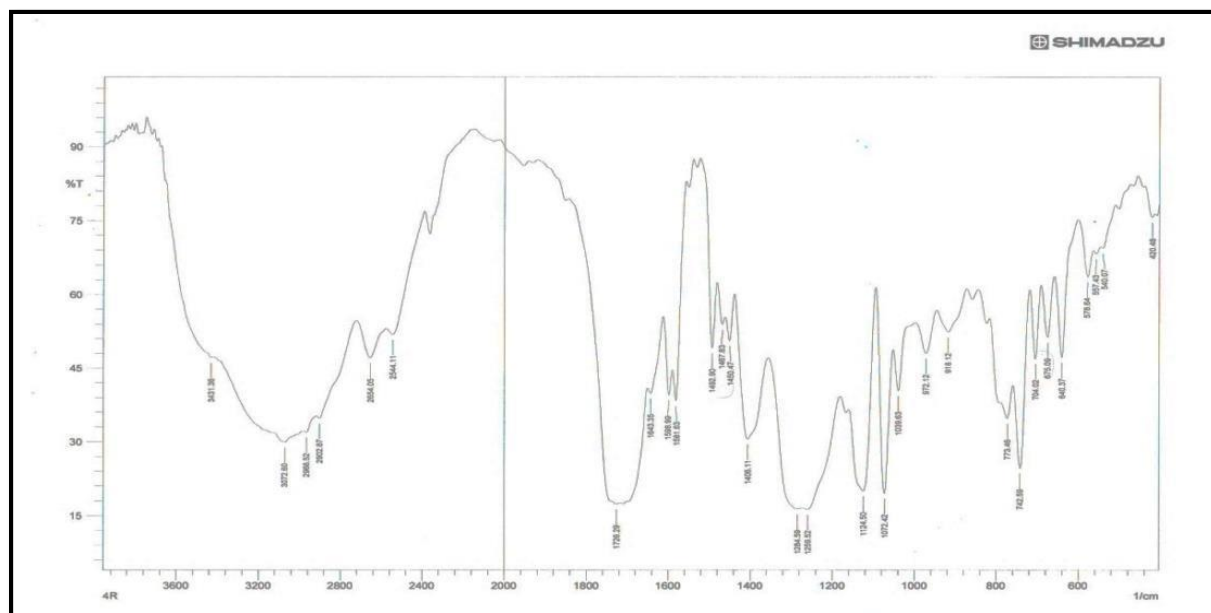
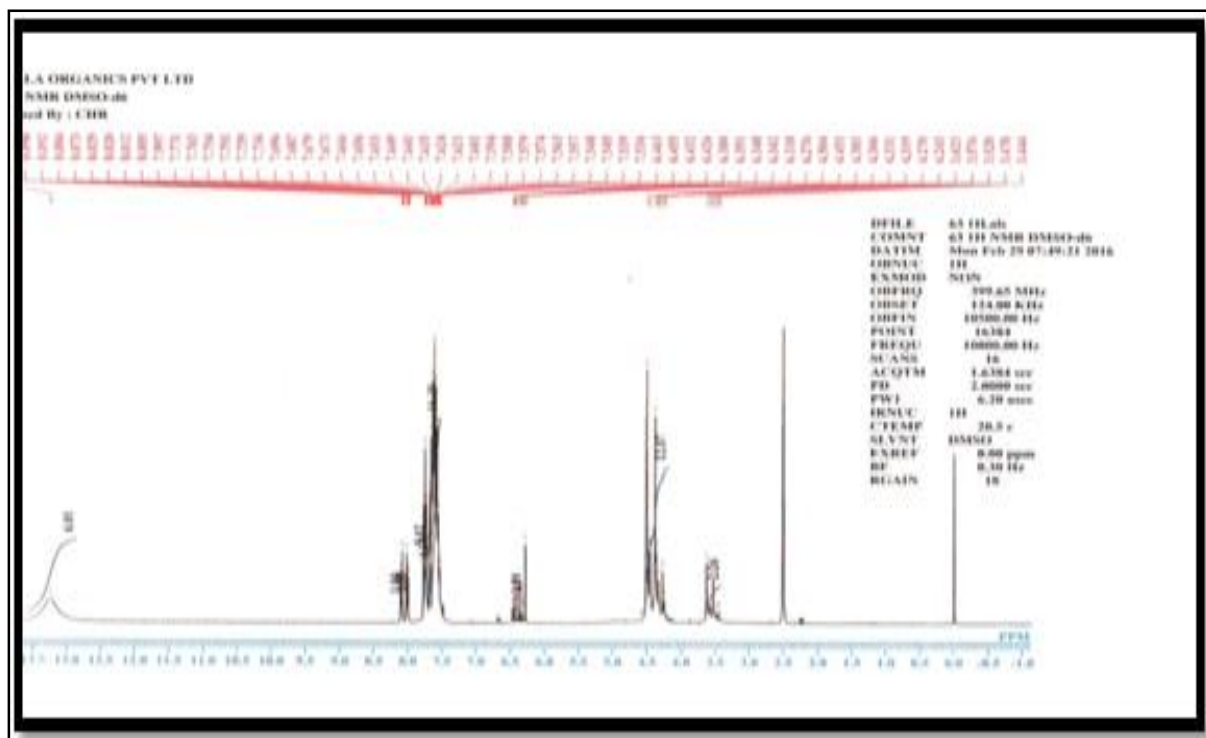


Figure (3-1): FT-IR of linear co-polymer spectrum.

The spectrum of ^1H NMR showed in Figure (3-2), which explain the singlet signal at 13.24 ppm characteristic of proton in carboxylic acid group, furthermore the multiples in the region 7.53- 8.10 ppm back to all protons in aromatic ring, the signals at 6.27-6.46 ppm for four protons of methylene in the structure of co-polymer, the multiples at 4.24- 4.50 ppm of methyl protons, but the triplet signal in 3.44- 3.62 ppm due to the proton of aliphatic alcohol so this spectrum was confirmed the structure of our target polymer.



The ^1H NMR spectrum (600 MHz, $(\text{CD}_3)_3\text{SO}$) of nano graft co-polymer showed in Figure (3-4), it's showed the appearance 13.12 (s, Protons of carboxylic groups), 7.79-7.48 (m, protons of aromatic ring), 6.46 (s, protons of methine group attached to the double bond), 5.91-5.56 (q, protons of methine groups that attached to oxygen's atoms), 4.28-4.23 (d, protons methylene groups).

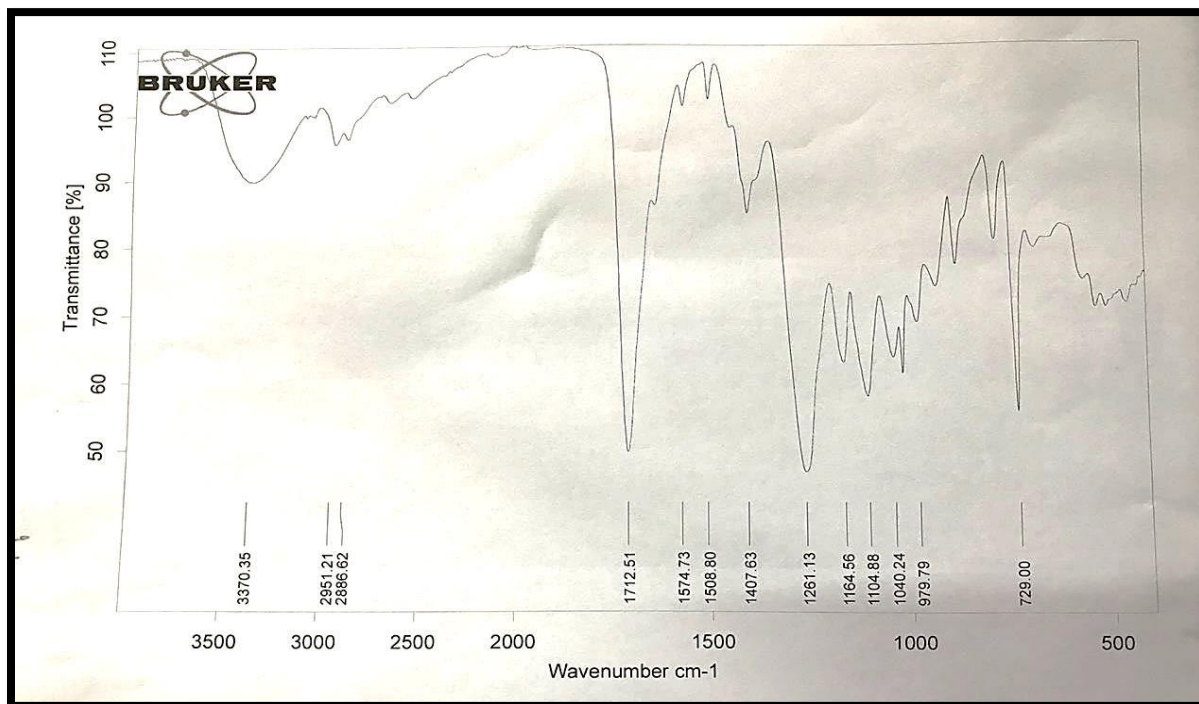


Figure (3-3): FT-IR spectrum of nano graft co-polymer

The spectrum of ^1H NMR (600 MHz, $(\text{CD}_3)_3\text{SO}$), Figure (3-4), it's showed the appearance 13.12 (s, Protons of carboxylic groups), 7.79-7.48 (m, protons of aromatic ring), 6.46 (s, protons of methine group attached to the double bond), 5.91-5.56 (q, protons of methine groups that attached to oxygen's atoms), 4.28-4.23 (d, protons methylene groups).

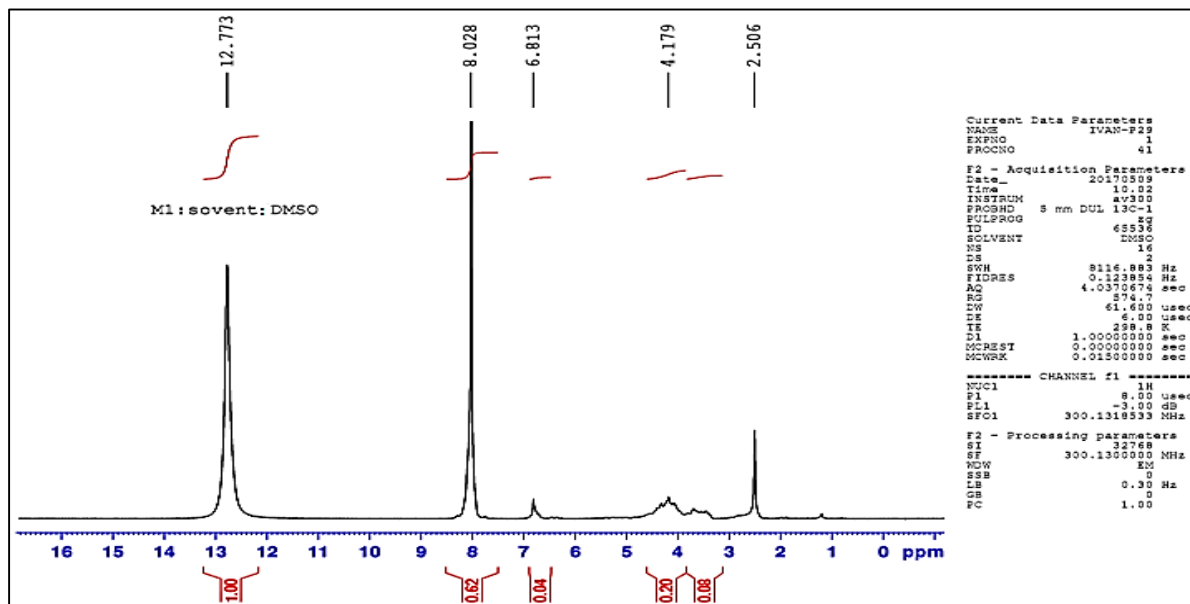


Figure (3-4): The ¹H NMR spectrum of nano graft co-polymer

The size of particles of the linear and graft co-polymers which prepared by using solubilization process was measured by the atomic force microscope (AFM); the results showed that the co-polymers are nanoparticles co-polymers, as shown below:

Figure (3-5 a, b &c) shows the outer surface of the nanoparticles of linear co-polymer. The roughness of this surface and the square root square are calculated according to the coefficient:

$$Rm = \sqrt{\sum_{i=1}^n \frac{(Z_i - Z_{av})^2}{N}}$$

Where N, Z = the number of measured points

The roughness coefficient of a linear co-polymer surface was 1.19 nm and the square root square was equal to 1.37 nm. This indicates that the bold size of the nanoparticles plays an important role in the roughness of the surface, its uniform

crystalline system, and the surface homogeneity, Also, the average of height of the particles was equal to 4.80 nm, as observe in Figure (3-5 a). Table (3-1), represents the total rate of the particle sizes of the common linear nanoparticle and the different proportions of these volumes; the results indicate that the molecular size of the linear co-polymer nanoparticle was 94.09 nm and Figure (3-6), represent the distribution of the different proportions of particle sizes of the linear co-polymer nanoparticle. On the other hand, Figure (3-7 a, b &c) shows the outer surface of the nanoparticles of graft co-polymer. The roughness coefficient of a graft co-polymer surface was 2.12 nm and the square root square was equal to 2.44 nm. This indicates that the bold size of the nanoparticles plays an important role in the roughness of the surface, its uniform crystalline system, and the surface homogeneity, Also, the average of height of the particles was equal to 8.3 nm, as observe in Figure (3-7 a). Table (3-2) represent the total rate of the particle sizes of the graft co-polymer nanoparticle and the different proportions of these volumes; the results indicate that the molecular size of the graft co-polymer nanoparticle was 74.39 nm and Figure (3-8) represent the distribution of the different proportions of particle sizes of the graft co-polymer nanoparticle

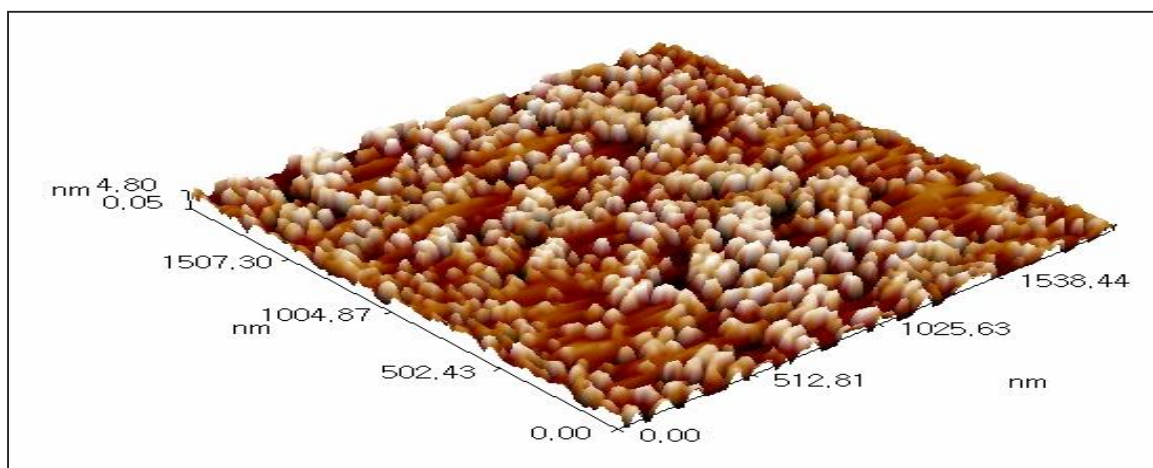


Figure (3-5 a): Image of Atomic Force Microscope for linear co-polymer shows 3D Image.

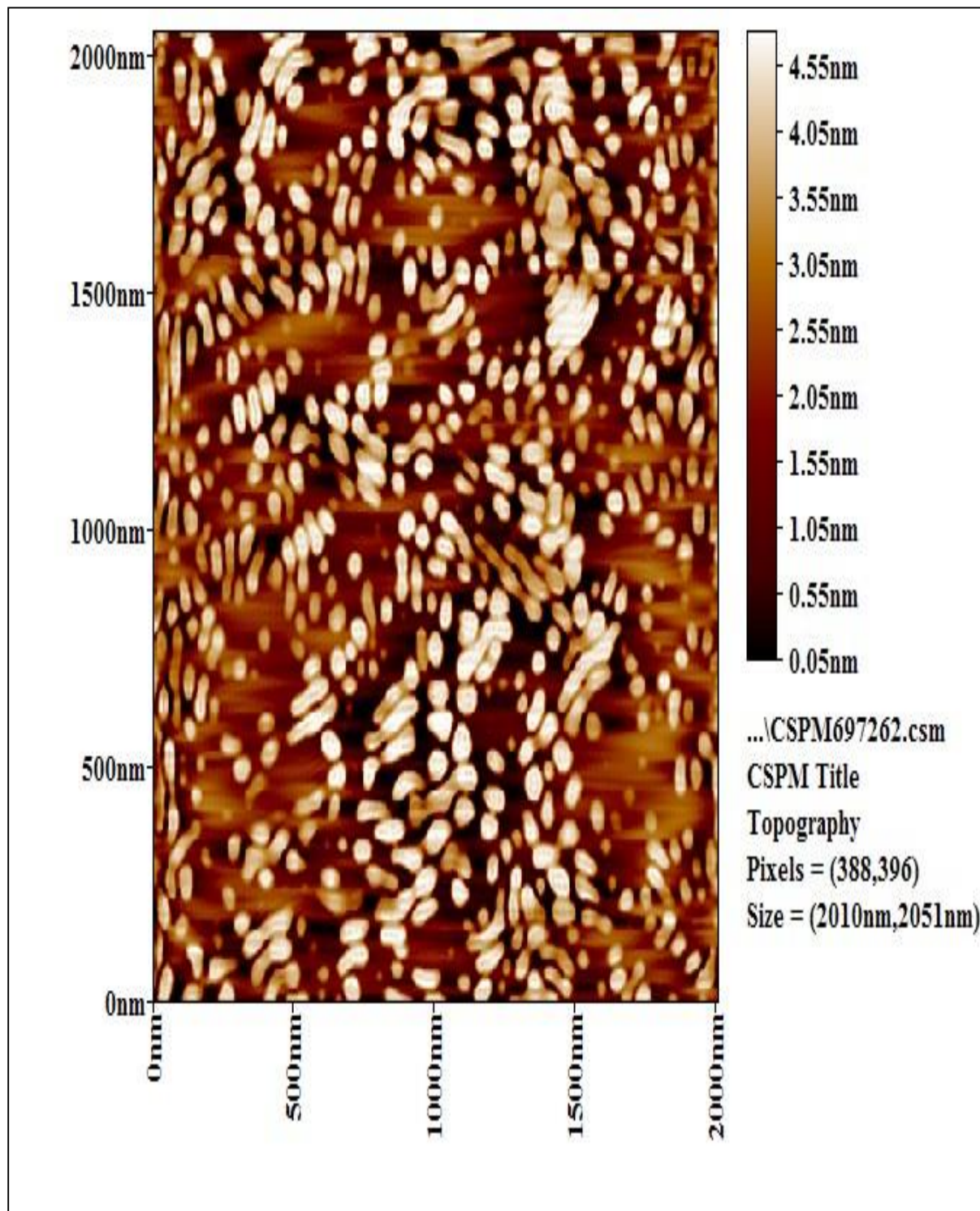


Figure (3-5 b): Image of Atomic Force Microscope for linear co-polymer shows 2D Image.

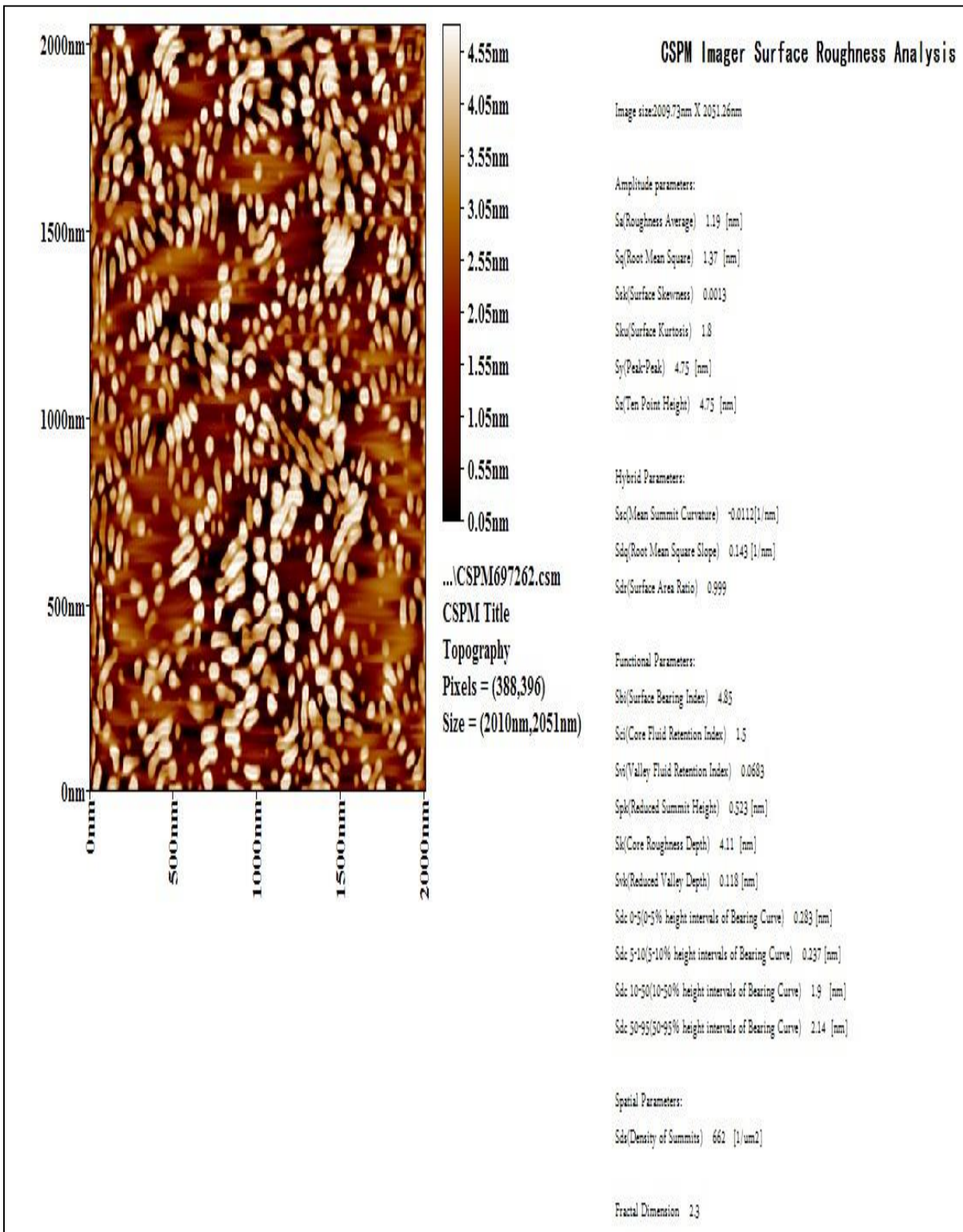


Figure (3-5 c): Image of Atomic Force Microscope for linear co-polymer shows 2D Image and showing all details of particles

Chapter Three - Results & Discussion

Table (3-1): The total rate of the particle sizes of the linear nano co-polymer nanoparticle and the different proportions of these volumes

Sample:1			Code: Sample Code		
Line No.: lineno			Grain No.:139		
Instrument: CSPM			Date:2021-04-23		
Avg. Diameter: 94.09 nm			<=10% Diameter:75.00 nm		
<=50% Diameter: 90.00 nm			<=90% Diameter:115.00 nm		

Diameter(n m)<	Volume (%)	Cumulatio n(%)	Diameter(n m)<	Volume (%)	Cumulatio n(%)	Diameter(n m)<	Volume (%)	Cumulatio n(%)
75.00	7.19	7.19	100.00	8.63	68.35	125.00	1.44	93.53
80.00	12.95	20.14	105.00	7.19	75.54	130.00	5.76	99.28
85.00	16.55	36.69	110.00	7.19	82.73	145.00	0.72	100.00
90.00	11.51	48.20	115.00	5.04	87.77			
95.00	11.51	59.71	120.00	4.32	92.09			

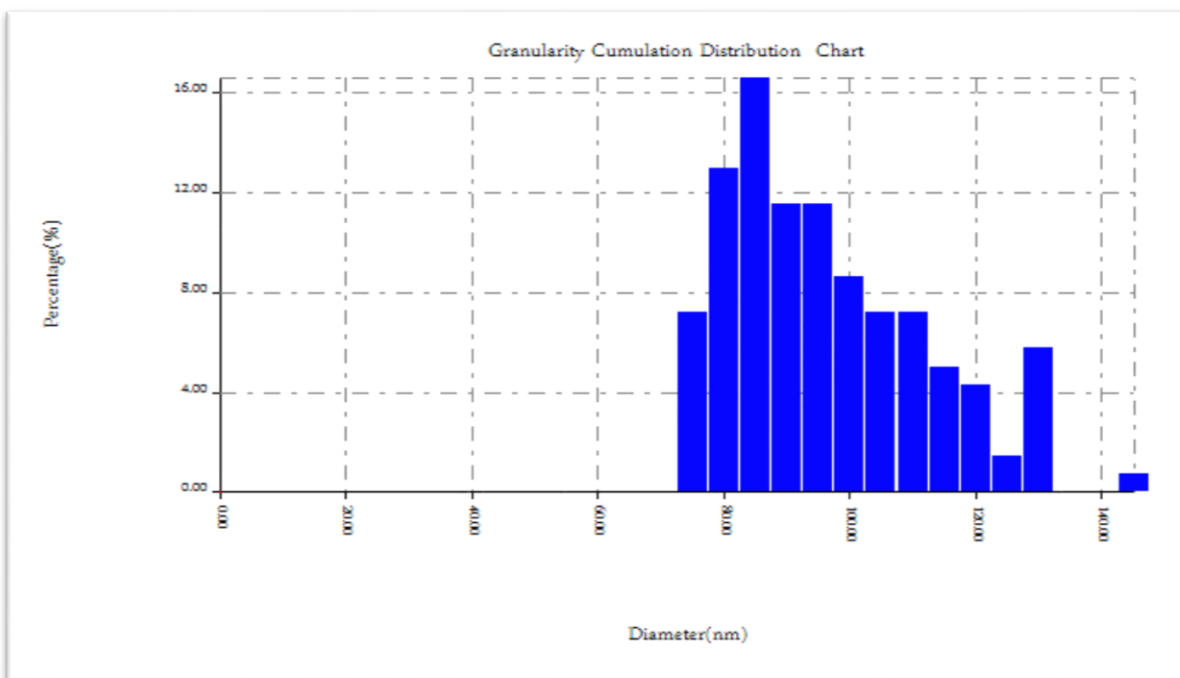


Figure (3-.6): Distribution of the different proportions of particle sizes of the linear co-polymer nanoparticle

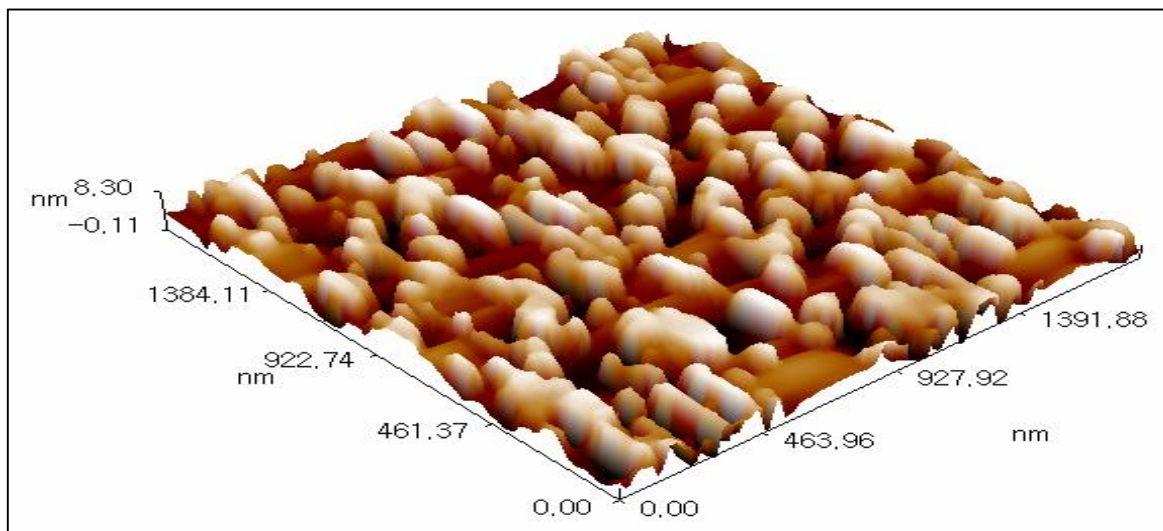


Figure (3-7 a): Image of Atomic Force Microscope for graft co-polymer shows 3D Image.

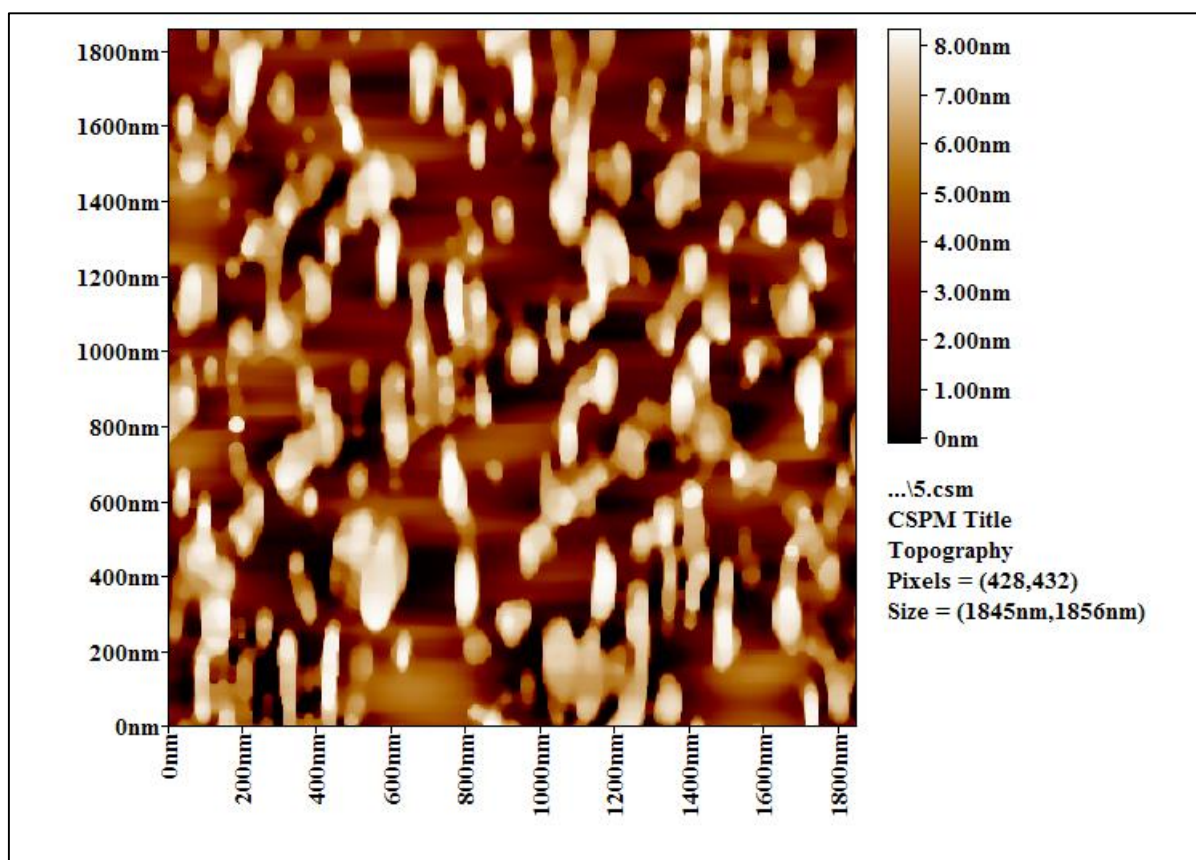


Figure (3-7 b): Image of Atomic Force Microscope for graft co-polymer shows 2D Image.

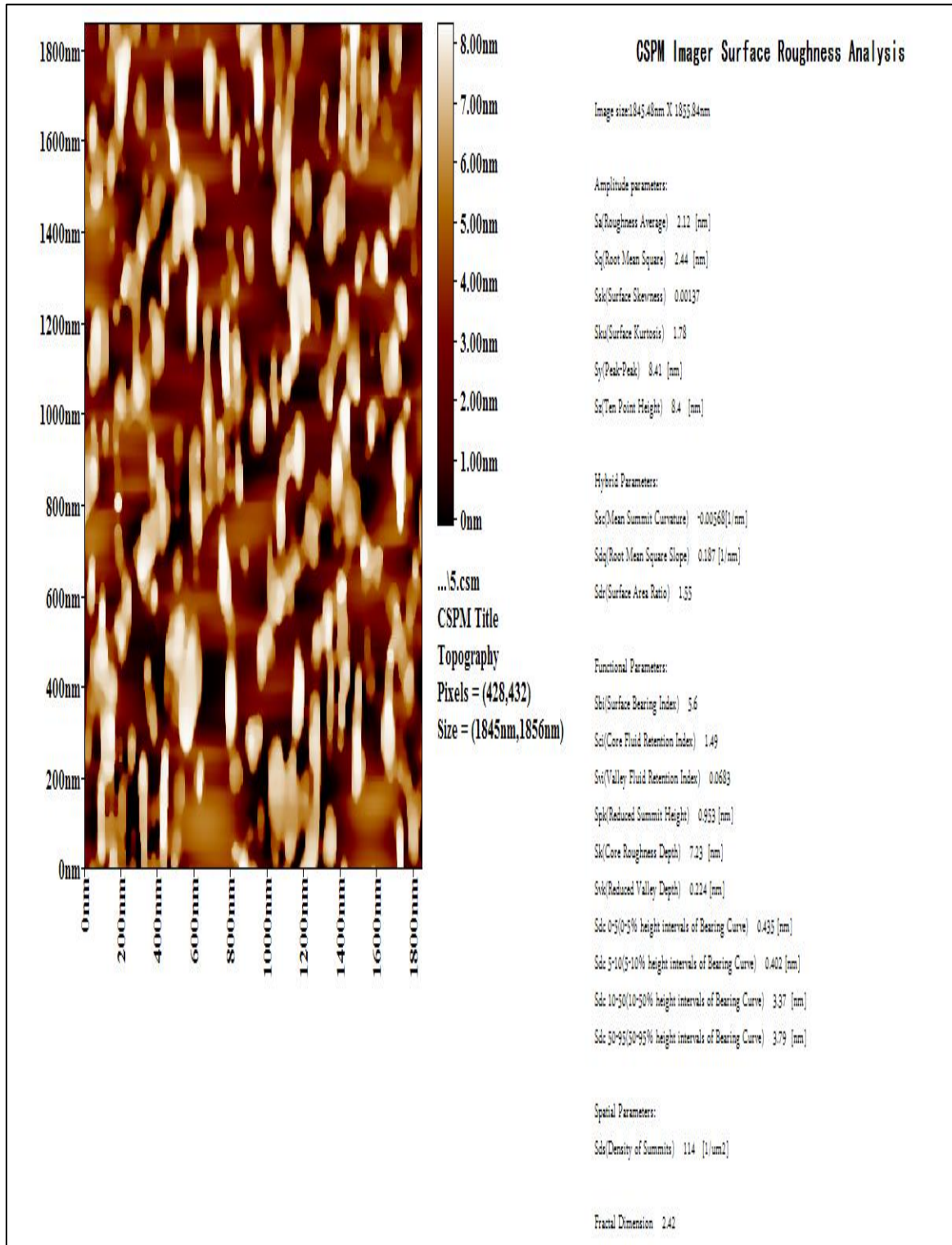


Figure (3-7 c): Image of Atomic Force Microscope for graft co-polymer shows 2D Image and showing all details of particles

Chapter Three - Results & Discussion

Table (3-2): The total rate of the particle sizes of the graft co-polymer nanoparticle and the different proportions of these volumes

Sample:2			Code: Sample Code		
Line No.: lineno			Grain No.:208		
Instrument: CSPM			Date:2021-05-31		
Avg. Diameter:74.39 nm			<=10% Diameter:0 nm		
<=50% Diameter:70.00 nm			<=90% Diameter:95.00 nm		

Diameter(n)<	Volum)<	Cumulatio)<	Diameter(n)<	Volum)<	Cumulatio)<	Diameter(n)<	Volum)<	Cumulatio)<
55.00	10.58	10.58	85.00	7.69	75.96	115.00	1.44	98.56
60.00	12.98	23.56	90.00	6.73	82.69	120.00	0.48	99.04
65.00	10.10	33.65	95.00	4.81	87.50	125.00	0.48	99.52
70.00	12.50	46.15	100.00	4.33	91.83	140.00	0.48	100.00
75.00	7.21	53.37	105.00	2.88	94.71			
80.00	14.90	68.27	110.00	2.40	97.12			

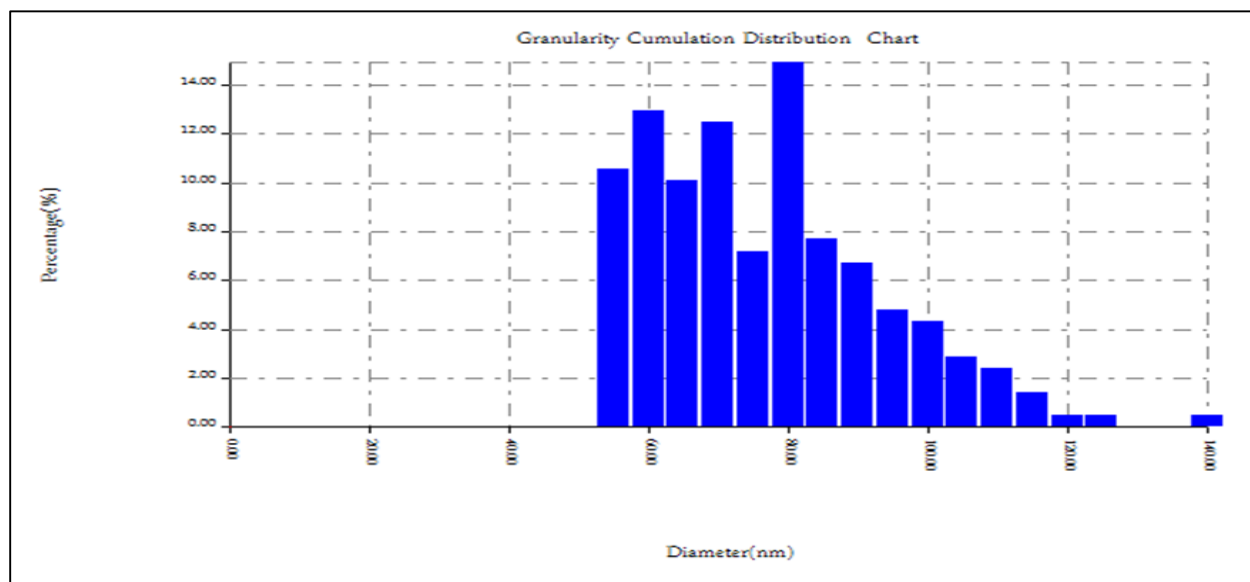


Figure (3-8): Distribution of the different proportions of particle sizes of nano graft co-polymer nanoparticle.

3.2 Removal of Pollutants

The pollutants were removed by using the adsorption process, where graft co-polymer nanoparticle were used as adsorbent surfaces with (Reactive Yellow145, Orange-G and Disperse Red 1) as adsorbate materials (pollutants).

3.3 Adsorption isotherm on the surface of the nano co-polymer.

The adsorption of Reactive Yellow145, Orange-G and Disperse Red 1 dyes were studied on the graft co-polymer nanoparticle, where adsorption isotherms were obtained at a temperature of 298K as shown in table (3-3) ,(3-4)and (3-5) for all dyes respectively and figure (3-9) , (3-10) and (3-11) for Reactive Yellow145, Orange-G and Disperse Red 1

It is evident from the drawing that the general form of adsorption isotherms is of type (S1) according to the classification of Giles). This indicates that the surface of the adsorbent material is a heterogeneous surface ^[114]. Also, when the covered part of the adsorbent surface increases, the adsorption temperature will decrease ^[111]. The increased shape of the isotherm with increasing the concentration of equilibrium confirms that the arrangement of the particles on the surface in vertical rows by hydrogen bonding^[115].

The dyes adsorption data were treated according to the following linear formula of the following logarithmic Freundlich equation:-

$$\text{Log } Q_e = \text{Log } K_f + 1 / n \text{ Log } C_e \dots\dots\dots(1-3).$$

C_e : Concentration of the adsorbate at equilibrium (mg/L).

Q_e : Quantity of the adsorbate material at equilibrium (mg/g).

Chapter Three - Results & Discussion

K_f , n : are isotherm constants indicate the capacity and intensity of adsorption respectively.

Tables (3-6),(3-7) and (3-8) and figures (3- 12), (3-13) and (3-14) show the extent to which the adsorption of Reactive Yellow145, Orange-G and Disperse Red 1 correspond to the Freundlich equation, and when drawing the relationship between $\text{Log } Q_e$ versus $\text{Log } C_e$ we get straight lines as shown in table (3-6),(3-7) and (3-8), and figures (3-12), (3-13) and(3-14) for all the dyes .

Table (3-3): adsorption of Reactive Yellow145 on the surface of the graft co-polymer nanoparticle at a temperature of 298K.

Temp	Con.(ppm)	C_e (mg/L)	Q_e (mg/g)
298K	1	0.0638	1.1702
	3	0.1702	3.5372
	5	0.2234	5.9707
	7	0.2765	8.4043

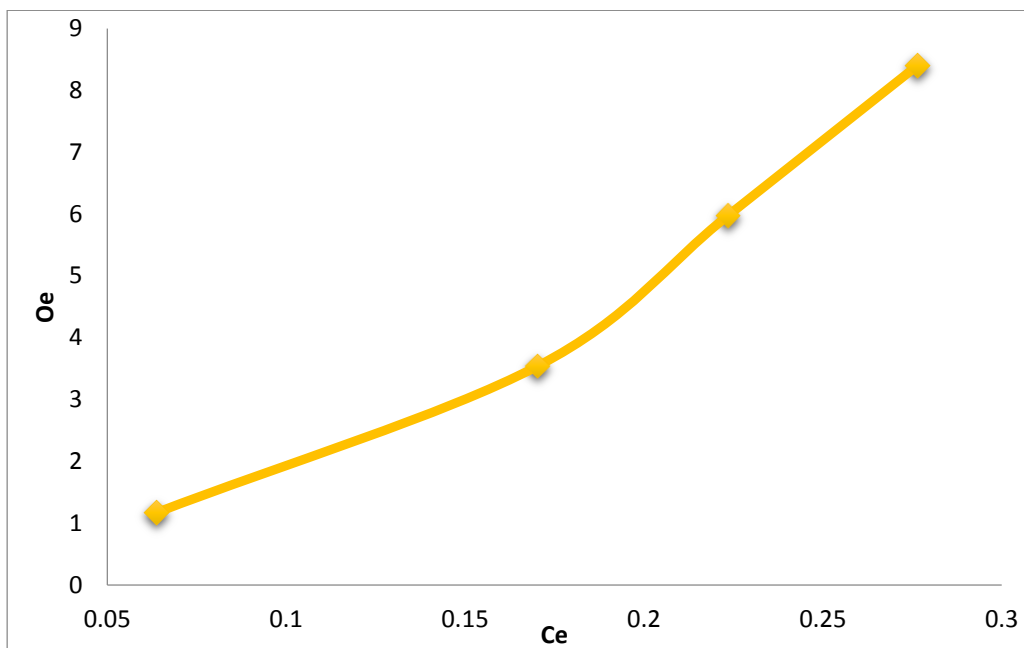


Figure (3-9): Adsorption isotherm Reactive Yellow145 dye on the surface of graft co-polymer.

Table (3-4): Adsorption of Orange-G dye on the surface of graft co-polymer nano particle at 298K.

Temp	Con.(ppm)	C_e (mg/L)	Q_e (mg/g)
298K	1	0.2641	0.7359
	3	0.6415	2.3585
	5	0.8301	4.1699
	7	0.9559	6.0441

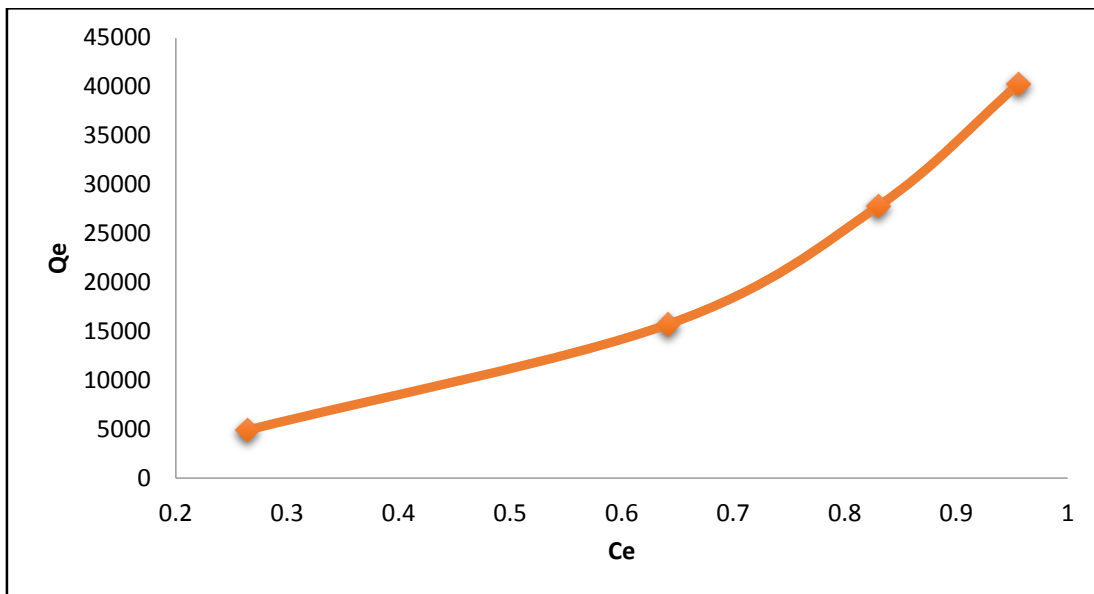


Figure (3-10): Adsorption isotherm Orange-G dye on the surface of graft copolymer.

Table (3-5): Adsorption of Disperse Red 1 dye on the surface of nano copolymer at 298K.

Temp	Con.(ppm)	C _e (mg/L)	Q _e (mg/g)
298K	1	0.25	1.125
	3	0.6554	3.5169
	5	0.8581	6.2128
	7	0.9932	9.0102

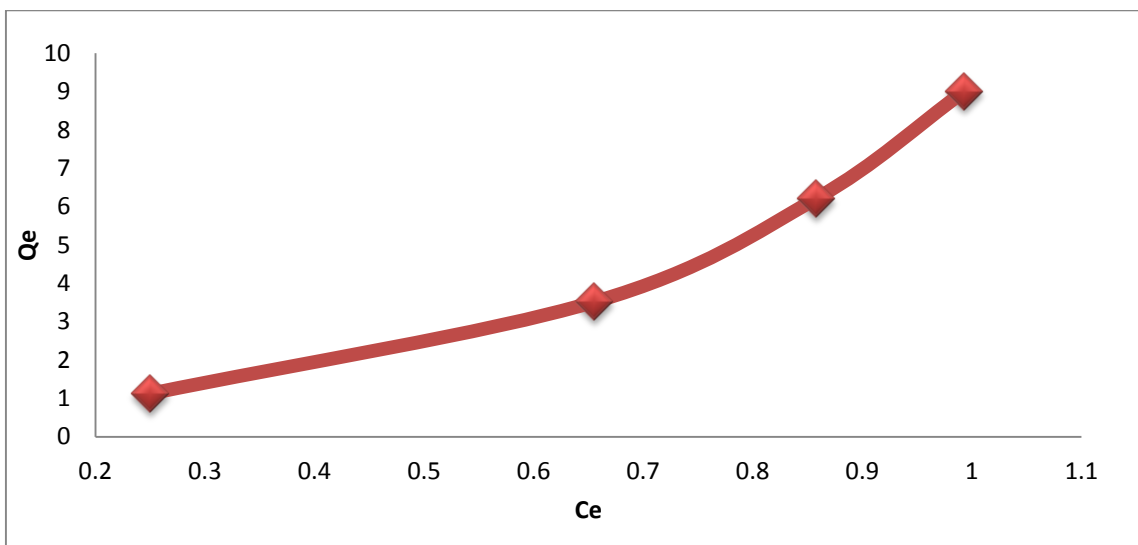


Figure (3-11): Adsorption isotherm Disperse Red 1 dye on the surface of graft copolymer

Table (3-6): Adsorption of Reactive Yellow145 dye on the surface of graft copolymer nanoparticle at 298K, 308K and 318K (by applying Freundlich equation).

T Conc (.ppm)	298K		308K		318K	
	-LogCe	LogQe	-LogCe	LogQe	-LogCe	Log Qe
1	1.1951	0.0682	0.769	0.0158	0.5583	-0.00436
3	0.769	0.5486	0.3604	0.5058	0.1536	0.4582
5	0.6509	0.776	0.2249	0.7407	0.0646	0.7137
7	0.5583	0.9245	0.1878	0.8997	0.0141	0.8773

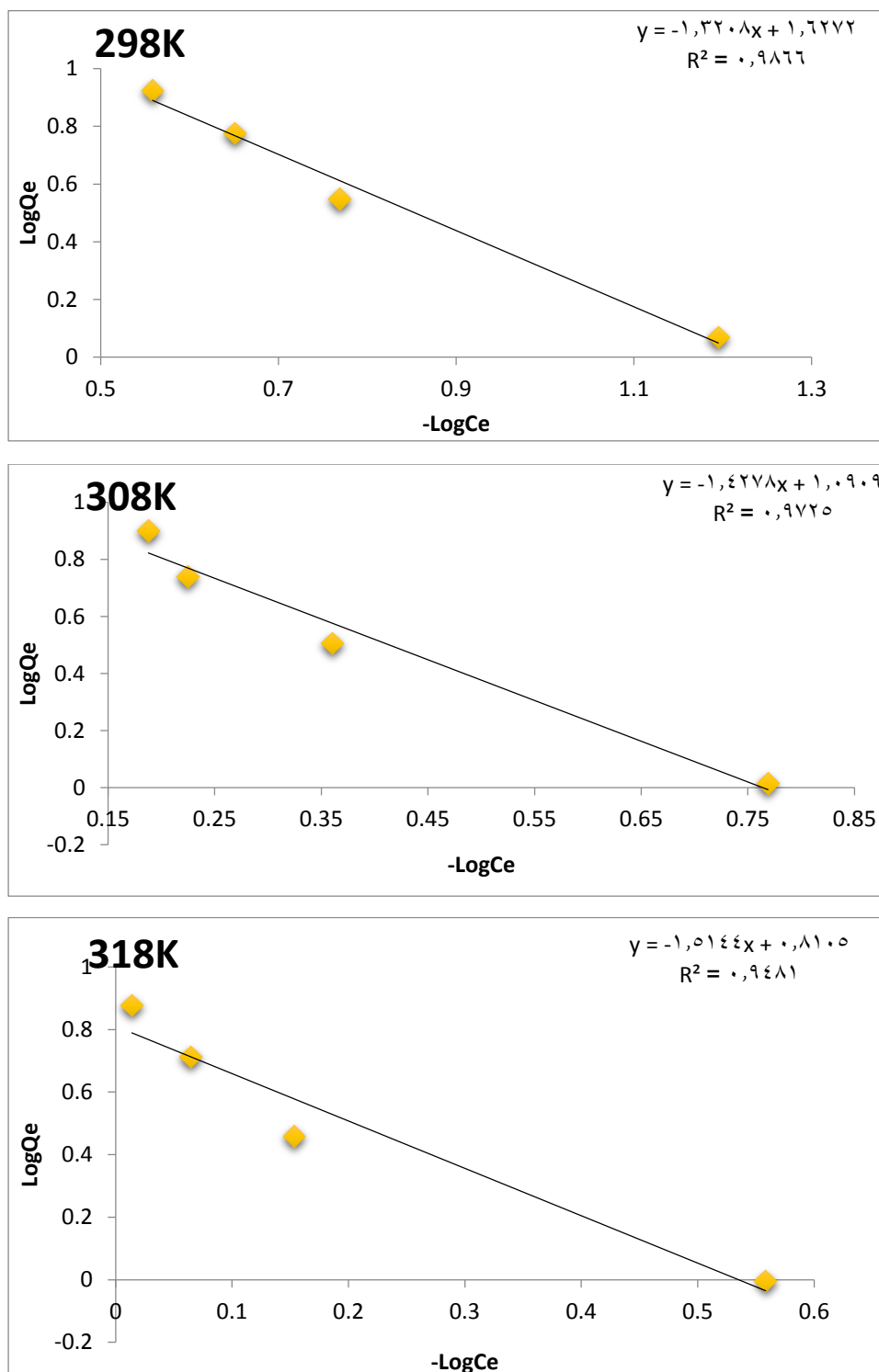


Figure (3-12): Apply Freundlich equation on adsorption of Reactive Yellow145 dye on the surface of graft co-polymer at 298K, 308K and318K.

Table (3-7): Adsorption of Orange-G dye on the surface of graft co-polymer nanoparticle at 298K, 308K and 318K (by applying Freundlich equation).

T Conc (ppm)	298K		308K		318K	
	-LogCe	LogQe	-LogCe	LogQe	-LogCe	LogQe
1	0.5782	-0.1331	0.8591	-0.0646	1.1226	-0.0344
3	0.1982	0.3726	0.409	0.4166	0.6963	0.4468
5	0.0808	0.6201	0.2876	0.6516	0.5782	0.6754
7	0.0195	0.78133	0.1928	0.8033	0.4854	0.8243

Table (3-8): Adsorption Disperse Red 1 on the surface of graft co-polymer nanoparticle at 298K,308K and 318K (by applying Freundlich equation).

T Conc.(ppm)	298K		308K		318K	
	LogCe	LOgQe	LOgCe	LogQe	LogCe	LogQe
1	0.602	-0.2041	0.7389	-0.1388	0.94005	-0.0212
3	0.1834	0.3046	0.2838	0.3462	0.60205	0.4191
5	0.0664	0.5697	0.102	0.5814	0.4144	0.6456
7	0.0029	0.7411	0.0335	0.749	0.3441	0.8007

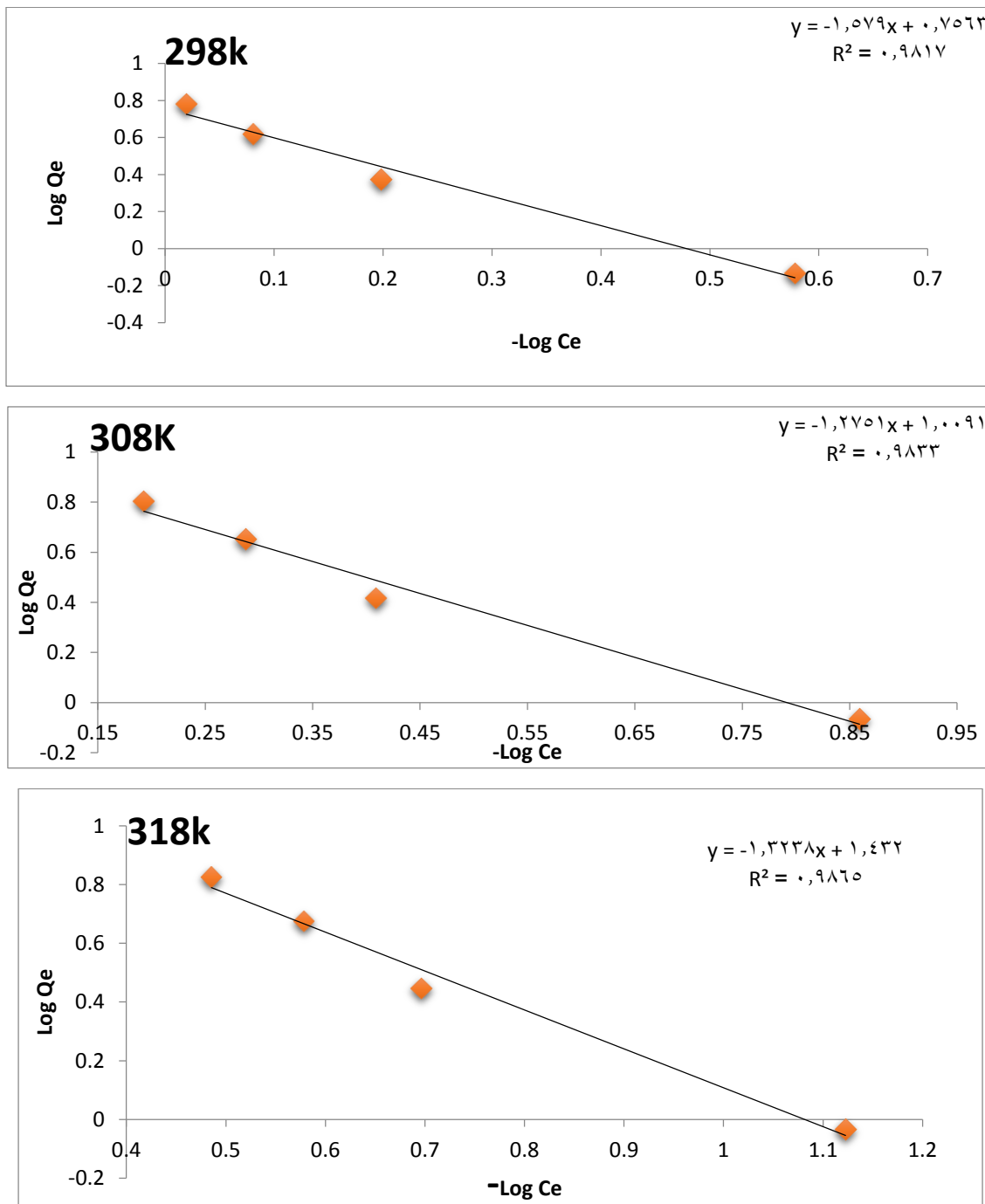


Figure (3-13): Apply Freundlich equation on adsorption of Orange-G dye on the surface of graft co-polymer at 298K, 308K and 318K.

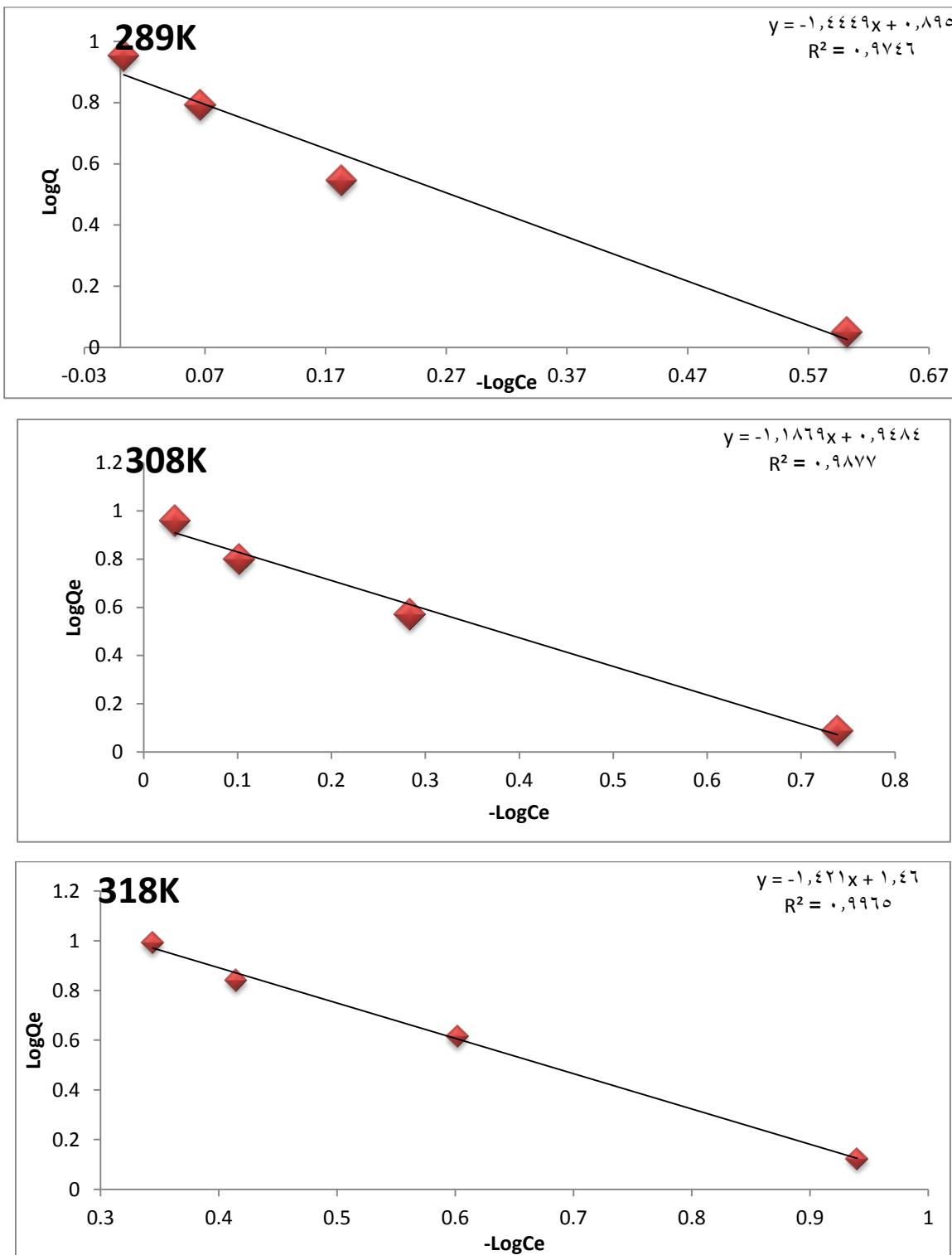


Figure (3-14): Apply Freundlich equation on adsorption of Disperse Red 1 dye on the surface of graft co-polymer nanoparticle at 298K,308K and 318K.

The adsorption data for Reactive Yellow145, Orange-G and Disperse Red 1 dyes were processed according to the linear relationship of the Langmuir equation as shown in table (3-9),(3-10) and (3-11) for all dyes respectively, and when drawing the relationship between (C_e / Q_e) versus C_e We obtain a linear relationship as shown in figure (3-15),(3-16) and (3-17) according to the following equation ^[116] .

$$C_e / Q_e = 1 / a b + (C_e / a) \dots\dots\dots(3-2).$$

where as:

Q_e : Adsorption capacity at equilibrium (mg / g).

C_e : Concentration of solute at equilibrium in units (mg / L).

a: Proportionality constant (is the theoretical maximum adsorption capacity(mg/g)).

b: Langmuir adsorption constant (L /mg)

Table (3-9): Adsorption of Reactive Yellow145 dye on the surface of graft co-polymer nanoparticle at 298K,308K and 318K (by applying Langmuir equation).

T Conc ppm	298K		T308K		T318K	
	Ce	Ce/Qe	Ce	Ce/Qe	Ce	Ce/Qe
1	0.0638	0.0545	0.1702	0.164	0.2765	0.3057
3	0.1702	0.0481	0.4361	0.136	0.7021	0.2444
5	0.2234	0.0374	0.5951	0.108	0.8617	0.1665
7	0.2765	0.0328	0.6489	0.0817	0.968	0.1283

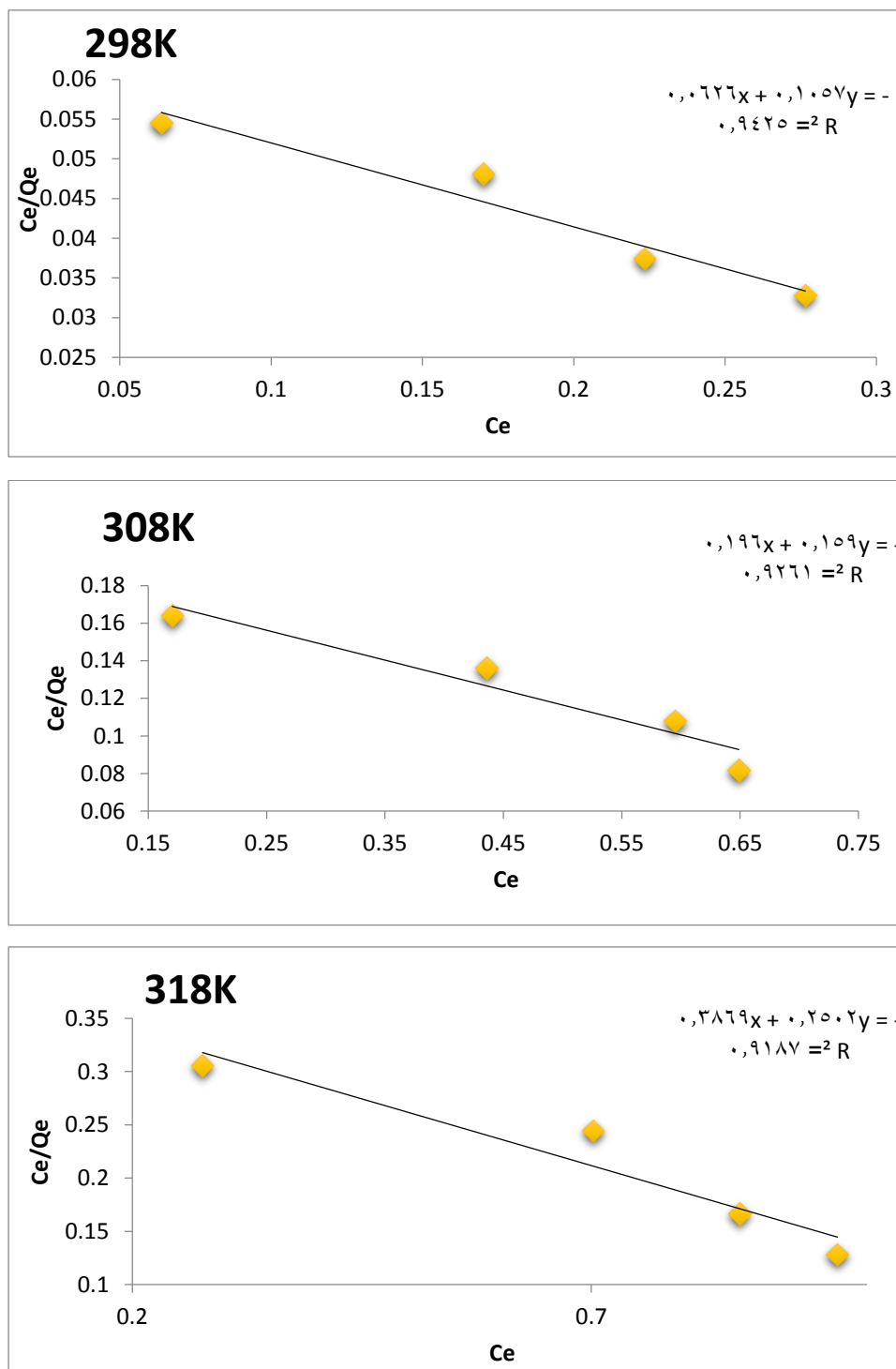


Figure (3-15): Apply Langmuir equation on adsorption of Reactive Yellow145 dye on the surface of graft co-polymer nanoparticle at 298k,308k and 318K

Chapter Three - Results & Discussion

Table (3-10): Adsorption of Orange-G dye on the surface of graft co-polymer nanoparticle at 298K, 308K and 318K (by applying Langmuir equation).

T Conc ppm	298K		308K		318K	
	Ce	Ce/Qe	Ce	Ce/Qe	Ce	Ce/Qe
1	0.2641	0.3588	0.1383	0.1604	0.0754	0.0815
3	0.6415	0.2719	0.3899	0.1493	0.2012	0.0718
5	0.8301	0.1990	0.5157	0.115	0.2641	0.0557
7	0.9559	0.1581	0.6415	0.1008	0.327	0.0490

Table (3-11): Adsorption of Disperse Red 1 dye on the surface of graft co-polymer at 298K, 308K and 318K (by applying Langmuir equation).

T Conc. ppm	298K		308K		318K	
	Ce	Ce/Qe	Ce	Ce/Qe	Ce	Ce/Qe
1	0.25	0.2222	0.1824	0.1487	0.1148	0.0864
3	0.6554	0.1863	0.5202	0.13998	0.25	0.0606
5	0.8581	0.1381	0.7905	0.1251	0.3851	0.0556
7	0.9932	0.1102	0.9256	0.1015	0.4527	0.046

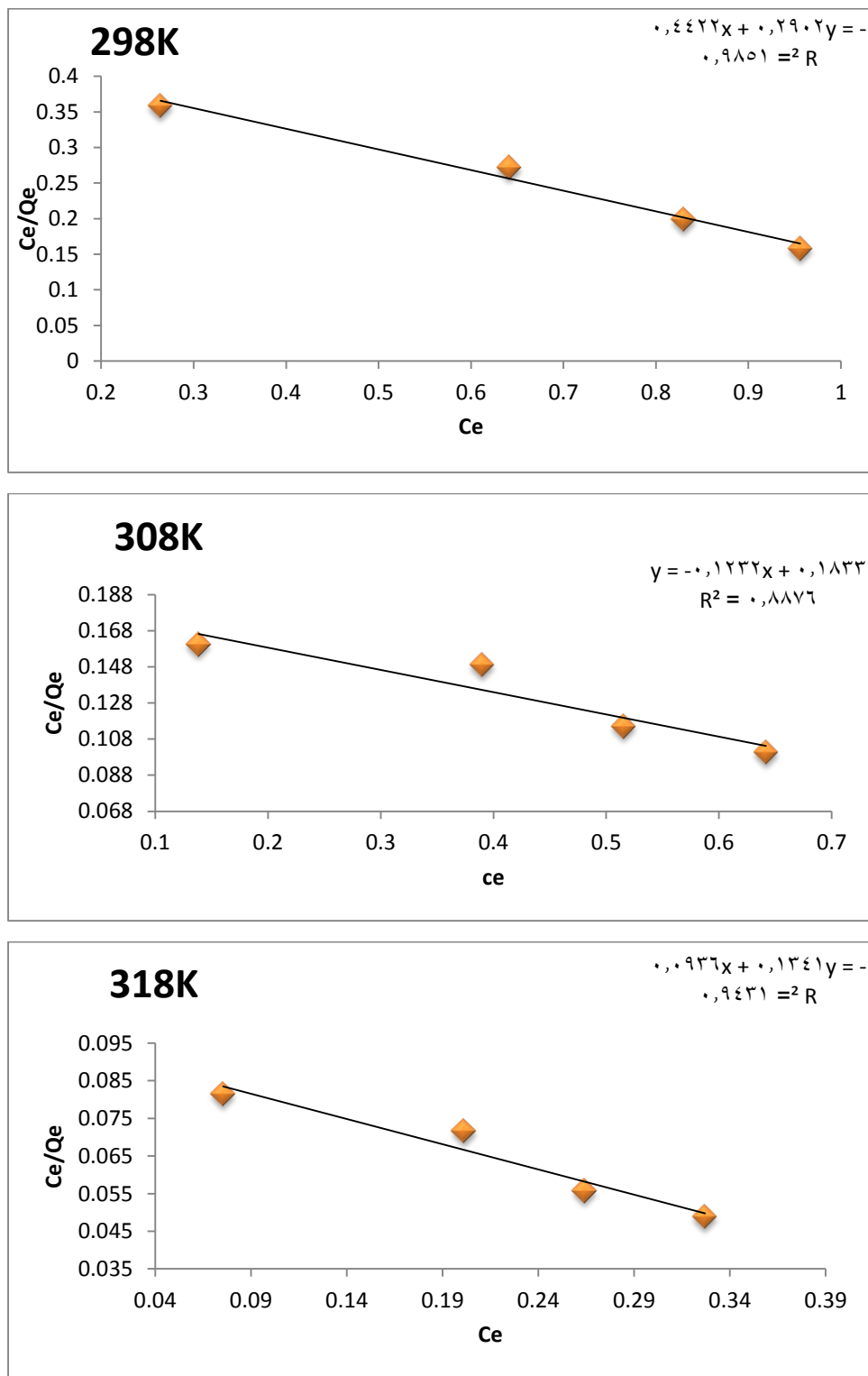


Figure (3-16): Apply Langmuir equation on adsorption of Orange-G dye on the surface of graft co-polymer nanoparticle at 298K,308K and 318K.

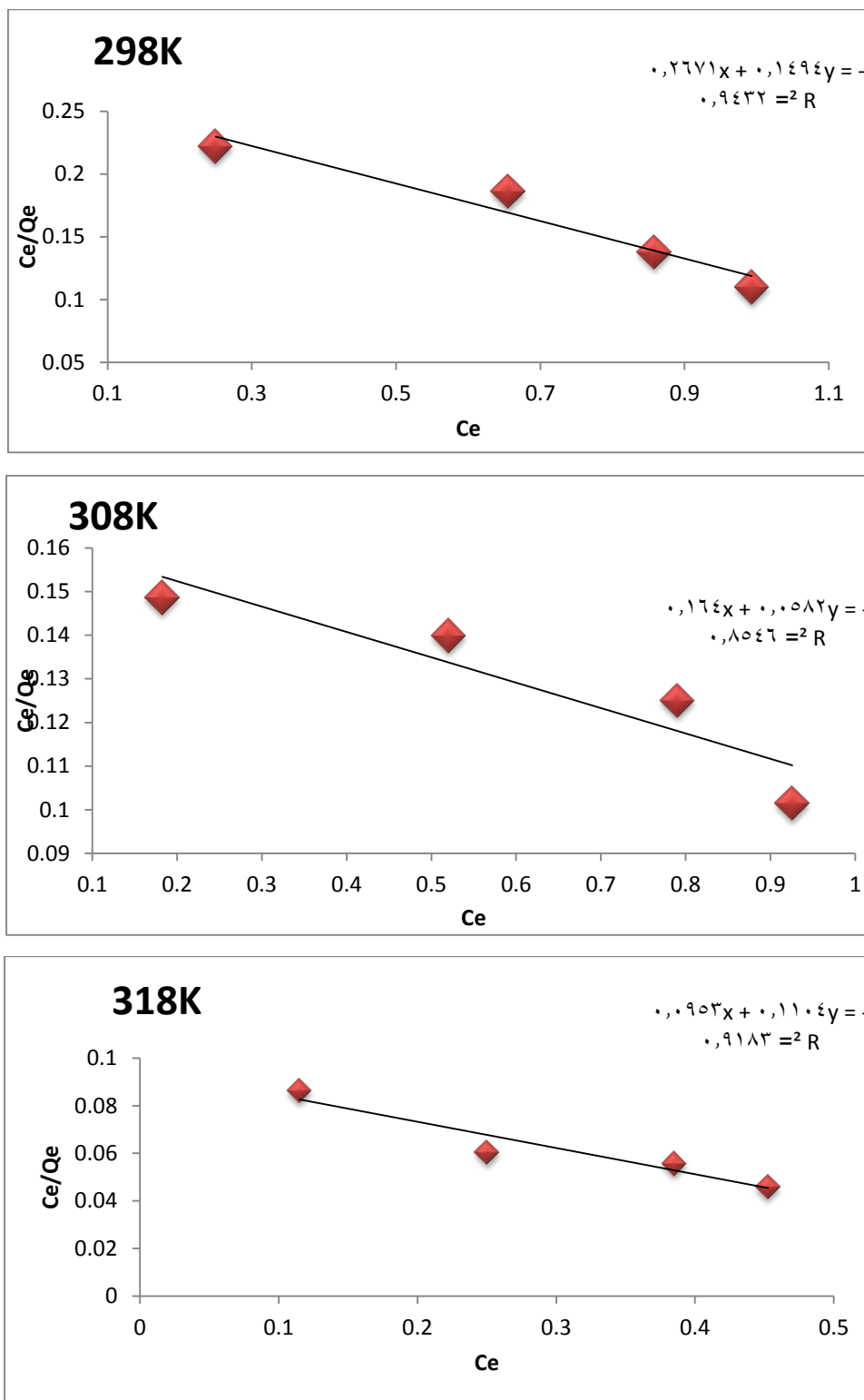


Figure (3-17): Apply Langmuir equation on adsorption of Disperse Red 1 dye on the surface of graft co-polymer at 298K, 308K and 318K

The adsorption data for Reactive Yellow145, Orange-G and Disperse Red 1 dyes were processed according to the linear relationship of the equation Temkin as shown in table (3-12),(3-13) and (3-14) for all dyes respectively and when drawing the relationship between (Q_e) values versus ($\ln C_e$) We obtain a linear relationship as shown in figure (3-18),(3-19) and(3-20) according to the following equation ^[117]
 $Q_e = B \ln A_T + B \ln C_e \dots \dots \dots (3-3).$

Q_e : Adsorption capacity at equilibrium (mg / g).

C_e : Concentration of solute at equilibrium in units (mg / L).

(A_T, B) are Temkin constants: A_T indicate equilibrium binding constant that corresponding to the maximum binding energy, while (B) is related to the heat of sorption.

Table (3-12): Adsorption of Reactive Yellow145 dye on the surface of graft co-polymer nanoparticle at 298K, 308K and 318K (by applying Temkin equation).

T Conc PPm	298K		308K		318K	
	-LnCe	Qe	-LnCe	Qe	-LnCe	Qe
1	2.752	1.1702	1.7707	1.0372	1.2855	0.9043
3	1.7707	3.5372	0.8298	3.2048	0.3536	2.8723
5	1.4987	5.9707	0.518	5.5053	0.1488	5.1728
7	1.2855	8.4043	0.4324	7.9388	0.0325	7.54

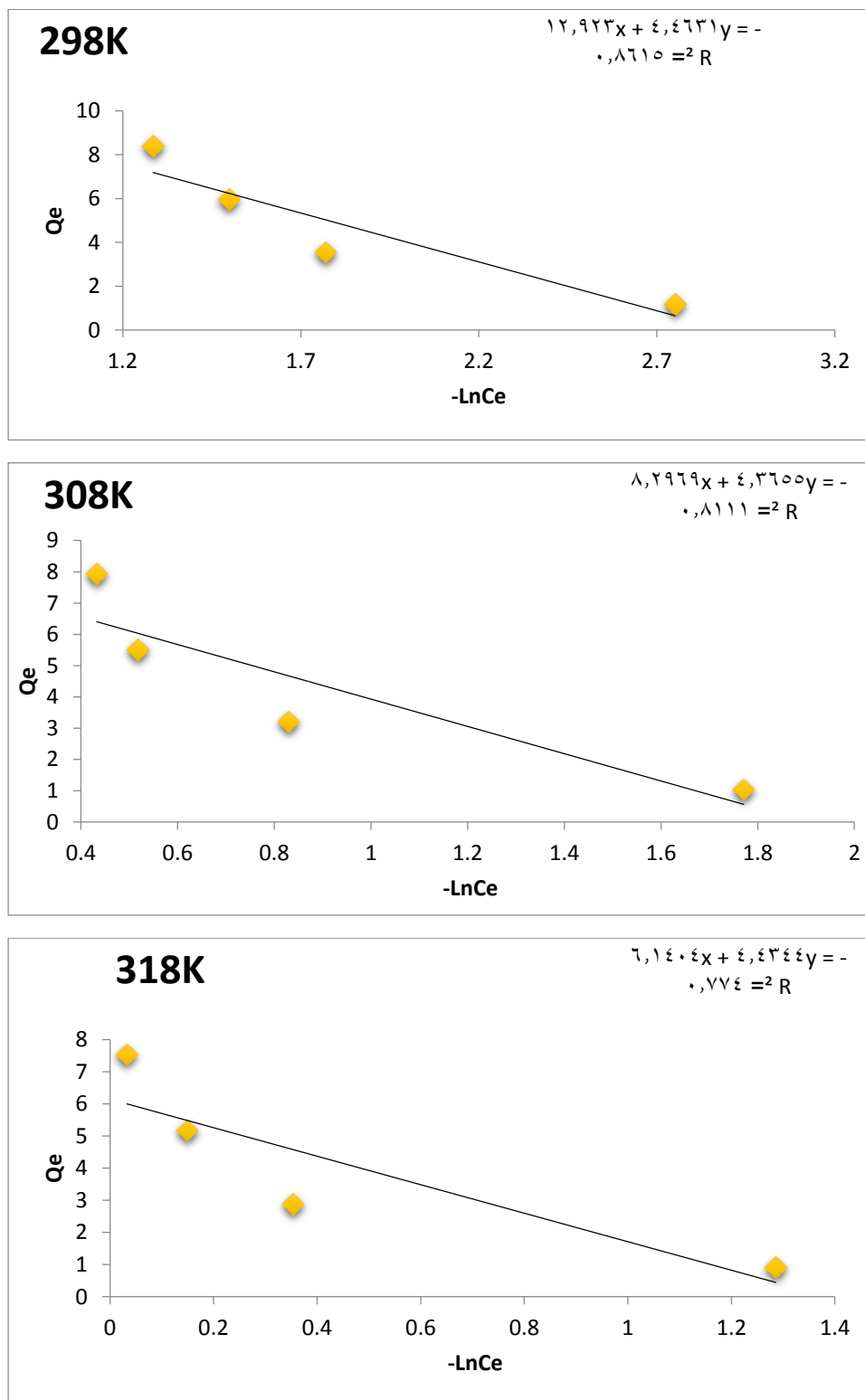


Figure (3-18): Apply Temkin equation on adsorption of Reactive Yellow145 dye on the surface of graft co-polymer nanoparticle at 298K, 308K and 318K.

Chapter Three - Results & Discussion

Table (3-13): Adsorption of Orange-G dye on surface of graft co-polymer nanoparticle at 298K, 308K and 318K (by applying Temkin equation).

T Conc. ppm	298K		308K		318K	
	-LnCe	Qe	-LnCe	Qe	-LnCe	Qe
1	1.3314	0.7359	1.9783	0.8617	2.5849	0.9246
3	0.4439	2.3585	0.9418	2.6101	1.6034	2.7988
5	0.1862	4.1699	0.6622	4.4843	1.3314	4.4834
7	0.0451	6.0441	0.4439	6.3585	1.1177	6.673

Table (3-14): Adsorption of Disperse Red 1 dye on the surface of graft co-polymer nanoparticle at 298K,308K and 318K (by applying Temkin equation).

T Conc. ppm	298K		308K		318K	
	-LnCe	Qe	-LnCe	Qe	-LnCe	Qe
1	1.3862	1.125	1.7015	1.2264	2.164	1.3278
3	0.4225	3.5169	0.6535	3.7197	1.3862	4.125
5	0.153	6.2128	0.2350	6.3142	0.9542	6.9223
7	0.0068	9.0102	0.0773	9.1116	0.7925	9.8209

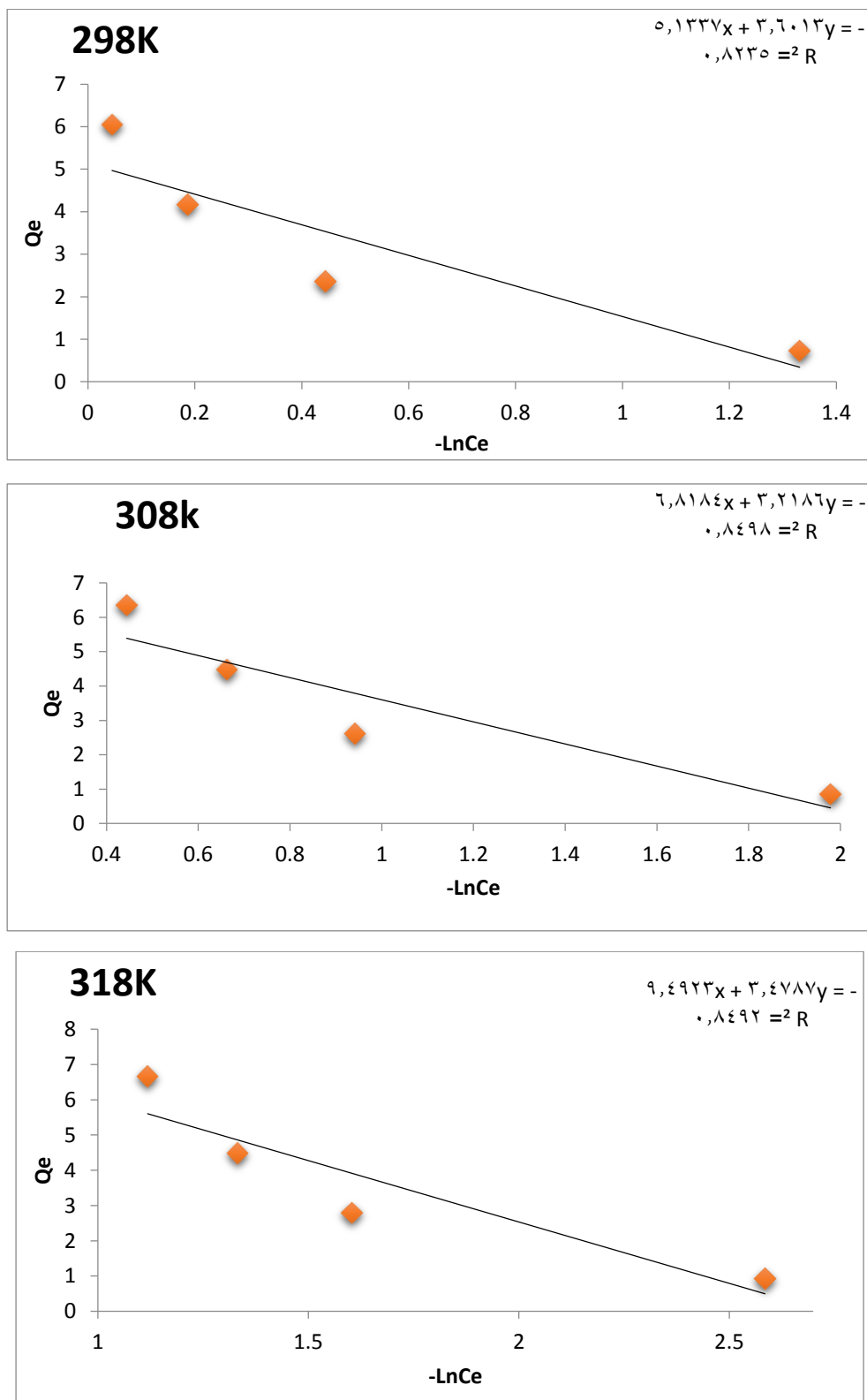


Figure (3-19): Apply Temkin equation on adsorption of Orange-G dye on the surface of graft co-polymer nanoparticle at 298K,308K and 318K.

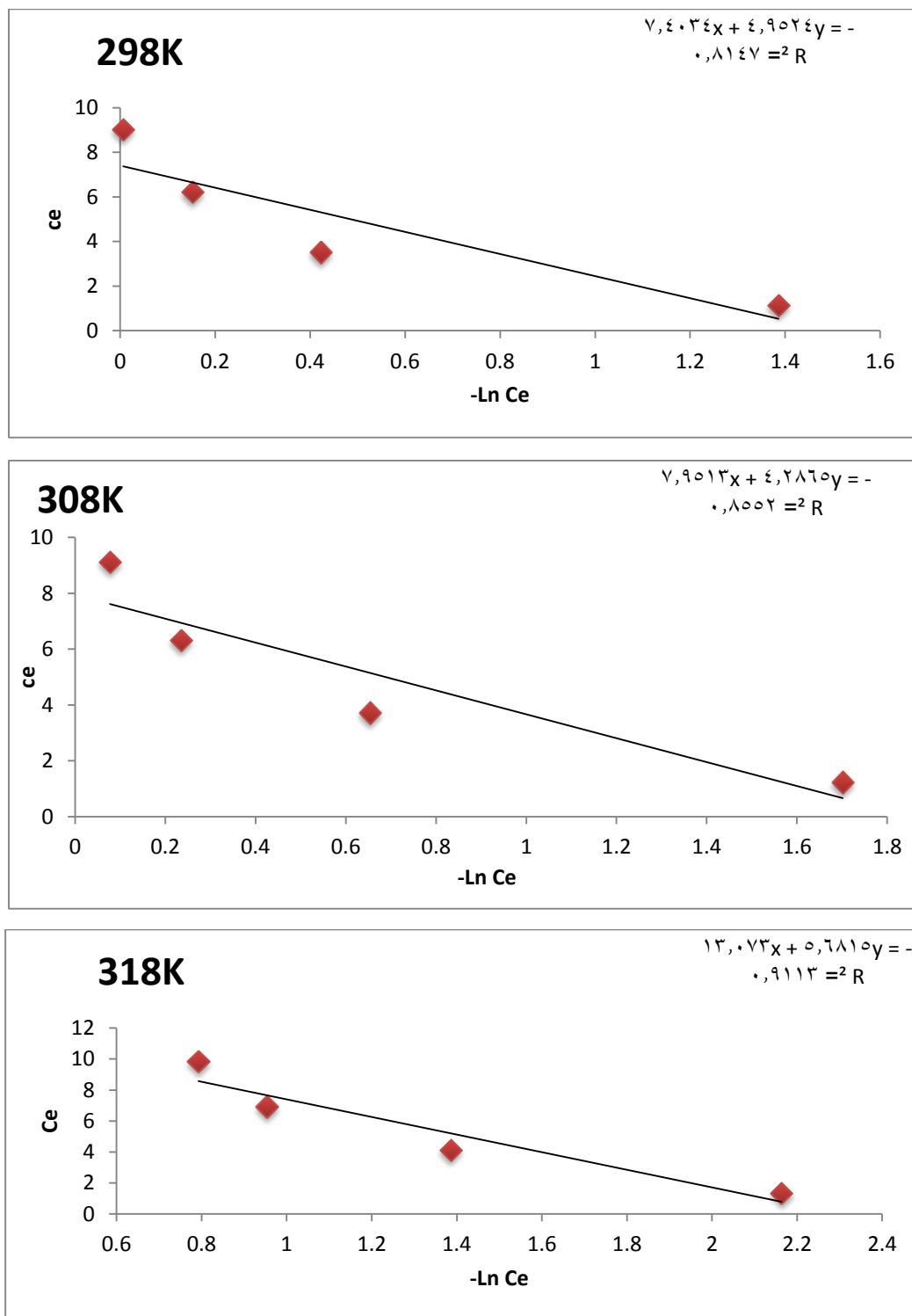


Figure (3-20): Apply Temkin equation on adsorption of Disperse Red 1 dye on the surface of graft co-polymer nanoparticle at 298K, 308 K and 318K.

The experimental Freundlich, Langmuir and Temkin constants and the correlation coefficient were calculated from the data of these lines for Reactive Yellow145, Orange-G and Disperse Red 1 Table (3-15). Table (3-15): shows the values of the Freundlich, Langmuir and Temkin constants via the adsorption of Reactive Yellow145, Orange-G and Disperse Red 1 dye on the surface of the graft co-polymer nanoparticle.

Table (3-15) shows that the values of (Slope), the correlation coefficient from the previous practical results that the Freundlich equation is more applicable than the Temkin and Lankmeyer equation on the adsorption process of Reactive Yellow145, Orange-G and Disperse Red 1 dyes due to the best apparent linear fit of the Freundlich isotherm in the previous figures. that the values of the constant K_f in the Freundlich equation are an approximate indicator of adsorption capacity, and n indicates the intensity of adsorption The greater it is, the more preferred it is in adsorption which are constants that include all the factors affecting the adsorption process.

The values of the constant, a of the Langmuir equation, represent a constant related to the maximum adsorption capacity, and the higher the value of the adsorption capacity the better. The values of the constant b are related to the adsorption energy. (A_T, B) are Temkin constants: A_T indicate equilibrium binding constant that corresponding to the maximum binding energy, while (B) is related to the heat of sorption.

Chapter Three - Results & Discussion

Table (3-15): The values of the Freundlich, Langmuir and Temkin constants via the adsorption of Reactive Yellow145, Orange-G and Disperse Red 1 dye on the surface of the nano graft co-polymer.

Disperse Red 1 dye				Orange-G dye			Reactive Yellow145dye		
Friendiash Transaction									
T(K)	-N	K _f	R ²	-N	K _f	R ²	-N	K _f	R ²
298	0.7571	282553.0502	0.9856	0.6332	38036.4520	0.9817	0.6920	52347.9887	0.9746
308	0.7003	82186.4080	0.9725	0.7841	68092.6129	0.9833	0.8425	59197.0411	0.9877
318	0.6282	43641.5332	0.9574	0.7556	180135.7865	0.9865	0.7037	192264.8972	0.9965
Langmuir Transaction									
T(K)	-a	-b	R ²	-a	-b	R ²	-a	-b	R ²
298	0.0632	-1.6849	0.799	-0.2297	-0.6562	0.9851	-0.4463	-0.55991	0.9431
308	0.4194	-0.8108	0.894	-0.5409	-0.6721	0.8875	-1.1481	-0.3541	0.8555
318	0.2664	-0.6467	0.860	-0.4966	-1.4332	0.9427	-0.6042	-1.1570	0.9175
Temkin Transaction									
T (K)	-B	A _T	R ²	-B	A _T	R ²	-B	-A _T	R ²
298	0.3453	3.3608	0.808	0.7015	4.1652	0.8235	0.6689	3.0288	0.8147
308	0.5261	3.4360	0.913	0.4720	4.6604	0.8498	0.5391	3.4993	0.8552
318	0.7221	3.3827	0.896	0.3667	4.2320	0.8608	0.4346	2.6401	0.9113

3.4 Effect of Temperature on Adsorption on the Surface of Nano Co-polymer

The effect of temperature on adsorption of Reactive Yellow145, Orange-G and Disperse Red 1 dye on the surface of the graft co-polymer was studied, and within the experimental heat range (298,308 and 318 K), as shown in Tables (3-16) to (3-18) and Figures (3-21) to(3-23) for Reactive Yellow145, Orange-G and Disperse Red 1 dyes respectively, which show adsorption isotherms assigned at these temperatures. The experimental results indicated that the adsorption of Orange-G and Disperse Red 1dye on the surface of the graft co-polymer increases with increasing temperature, i.e. the endothermic process within the experimental thermal range (298,308 and 318 K) ^[118]. Any occurrence of chemical adsorption (needs high temperatures). The adsorption of the Reactive Yellow145 dye results on the surface of the graft co-polymer nanoparticle showed that it decreased with increasing temperature, meaning that the process is of the exothermic process ^[119]. Any physical adsorption (need slow temperatures).

Table (3-16): Effect of temperature on adsorption of Reactive Yellow145 dye.

T Conc. (ppm)	298K		308K		318K	
	Ce mg/L	Qe mg/g	Ce mg/L	Qe mg/g	Ce mg/L	Qe mg/g
1	0.0638	1.1702	0.1702	1.0372	0.2765	0.9043
3	0.1702	3.5372	0.4361	3.2048	0.7021	2.8723
5	0.2234	5.9707	0.5957	5.5053	0.8617	5.1728
7	0.2765	8.4043	0.6489	7.9388	0.968	7.545

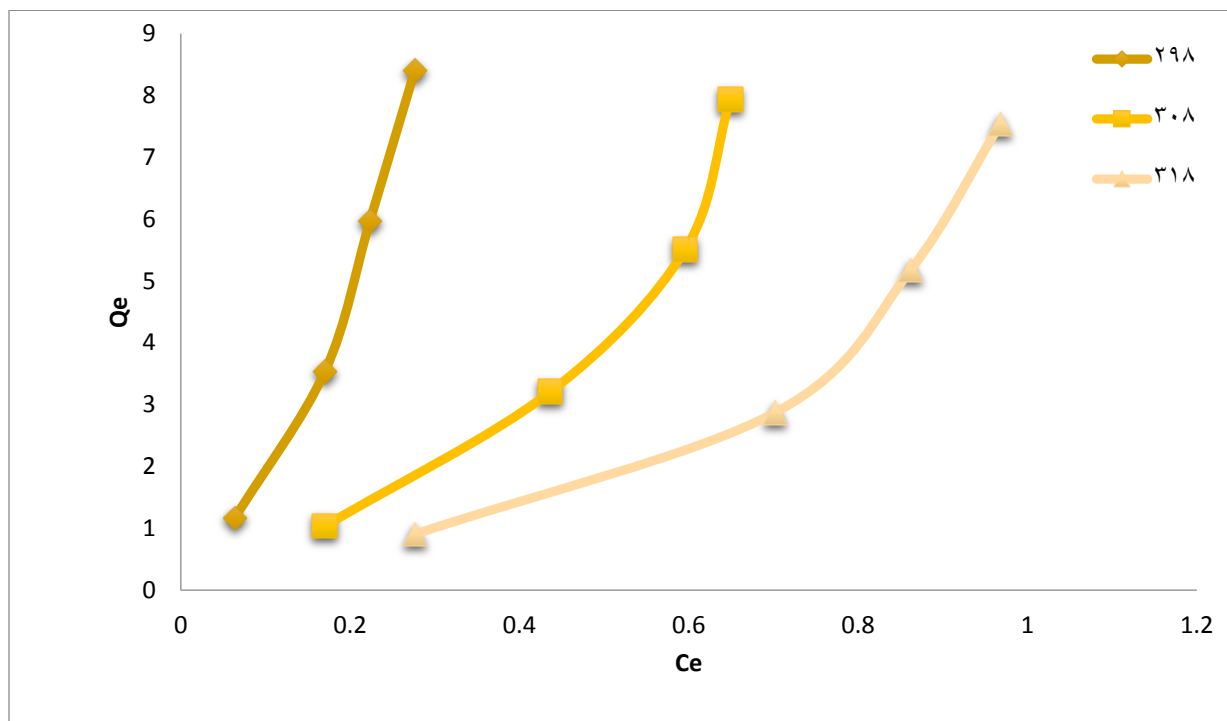


Figure (3-21): Effect of temperature on adsorption of graft co-polymer at (1, 3, 5 and 7 ppm) of Reactive Yellow 145 dye.

Table (3-17): Effect of temperature on adsorption of Orange-G.

T \ Conc. (ppm)	298K		308K		318K	
	Ce mg/L	Qe mg/g	Ce mg/L	Qe mg/g	Ce mg/L	Qe mg/g
1	0.2641	0.7359	0.1383	0.8617	0.0754	0.9246
3	0.6415	2.3585	0.3899	2.6101	0.2012	2.7988
5	0.8301	4.1699	0.5157	4.4843	0.2641	4.4834
7	0.9559	6.0441	0.6415	6.3585	0.327	6.673

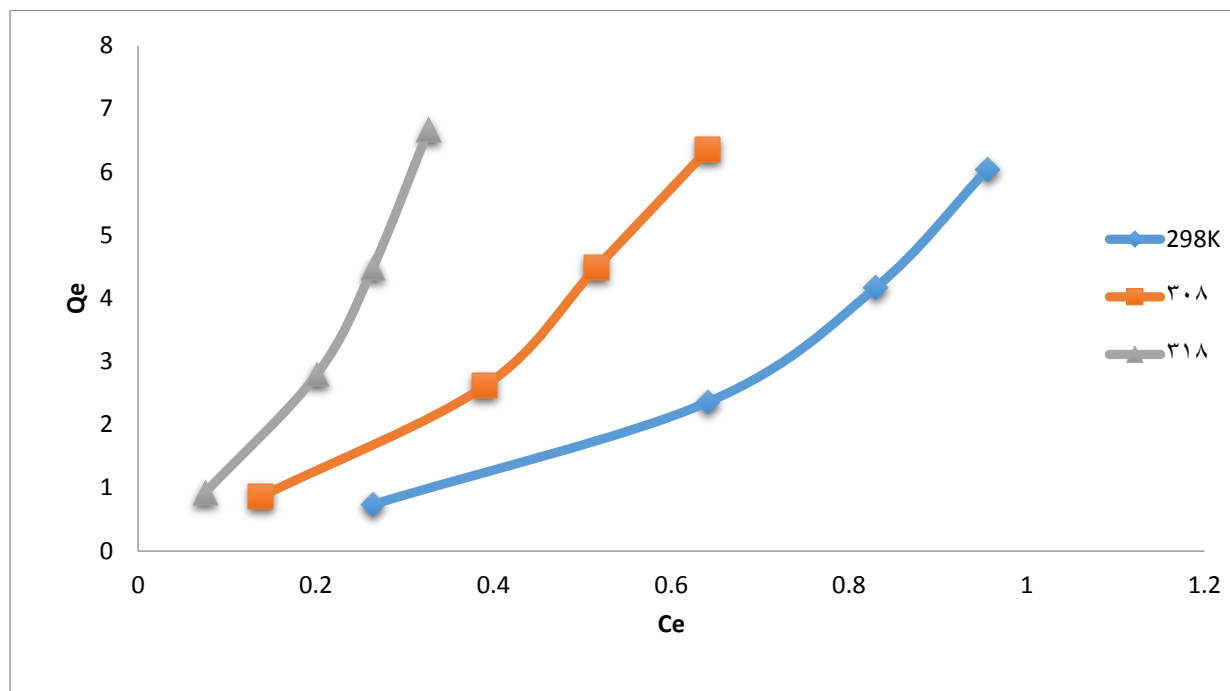


Figure (3-22): Effect of temperature on adsorption of graft co-polymer at (1, 3, 5 and 7ppm) of Orange-G.dye .

Table (3-18): Effect of temperature on adsorption of Disperse Red 1 dye.

T Conc (ppm)	298K		308K		318K	
	Ce mg/L	Qe mg/g	Ce mg/L	Qe mg/g	Ce mg/L	Qe mg/g
1	0.2500	1.1250	0.1824	1.2264	0.11486	1.3278
3	0.6554	3.5169	0.5202	3.7197	0.25	4.125
5	0.8581	6.2128	0.7905	6.3142	0.3851	6.9223
7	0.9932	9.0102	0.9256	9.1116	0.4527	9.8209

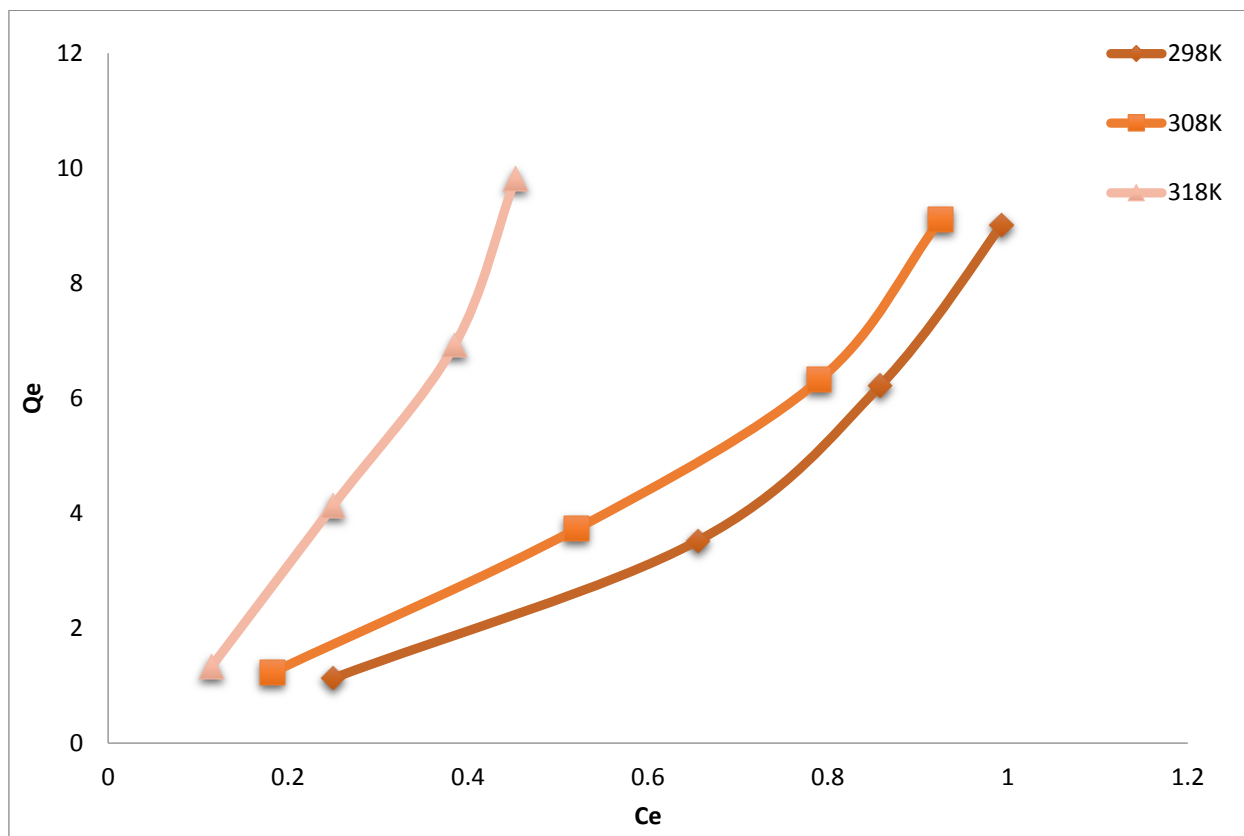


Figure (3-23): Effect of temperature on adsorption of graft co-polymer at (1, 3 ,5 and 7ppm) of Disperse Red 1 dye.

The results showed the percentage of removal of Orange-G and Disperse Red 1 dye by the effect of temperature, as it increases with increasing temperature, that is, the increase in temperature increases the amount of adsorbed material on the surface of the graft co-polymer, that is, the processes of adsorption and absorption occur, and thus this leads to an increase in the percentage of removal when the temperature is increased, as in Table (3-19) and (3-20) for Orange-G and Disperse Red 1 dye respectively.

As for the results of the percentage of Reactive Yellow145 removal, it decreased with increasing temperature, That is, by increasing the temperature, the amount of the adsorbate material on the surface of the graft co-polymer nanoparticle decreases, i.e. the occurrence of an desorption process on the

adsorbent surface when the temperature increases, that is, the speed of the particles diffusion on the surface of the graft co-polymer nanoparticle decreases, and therefore the percentage of removal will decrease when the temperature is increased, as shown in Table (3-21)

Table (3-19): The percentage of Orange-G removal due to the effect of temperature.

T(K)	Conc.(ppm)	Re%=$\frac{C_o - C_e}{C_o} \times 100\%$
298K	1	73.5900
	3	78.0000
	5	83.0000
	7	86.3400
308K	1	86.7700
	3	87.0000
	5	89.0000
	7	90.0000
318K	1	92.5400
	3	93.2900
	5	94.7100
	7	95.3200

Table (3-20): The percentage of Disperse Red 1 removal due to the effect of temperature.

T(K)	. Conc.(ppm)	Re%=$\frac{c_o - c_e}{c_o} \times 100\%$
298	1	75
	3	78.1533
	5	82.8380
	7	85.8114
308	1	81.7600
	3	82.6600
	5	84.1500
	7	86.7771
318	1	88.5140
	3	91.6666
	5	92.2980
	7	93.5328

Table (3-21): The percentage of Reactive Yellow145 removal due to the effect of temperature.

T(K)	Conc.(ppm)	Re%= $\frac{c_o - c_e}{c_o} \times 100\%$
298	1	93.6200
	3	94.3266
	5	95.5320
	7	96.0500
308	1	82.9800
	3	85.4633
	5	88.0860
	7	90.7300
318	1	72.3500
	3	76.5966
	5	82.7660
	7	86.1714

3-5 Calculation the Thermodynamic Values of ΔH , ΔS and ΔG .

The thermodynamic values represented by the values of ΔS , ΔG , ΔH , were calculated, where the value of ΔH was calculated by drawing the relationship between $\text{Log } X_m$ (versus the reciprocal of temperature $(1 / T)$ and its value is shown in Tables (3-24) to(3-26) for Reactive Yellow145, Orange-G and Disperse Red 1 dye on the surface of the nano graft co-polymer respectively, based on the Vant-Hoff-Arrhenius Equation ^[120].

$$\text{Log } X_m = (- \Delta H / 2.303RT) + \text{Constant} \dots\dots (3-1)$$

Where:

$\text{Log } X_m$: Logarithm of greatest adsorbed quantity (mg / g)

R: general constant for gases.(8.314 Jmol⁻¹)

T: temperature (K).

Cons. : Constant of the van der Hoff equation.

A linear relationship was obtained and from the slope of this relationship, as in figures (3-24), (3-25) and (3-26) the value of ΔH , was calculated, and the slope is equal to:

$$\text{Slope} = -\Delta H / 2.303R$$

The value of change in free energy (ΔG) was calculated from the following equation.

$$\Delta G = - R T \text{Ln} (Q_e / C_e) \dots\dots\dots (3-2)$$

When applying the Gibbs equation^[121], the values of the change are obtained by entropy) S (Δ whose value is listed in table ,(3-25) for the Reactive Yellow145, Orange-G and Disperse Red 1 dyes ,respectively, and the equation is:

$$\Delta G = \Delta H -T\Delta S \dots\dots\dots (3-3)$$

Chapter Three - Results & Discussion

Table (3-22): shows the values of $1 / T$, $\text{Log } X_m$ of Reactive Yellow145 on the surface of nano graft co-polymer within the experimental heat range (298,308 and 318 K)

Temp(K)	X_m (mg/g)	$1/T \times 10^{-3} \text{ K}^{-1}$	Log X_m
298	8.4043	3.3557	0.9245
308	7.9388	3.2467	0.8997
318	1.014	3.1446	0.8773

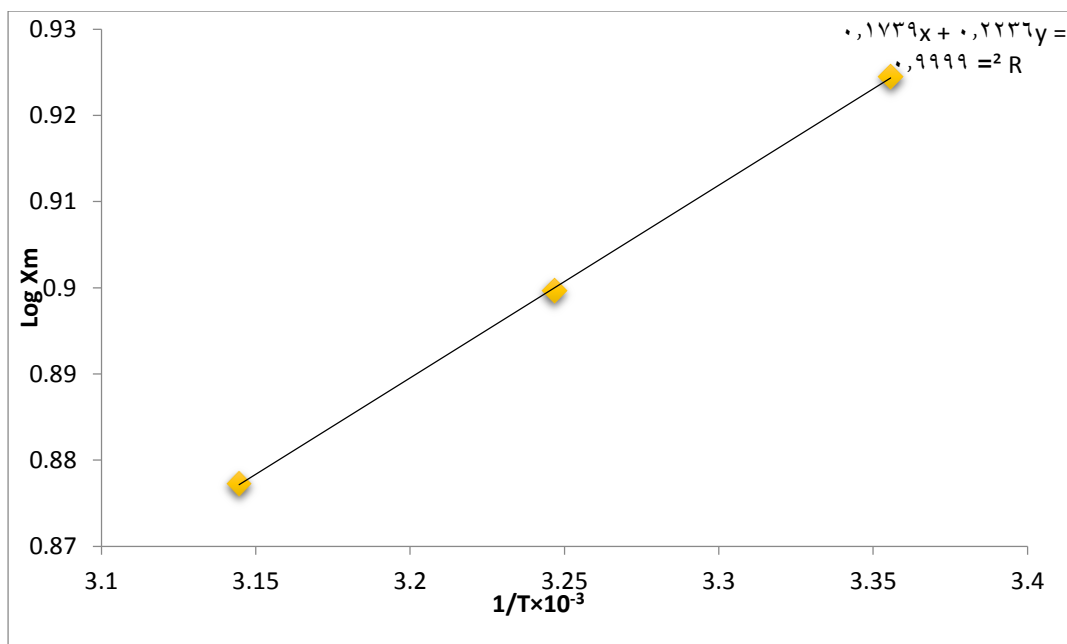


Figure (3-24): shows a graph between the logarithms of the highest value in the reciprocal of the temperature of the Reactive Yellow145 dye.

Table (3-23): shows the values of $1 / T$, $\text{Log } X_m$ of Orange-G on the surface of nano graft co-polymer nanoparticle within the experimental heat range (298,308 and 318 K).

T(K)	X_m(mg/g)	1/T×10⁻³ K⁻¹	LogX_m
298	6.0441	3.3557	0.78133
308	6.3585	3.2467	0.8033
318	6.673	3.1446	0.8243

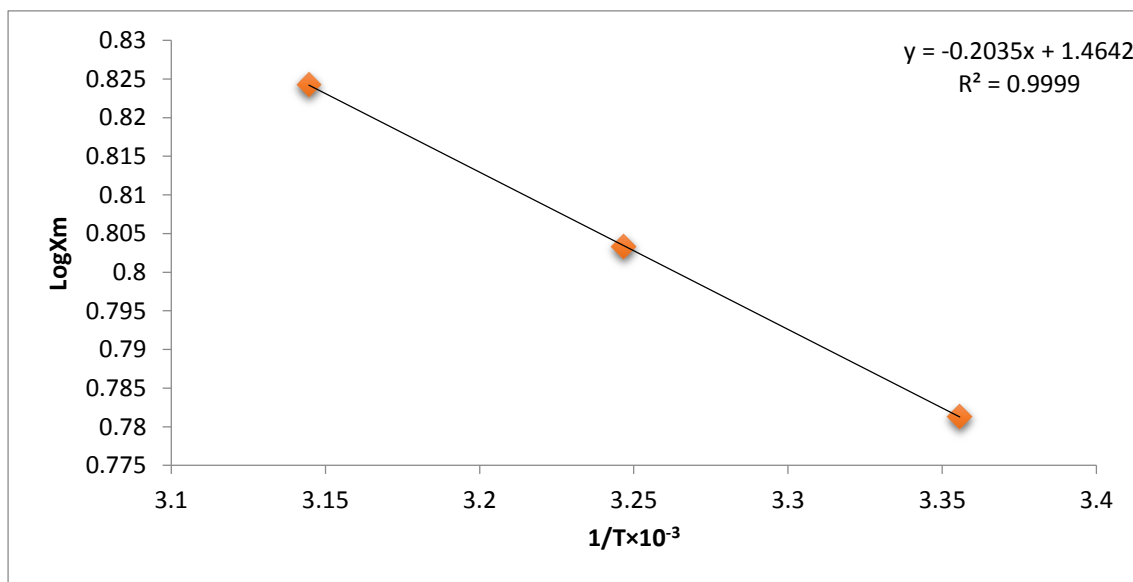


Figure (3-25): shows a graph between the logarithms of the highest value in the reciprocal of the temperature of the Orange-G dye.

Table (3-24): shows the values of $1 / T$ and $\text{Log } X_m$ of Disperse Red 1 on the surface of nano graft co-polymer within the experimental heat range (298,308 and 318K).

Temp(k)	X_m	$1/T \times 10^{-3} \text{ K}^{-1}$	$\text{Log } X_m$
298	9.0102	3.3557	0.9547
308	9.1116	3.2467	0.9595
318	9.8209	3.1446	0.9921

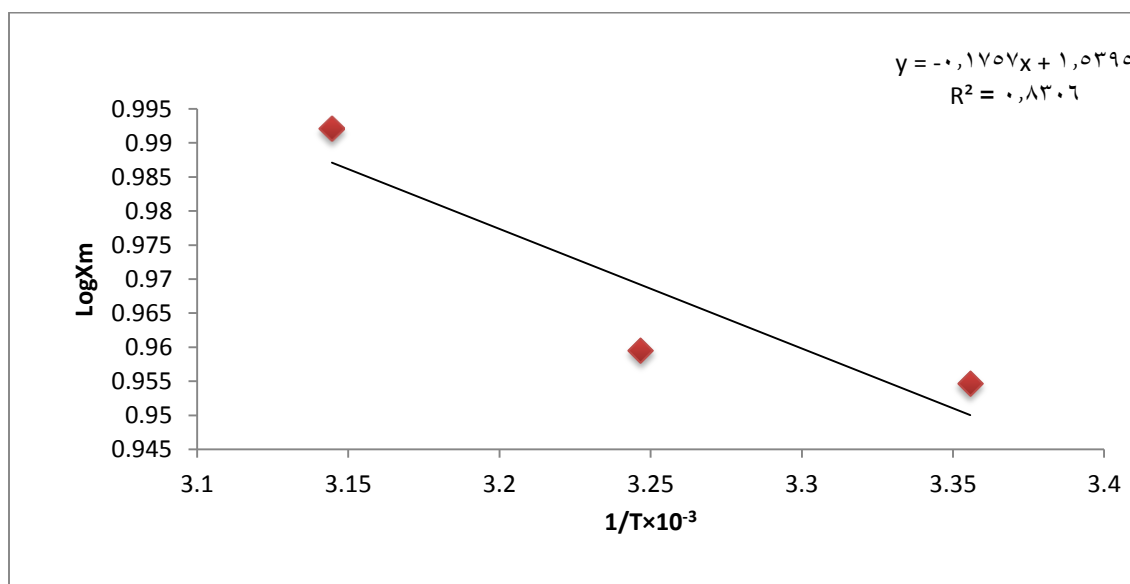


Figure (3-26) shows a graph between the logarithm of the highest value in the reciprocal of the temperature of the Disperse Red 1 dye.

Table (3-25): shows the values of the thermodynamic functions ΔH , ΔG , and ΔS to remove Reactive Yellow145, Orange-G and Disperse Red 1 dyes on the surface of the graft co-polymer at different temperature.

Dyes	T(K).	ΔH KJ /mol	ΔG KJ/mol	ΔS J/mol. K
Reactive Yellow145	298	-4.2813	-8.4591	14.0194
	308		-6.4125	6.9194
	318		5.4271	3.6031
Orang-G	298	3.9002	-4.5688	28.4194
	308		-5.8735	31.7327
	318		-7.9734	37.338
Disperse Red 1	298	3.3641	-5.4634	29.6224
	308		-5.8558	29.9350
	318		-8.1352	36.1613

The results of adsorption of both the Orange-G and dispersion red dye showed that the positive (ΔH) values mean that the adsorption on the surface of the nano co-polymer is an endothermic process [122]. It also indicates an increase in the interaction of the adsorbing molecules of the pollutants and the surface of the graft co-polymer nanoparticle with increasing temperature. While the Reactive

Chapter Three - Results & Discussion

Yellow145,dye results showed that the (ΔH) values are negative, this means that the adsorption on the surface of the nano co-polymer is a exothermic process ^[123].

The negative (ΔG) values indicate that the adsorption on the surface of the graft co-polymer nanoparticle is spontaneous, but if the values are positive, it indicates that the process is not spontaneous^[124].

As for the negative (ΔS) values, it indicates that the adsorbed particles are irregular on the adsorbent surface, as a result of their binding to the surface. Whereas if the values are positive, then it is an indication that the adsorbed molecules are less regular when adsorption and absorption processes occur^[125,126].

CONCLUSION

AND

FUTURE WORK

Conclusion

In this project the following points were concluded:

1-This grafted nano-copolymer produced by the reaction Terphthalic acid with Glycerol preparing a linear co-polymer as a first step b of Maleic anhydride was added to the resulting linear co-polymer solution to get the graft nano co-polymer characterized by techniques (FT-IR, 1H-NMR and AFM). The AFM results showed that the average particle size of the nano co-polymer is 74.39 nm, this proves that the prepared co-polymer is nano scale. prepared polymer is nanoscale. the presence of rigid aromatic rings, stemmed from the Terphthalic acid, lead to more rigid structures, which should be more prone to crystallize than fully aliphatic polymer. Molar proportion between Terphthalic acid ,Glycerol and Maleic anhydride used for the synthesis of polymer contributed to the formation of ramified polymer having carbonyl groups in relation to alcohol groups. Furthermore, a higher amount of Terphthalic acid indicated that the molecular motions, due to the rigidity of the aromatic rings should facilitate the packing of the polymer chains in crystalline lattices.

2- The adsorption of dyes (Reactive Yellow145 , Orange-G and dispersion red) were studied on a nano-copolymer by changing the temperature and by the constant pH of the solution. The results showed that the absorption of dyes (, Orange-G and dispersion red) increases with increasing temperature, while (Reactive Yellow145) decreases with increasing temperature

2. Future Work

We suggest the following:

- 1- Calculate the adsorption amount with other dyes using different polymers by other operations.
- 2- Use of nanoparticles polymers as drug delivery systems.
- 3- Use of other processes to remove pollutants from water, air and land.
- 4- Use other types of hydroxyl compounds to provide a greater number of points of connection with the carboxylic compounds

Reference

Reference

- [1] N. M. Aljamali, A. K. Thamer, and A. M. Sabea, "Review on electronic instruments and its nano-skill solicitations," *J. Electr. Power Syst. Eng.*, vol. 7, no. 3, pp. 11–19, 2021.
- [2] M. Sajid, "Nanomaterials: types, properties, synthesis, emerging materials, and toxicity concerns," *Curr. Opin. Environ. Sci. Heal.*, p. 100319, 2021.
- [3] A. K. Yetisen *et al.*, "Art on the Nanoscale and Beyond," *Adv. Mater.*, vol. 28, no. 9, pp. 1724–1742, 2016.
- [4] R. U. Ayres, "Extensions of the Body," in *The History and Future of Technology*, Springer, 2021, pp. 33–56.
- [6] S. Rayamajhi, "Engineering synthetic and natural vesicular system for tumor-targeted drug delivery." 2021.
- [5] T. Bertók, *Glyconanotechnology: Nanoscale Approach for Novel Glycan Analysis and Their Medical Use*. CRC Press, 2019.
- [7] G. D. Kalita, "Chapter-1 Nanotechnology," *Chem. Sci.*, vol. 1, p. 1, 2020.
- [8] L. H. Madkour, "Introduction to nanotechnology (NT) and nanomaterials (NMs)," in *Nanoelectronic Materials*, Springer, 2019, pp. 1–47.
- [9] S. E. Hunyadi Murph, "An Introduction to Nanotechnology," in *Anisotropic and Shape-Selective Nanomaterials*, Springer, 2017, pp. 3–5.
- [10] R. Foulkes, E. Man, J. Thind, S. Yeung, A. Joy, and C. Hoskins, "The regulation of nanomaterials and nanomedicines for clinical application: Current and future perspectives," *Biomater. Sci.*, vol. 8, no. 17, pp. 4653–4664, 2020.
- [11] V. Dave, S. Sur, and N. Gupta, "Current Framework, Ethical Consideration and Future Challenges of Regulatory Approach for Nano-Based Products," *Nanopharmaceutical Adv. Deliv. Syst.*, pp. 447–472, 2021.
- [12] M. Claville *et al.*, "NanoHU: A Boundary-Spanning Education Model for Maximizing Human and Intellectual Capital," *ACS Symp. Ser.*, vol. 1328, pp.

- 83–102, 2019, doi: 10.1021/bk-2019-1328.ch006.
- [13] K. Schwab and N. Davis, *Shaping the future of the fourth industrial revolution: A guide to building a better world*. Currency, 2018.
- [14] Y. Fang, G. Chen, M. Bick, and J. Chen, “Smart textiles for personalized thermoregulation,” *Chem. Soc. Rev.*, 2021.
- [15] E. L. Ayuk, M. O. Ugwu, and S. B. Aronimo, “A review on synthetic methods of nanostructured materials,” *Chem. Res. J.*, vol. 2, no. 5, pp. 97–123, 2017.
- [16] T. P. Yadav, R. M. Yadav, and D. P. Singh, “Mechanical milling: a top down approach for the synthesis of nanomaterials and nanocomposites,” *Nanosci. Nanotechnol.*, vol. 2, no. 3, pp. 22–48, 2012.
- [17] K. J. Klabunde and G. B. Sergeev, *Nanochemistry*. Newnes, 2013.
- [18] R. Keçili, S. Büyüktiryaki, and C. M. Hussain, “Advancement in bioanalytical science through nanotechnology: past, present and future,” *TrAC Trends Anal. Chem.*, vol. 110, pp. 259–276, 2019.
- [19] P. N. Sudha, K. Sangeetha, K. Vijayalakshmi, and A. Barhoum, “Nanomaterials history, classification, unique properties, production and market,” in *Emerging applications of nanoparticles and architecture nanostructures*, Elsevier, 2018, pp. 341–384.
- [20] C. J. Chirayil, J. Abraham, R. K. Mishra, S. C. George, and S. Thomas, “Instrumental techniques for the characterization of nanoparticles,” in *Thermal and Rheological Measurement Techniques for Nanomaterials Characterization*, Elsevier, 2017, pp. 1–36.
- [21] T. E. Twardowski, *Introduction to nanocomposite materials: properties, processing, characterization*. DEStech Publications, Inc, 2007.
- [22] D. K. Eric, “Engines of creation. The coming era of nanotechnology,” *Anchor B.*, 1986.
- [23] J. Paull and K. Lyons, “Nanotechnology: the next challenge for organics,” *J. Org. Syst.*, vol. 3, no. 1, pp. 3–22, 2008.
- [24] S. A. M. Ealia and M. P. Saravanakumar, “A review on the classification, characterisation, synthesis of nanoparticles and their application,” in *IOP*

- conference series: materials science and engineering, 2017, vol. 263, no. 3, p. 32019.
- [25] M. Z. Rong, M. Q. Zhang, and W. H. Ruan, "Surface modification of nanoscale fillers for improving properties of polymer nanocomposites: a review," *Mater. Sci. Technol.*, vol. 22, no. 7, pp. 787–796, 2006.
- [26] K. K. Sadasivuni *et al.*, "Silver nanoparticles and its polymer nanocomposites—Synthesis, optimization, biomedical usage, and its various applications," in *Polymer nanocomposites in biomedical engineering*, Springer, 2019, pp. 331–373.
- [27] B. Thomas, M. C. Raj, J. Joy, A. Moores, G. L. Drisko, and C. Sanchez, "Nanocellulose, a versatile green platform: from biosources to materials and their applications," *Chem. Rev.*, vol. 118, no. 24, pp. 11575–11625, 2018.
- [28] T. Hillie, M. Munasinghe, M. Hlope, and Y. Deraniyagala, "Nanotechnology, water and development," 2006.
- [29] J. K. Patra *et al.*, "Nano based drug delivery systems: recent developments and future prospects," *J. Nanobiotechnology*, vol. 16, no. 1, pp. 1–33, 2018.
- [30] R. Misra, S. Acharya, and S. K. Sahoo, "Cancer nanotechnology: application of nanotechnology in cancer therapy," *Drug Discov. Today*, vol. 15, no. 19–20, pp. 842–850, 2010.
- [31] L. Yang, L. Yang, L. Ding, F. Deng, X.-B. Luo, and S.-L. Luo, "Principles for the application of nanomaterials in environmental pollution control and resource reutilization," in *Nanomaterials for the Removal of Pollutants and Resource Reutilization*, Elsevier, 2019, pp. 1–23.
- [32] A. M. Youssef, "Polymer nanocomposites as a new trend for packaging applications," *Polym. Plast. Technol. Eng.*, vol. 52, no. 7, pp. 635–660, 2013.
- [33] F. Guo, S. Aryana, Y. Han, and Y. Jiao, "A review of the synthesis and applications of polymer–nanoclay composites," *Appl. Sci.*, vol. 8, no. 9, p. 1696, 2018.
- [34] M. Sumesh, U. J. Alengaram, M. Z. Jumaat, K. H. Mo, and M. F. Alnahhal, "Incorporation of nano-materials in cement composite and geopolymer based paste and mortar—A review," *Constr. Build. Mater.*, vol. 148, pp. 62–

- 84, 2017.
- [35] W. S. Khan, N. N. Hamadneh, and W. A. Khan, "Polymer nanocomposites—synthesis techniques, classification and properties," *Sci. Appl. Tailored Nanostructures*, vol. 50, 2016.
- [36] E. Umut, "Surface modification of nanoparticles used in biomedical applications," *Mod. Surf. Eng. Treat.*, vol. 20, pp. 185–208, 2013.
- [37] F. Hussain, M. Hojjati, M. Okamoto, and R. E. Gorga, "Polymer-matrix nanocomposites, processing, manufacturing, and application: an overview," *J. Compos. Mater.*, vol. 40, no. 17, pp. 1511–1575, 2006.
- [38] G. Schmidt and M. M. Malwitz, "Properties of polymer–nanoparticle composites," *Curr. Opin. Colloid Interface Sci.*, vol. 8, no. 1, pp. 103–108, 2003.
- [39] X. Chen and S. S. Mao, "Titanium dioxide nanomaterials: synthesis, properties, modifications, and applications," *Chem. Rev.*, vol. 107, no. 7, pp. 2891–2959, 2007.
- [40] S. Mallakpour, C. M. Hussain, and S. Kaushik, "Nanoproducts: Biomedical, Environmental, and Energy Applications," *Handb. Consum. Nanoproducts*, pp. 1–26, 2021.
- [41] G. E. J. Poinern, *A laboratory course in nanoscience and nanotechnology*. CRC Press, 2014.
- [42] S. Chen, E. Olson, S. Jiang, and X. Yong, "Nanoparticle assembly modulated by polymer chain conformation in composite materials," *Nanoscale*, vol. 12, no. 27, pp. 14560–14572, 2020.
- [43] C. Wu et al., "A novel mechanism linking ferroptosis and endoplasmic reticulum stress via the circPtpn14/miR-351-5p/5-LOX signaling in melatonin-mediated treatment of traumatic brain injury," *Free Radic. Biol. Med.*, vol. 178, pp. 271–294, 2022.
- [44] C. L. Seebon, "A Correlational Study of Emotional Intelligence and Resilience in Asset Managers During the Global Pandemic Explored Through Chaos and Intentional Change Theories." Franklin University, 2022.
- [54] E. A. Larsen, "Classification of EEG signals in a brain-computer interface

- system.” Institutt for datateknikk og informasjonvitenskap, 2011.
- [46] Z. Benzait and L. Trabzon, “A review of recent research on materials used in polymer–matrix composites for body armor application,” *J. Compos. Mater.*, vol. 52, no. 23, pp. 3241–3263, 2018.
- [47] H. E. Andås, “Emerging technology trends for defence and security,” 2020.
- [48] M. Sahoo, S. Vishwakarma, C. Panigrahi, and J. Kumar, “Nanotechnology: Current applications and future scope in food,” *Food Front.*, vol. 2, no. 1, pp. 3–22, 2021.
- [49] C. Silvestre, D. Duraccio, and S. Cimmino, “Food packaging based on polymer nanomaterials,” *Prog. Polym. Sci.*, vol. 36, no. 12, pp. 1766–1782, 2011.
- [50] A. Abaee, M. Mohammadian, and S. M. Jafari, “Whey and soy protein-based hydrogels and nano-hydrogels as bioactive delivery systems,” *Trends Food Sci. Technol.*, vol. 70, pp. 69–81, 2017.
- [51] J. Bott, A. Störmer, and R. Franz, “A comprehensive study into the migration potential of nano silver particles from food contact polyolefins,” in *Chemistry of food, food supplements, and food contact materials: from production to plate*, ACS Publications, 2014, pp. 51–70.
- [52] M. M. Berekaa, “Nanotechnology in food industry; advances in food processing, packaging and food safety,” *Int J Curr Microbiol App Sci*, vol. 4, no. 5, pp. 345–357, 2015.
- [53] A. Castaldo, E. Gambale, and G. Vitiello, “Aluminium Nitride Doping for Solar Mirrors Self-Cleaning Coatings,” *Energies*, vol. 14, no. 20, p. 6668, 2021.
- [54] D. Ming, Y. U. Lianhua, and C. Xiaobo, “On redundancy-modified NAND multiplexing,” *J. Syst. Eng. Electron.*, vol. 29, no. 4, pp. 864–872, 2018.
- [55] D. Gubsky and V. Zemlyakov, “Advanced microwave equipment simulator for engineering education,” *Int. J. Electr. Eng. Educ.*, vol. 56, no. 1, pp. 92–101, 2019.
- [56] H. Gunneriusson, “Nothing is Taken Serious Until it gets Serious: Countering Hybrid Threats,” *Def. Against Terror. Rev.*, vol. 4, no. 1, pp. 47–70, 2012.

- [57] T. J. Henderson, G. Emmett, R. M. Dorsey, C. B. Millard, R. D. LeClaire, and H. Salem, "The structural biology, biochemistry, toxicology, and military use of the ricin toxin and the associated treatments and medical countermeasures for ricin exposure," in *Chemical Warfare Agents*, CRC Press, 2019, pp. 203–226.
- [58] B. Van der Bruggen, M. Mänttari, and M. Nyström, "Drawbacks of applying nanofiltration and how to avoid them: a review," *Sep. Purif. Technol.*, vol. 63, no. 2, pp. 251–263, 2008.
- [59] N. Hilal, H. Al-Zoubi, N. A. Darwish, A. W. Mohamma, and M. A. Arabi, "A comprehensive review of nanofiltration membranes: Treatment, pretreatment, modelling, and atomic force microscopy," *Desalination*, vol. 170, no. 3, pp. 281–308, 2004.
- [60] D.-X. Wang, M. Su, Z.-Y. Yu, X.-L. Wang, M. Ando, and T. Shintani, "Separation performance of a nanofiltration membrane influenced by species and concentration of ions," *Desalination*, vol. 175, no. 2, pp. 219–225, 2005.
- [61] A. Santafé-Moros, J. M. Gozávez-Zafrilla, and J. Lora-García, "Applicability of the DSPM with dielectric exclusion to a high rejection nanofiltration membrane in the separation of nitrate solutions," *Desalination*, vol. 221, no. 1–3, pp. 268–276, 2008.
- [62] J. M. K. Timmer, *Properties of nanofiltration membranes: model development and industrial application*. Technische Universiteit Eindhoven Eindhoven, The Netherlands, 2001.
- [63] W. Huang, Y. Wang, C. Chen, J. L. M. Law, M. Houghton, and L. Chen, "Fabrication of flexible self-standing all-cellulose nanofibrous composite membranes for virus removal," *Carbohydr. Polym.*, vol. 143, pp. 9–17, 2016.
- [64] B. P. Baldigo, K. M. Roy, and C. T. Driscoll, "Response of fish assemblages to declining acidic deposition in Adirondack Mountain lakes, 1984–2012," *Atmos. Environ.*, vol. 146, pp. 223–235, 2016.
- [65] A. Inyinbor Adejumo, O. Adebese Babatunde, P. Oluyori Abimbola, A. Adelani Akande Tabitha, O. Dada Adewumi, and A. Oreofe Toyin, "Water pollution: effects, prevention, and climatic impact," *Water Challenges an Urban. World*, vol. 33, pp. 33–47, 2018.

- [66] P. Chowdhary, R. N. Bharagava, S. Mishra, and N. Khan, "Role of industries in water scarcity and its adverse effects on environment and human health," in *Environmental concerns and sustainable development*, Springer, 2020, pp. 235–256.
- [67] S. Madhav *et al.*, "Water pollutants: sources and impact on the environment and human health," *Sensors Water Pollut. Monit. Role Mater.*, pp. 43–62, 2020.
- [68] I. C. Ossai, A. Ahmed, A. Hassan, and F. S. Hamid, "Remediation of soil and water contaminated with petroleum hydrocarbon: A review," *Environ. Technol. Innov.*, vol. 17, p. 100526, 2020.
- [69] R. Altenburger *et al.*, "Future water quality monitoring: improving the balance between exposure and toxicity assessments of real-world pollutant mixtures," *Environ. Sci. Eur.*, vol. 31, no. 1, pp. 1–17, 2019.
- [70] A. Reife and H. S. Freeman, "Pollution Prevention in the Production of Dyes and Pigments.," *Text. Chem. Color. Am. Dyest. Report.*, vol. 32, no. 1, 2000.
- [71] G. M. Balusescu and O. Horhogeia, "Nano-Killers. Aluminium Toxicity in the Human Body," in *Proceedings of the 15th International RAIS Conference, November 6-7, 2019*, 2019, no. 012MB.
- [72] A. W. Kalsido, B. Tekola, B. Mogessie, and E. Alemayehu, "Excess fluoride issues and mitigation using low-cost techniques from groundwater: A review," *Cost Eff. Technol. Solid Waste Wastewater Treat.*, pp. 241–263, 2022.
- [73] K. J. Pieper, M. Tang, and M. A. Edwards, "Flint water crisis caused by interrupted corrosion control: Investigating 'ground zero' home," *Environ. Sci. Technol.*, vol. 51, no. 4, pp. 2007–2014, 2017.
- [74] K. Aoshima, "Itai-itai disease: renal tubular osteomalacia induced by environmental exposure to cadmium—historical review and perspectives," *Soil Sci. Plant Nutr.*, vol. 62, no. 4, pp. 319–326, 2016.
- [75] M. S. Samuel *et al.*, "Nanomaterials as adsorbents for As (III) and As (V) removal from water: A review," *J. Hazard. Mater.*, vol. 424, p. 127572, 2022.
- [76] M. K. Yadav, D. Saidulu, A. K. Gupta, P. S. Ghosal, and A. Mukherjee, "Status

- and management of arsenic pollution in groundwater: A comprehensive appraisal of recent global scenario, human health impacts, sustainable field-scale treatment technologies,” *J. Environ. Chem. Eng.*, vol. 9, no. 3, p. 105203, 2021, doi: 10.1016/j.jece.2021.105203.
- [77] T. T. Mensinga, G. J. A. Speijers, and J. Meulenbelt, “Health implications of exposure to environmental nitrogenous compounds,” *Toxicol. Rev.*, vol. 22, no. 1, pp. 41–51, 2003.
- [78] A. K. Susheela, A. Mudgal, and G. Keast, “Fluoride in water: An overview,” *Water Front*, vol. 1, no. 13, pp. 11–13, 1999.
- [79] M. Diana, M. Felipe-Sotelo, and T. Bond, “Disinfection byproducts potentially responsible for the association between chlorinated drinking water and bladder cancer: A review,” *Water Res.*, vol. 162, pp. 492–504, 2019.
- [80] S. Kuppusamy, N. R. Maddela, M. Megharaj, and K. Venkateswarlu, “Ecological impacts of total petroleum hydrocarbons,” in *Total petroleum hydrocarbons*, Springer, 2020, pp. 95–138.
- [81] D.-G. JRC, “Integrated Pollution Prevention and Control (IPPC) Reference Document on Best Available Techniques for the Textiles Industry Draft dated February 2001.”
- [82] A. Gürses, M. Açıkyıldız, K. Güneş, and M. S. Gürses, “Dyes and pigments: their structure and properties,” in *Dyes and Pigments*, Springer, 2016, pp. 13–29.
- [83] M. F. Hanafi and N. Sapawe, “A review on the water problem associate with organic pollutants derived from phenol, methyl orange, and remazol brilliant blue dyes,” *Mater. Today Proc.*, vol. 31, pp. A141–A150, 2020.
- [84] T. L. Vigo, *Textile processing and properties: Preparation, dyeing, finishing and performance*. Elsevier, 2013.
- [85] H. S. Altundoğan, A. Topdemir, M. Çakmak, and N. Bahar, “Hardness removal from waters by using citric acid modified pine cone,” *J. Taiwan Inst. Chem. Eng.*, vol. 58, pp. 219–225, 2016.
- [86] R. L. Singh, *Principles and applications of environmental biotechnology for a*

- sustainable future*. Springer, 2017.
- [87] P. Grennfelt, A. Engleryd, M. Forsius, Ø. Hov, H. Rodhe, and E. Cowling, "Acid rain and air pollution: 50 years of progress in environmental science and policy," *Ambio*, vol. 49, no. 4, pp. 849–864, 2020.
- [88] G. L. Sun, E. Reynolds, and A. M. Belcher, "Using yeast to sustainably remediate and extract heavy metals from waste waters," *Nat. Sustain.*, vol. 3, no. 4, pp. 303–311, 2020.
- [89] E. L. Ungureanu, A. D. Soare, A. L. Mocanu, S. C. Iorga, G. Mustatea, and M. E. Popa, "Occurrence of Potentially Toxic Elements in Bottled Drinking Water—Carcinogenic and Non-Carcinogenic Risks Assessment in Adults via Ingestion," *Foods*, vol. 11, no. 10, p. 1407, 2022.
- [90] A. R. Khudhair, S. T. H. Sherazi, and M. N. Al-Baiati, "Adsorption of methylene blue from aqueous solutions by using a novel nano co-polymer," in *AIP Conference Proceedings*, 2020, vol. 2290, no. 1, p. 30021.
- [91] S. H. Guzar, A. S. Al-mayali, and M. N. Al-Baiati, "Removal of Pollution with Dye Orange-G from Waste Water by Using Novel Nano Co_ polymer," *NeuroQuantology*, vol. 20, no. 2, p. 44, 2022.
- [92] Z. M. Shaker, E. S. Hamida, and M. N. Al-baiati, "Removal of pollutants from wastewater using a nano," pp. 1–12.
- [93] K. Siddique, M. Rizwan, M. J. Shahid, S. Ali, R. Ahmad, and H. Rizvi, "Textile wastewater treatment options: a critical review," *Enhancing cleanup Environ. Pollut.*, pp. 183–207, 2017.
- [94] S. Thakur and M. S. Chauhan, "Treatment of dye wastewater from textile industry by electrocoagulation and Fenton oxidation: a review," *Water Qual. Manag.*, pp. 117–129, 2018.
- [95] K. Miazek, W. Iwanek, C. Remacle, A. Richel, and D. Goffin, "Effect of metals, metalloids and metallic nanoparticles on microalgae growth and industrial product biosynthesis: a review," *Int. J. Mol. Sci.*, vol. 16, no. 10, pp. 23929–23969, 2015.
- [96] A. Gürses, M. Açıkyıldız, K. Güneş, and M. S. Gürses, *Dyes and pigments*. Springer, 2016.

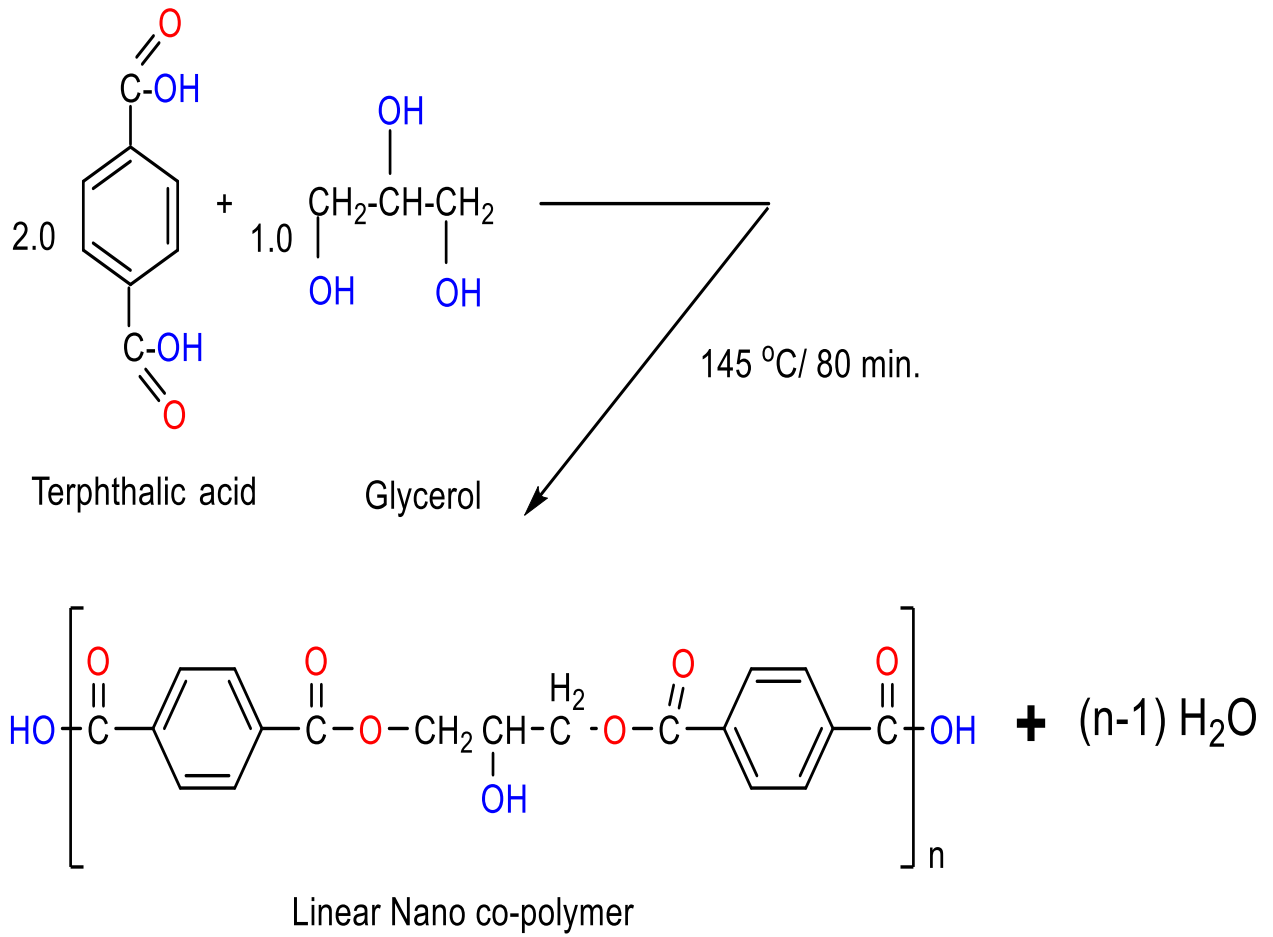
- [97] F. M. Bezerra *et al.*, "The role of β -cyclodextrin in the textile industry," *Molecules*, vol. 25, no. 16, p. 3624, 2020.
- [98] N. N. Patil and S. R. Shukla, "Degradation of Reactive Yellow 145 dye by persulfate using microwave and conventional heating," *J. Water Process Eng.*, vol. 7, pp. 314–327, 2015.
- [99] S. Singh, K. Pakshirajan, and A. Daverey, "Enhanced decolourization of Direct Red-80 dye by the white rot fungus *Phanerochaete chrysosporium* employing sequential design of experiments," *Biodegradation*, vol. 21, no. 4, pp. 501–511, 2010.
- [100] D. Śmigiel-Kamińska, J. Pośpiech, J. Makowska, P. Stepnowski, J. Wąs-Gubała, and J. Kumirska, "The identification of polyester fibers dyed with disperse dyes for forensic purposes," *Molecules*, vol. 24, no. 3, p. 613, 2019.
- [101] Y. Yang and S. Li, "One-Step Dyeing of Polyester/Cotton With Disperse/Reactive Dyes," *Text. Chem. Color. Am. Dyest. Report.*, vol. 32, no. 3, 2000.
- [102] V. Ahuja, T. Platzek, H. Fink, A. Sonnenburg, and R. Stahlmann, "Study of the sensitising potential of various textile dyes using a biphasic murine local lymph node assay," *Arch. Toxicol.*, vol. 84, no. 9, pp. 709–718, 2010.
- [103] P. Gharbani, "Modeling and optimization of reactive yellow 145 dye removal process onto synthesized MnOX-CeO₂ using response surface methodology," *Colloids Surfaces A Physicochem. Eng. Asp.*, vol. 548, pp. 191–197, 2018.
- [104] S. Alahiane, A. Sennaoui, F. Sakr, M. Dinne, S. Qourzal, and A. Assabbane, "Photo-mineralization of azo dye reactive yellow 145 in aqueous medium by TiO₂-coated non-woven fibres," *Mediterr. J. Chem.*, vol. 10, no. 2, pp. 107–115, 2020.
- [105] M. Arulkumar, P. Sathishkumar, and T. Palvannan, "Optimization of Orange G dye adsorption by activated carbon of *Thespesia populnea* pods using response surface methodology," *J. Hazard. Mater.*, vol. 186, no. 1, pp. 827–834, 2011.

- [106] S. Wang, X. Li, S. Wang, Y. Li, and Y. Zhai, "Synthesis of γ -alumina via precipitation in ethanol," *Mater. Lett.*, vol. 62, no. 20, pp. 3552–3554, 2008.
- [107] X.-R. Xu and X.-Z. Li, "Degradation of azo dye Orange G in aqueous solutions by persulfate with ferrous ion," *Sep. Purif. Technol.*, vol. 72, no. 1, pp. 105–111, 2010.
- [108] J. Koh, "Dyeing with disperse dyes," *Text. Dye.*, vol. 10, pp. 195–220, 2011.
- [109] J. R. Aspland, "The structure and properties of disperse dyes and related topics," *Text. Chem. Color.*, vol. 25, no. 1, pp. 21–25, 1993.
- [110] M. Elapasery, A. M. Hussein, A. A. Eladasy, M. O. Saleh, and M. Kamel, "Microwave Assisted Synthesis of Some Azo Disperse Dyes with Antibacterial Activities. Part 1," *Egypt. J. Chem.*, vol. 62, no. 5, pp. 853–859, 2019.
- [111] W. N. Saeed, "Removal of azo benzidine reactive dye from aqueous solution by adsorption onto ZnO surface," *J. Kerbala Univ.*, vol. 1, no. 12, pp. 11–18, 2014.
- [112] J. Workman Jr and A. Springsteen, *Applied spectroscopy: a compact reference for practitioners*. Academic Press, 1998.
- [113] J. Murrell and E. A. Bucher, "Properties of liquids and solution John Wiley and sons," *New York*, vol. 255, 1982.
- [114] I. Langmuir, "The adsorption of gases on plane surfaces of glass, mica and platinum.," *J. Am. Chem. Soc.*, vol. 40, no. 9, pp. 1361–1403, 1918.
- [115] M. J. Temkin and V. Pyzhev, "Recent modifications to Langmuir isotherms," 1940.
- [116] V. P. Ravi, R. V. Jasra, and T. S. G. Bhat, "Adsorption of phenol, cresol isomers and benzyl alcohol from aqueous solution on activated carbon at 278, 298 and 323 K," *J. Chem. Technol. Biotechnol.*, vol. 71, no. 2, pp. 173–179, 1998, doi: 10.1002/(SICI)1097-4660(199802)71:2<173::AID-JCTB818>3.0.CO;2-N.
- [117] N. Mohammadi, H. Khani, V. K. Gupta, E. Amereh, and S. Agarwal, "Adsorption process of methyl orange dye onto mesoporous carbon material—kinetic and thermodynamic studies," *J. Colloid Interface Sci.*, vol. 362, no. 2, pp. 457–462, 2011.

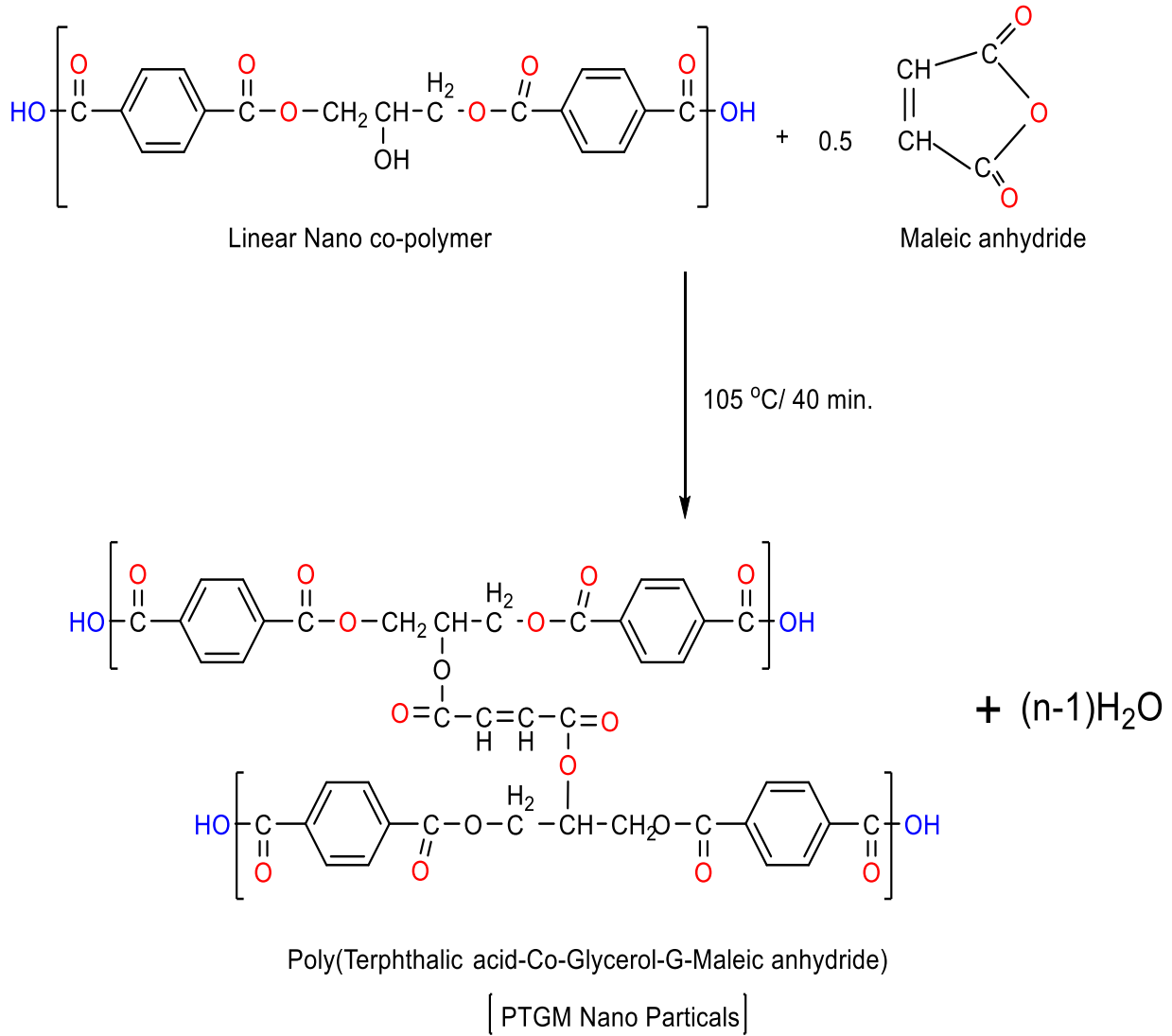
- [118] W. J. Weber Jr and J. C. Morris, "Kinetics of adsorption on carbon from solution," *J. Sanit. Eng. Div.*, vol. 89, no. 2, pp. 31–59, 1963.
- [119] A. A. Jalil *et al.*, "Adsorption of methyl orange from aqueous solution onto calcined Lapindo volcanic mud," *J. Hazard. Mater.*, vol. 181, no. 1–3, pp. 755–762, 2010.
- [120] H. S. M. Suhaimi, C. P. Leo, and A. L. Ahmad, "Hydrogen separation using polybenzimidazole membrane with palladium nanoparticles stabilized by polyvinylpyrrolidone," *Int. J. Energy Res.*, vol. 45, no. 10, pp. 15171–15181, 2021.
- [121] J. Penfold and R. K. Thomas, "Counterion Condensation, the Gibbs Equation, and Surfactant Binding: An Integrated Description of the Behavior of Polyelectrolytes and Their Mixtures with Surfactants at the Air–Water Interface," *J. Phys. Chem. B*, vol. 124, no. 28, pp. 6074–6094, 2020.
- [122] Y.-H. Deng, "Analysis of misidentifications in TEM characterization of perovskite material," *arXiv Prepr. arXiv2009.04086*, 2020.
- [123] P. Saha, S. Chowdhury, S. Gupta, and I. Kumar, "Insight into adsorption equilibrium, kinetics and thermodynamics of Malachite Green onto clayey soil of Indian origin," *Chem. Eng. J.*, vol. 165, no. 3, pp. 874–882, 2010.
- [124] Y. Jin, C. Zeng, Q.-F. Lü, and Y. Yu, "Efficient adsorption of methylene blue and lead ions in aqueous solutions by 5-sulfosalicylic acid modified lignin," *Int. J. Biol. Macromol.*, vol. 123, pp. 50–58, 2019.
- [125] N. Y. Mezenner and A. Bensmaili, "Kinetics and thermodynamic study of phosphate adsorption on iron hydroxide-eggshell waste," *Chem. Eng. J.*, vol. 147, no. 2–3, pp. 87–96, 2009.
- [126] L. Cottet, C. A. P. Almeida, N. Naidek, M. F. Viante, M. C. Lopes, and N. A. Debacher, "Adsorption characteristics of montmorillonite clay modified with iron oxide with respect to methylene blue in aqueous media," *Appl. Clay Sci.*, vol. 95, pp. 25–31, 2014.

الخلاصة

في هذا العمل ، تم تحضير البوليمر النانوي المطبق بواسطة عملية الأسترة ، عن طريق الذوبان لتحضير بوليمر خطي كخطوة أولى من تفاعل (2.0 مول) حمض تيرفثاليك مع (1.0 مول) جلسرين. تمت إضافة حوالي (0.5 مول) من أنهيدريد الماليك إلى محلول البوليمر الخطي الناتج للحصول على البوليمر النانوي المشترك كما موضح في المعادلات ادناه :



الخطوة الأولى؛ تحضير النانو بوليمر المشترك الخطي.



الخطوة الثانية: تحضير النانوبوليمر المشترك المطعم PTGM.

شخص البوليمر المشترك النانوي المحضر بواسطة مطيافية الأشعة تحت الحمراء (FT-IR) ، الرنين النووي المغناطيسي البروتوني (H-NMR) ، وقياس حجم الجسيمات للبوليمر المشترك النانوي بواسطة تقنية مجهر القوة الذرية (AFM) ؛ تبين إن البوليمر يميل الى إمتزاز اصباغ المنسوجات (الصفراء الفعالة 145 ، البرتقالي-G و تفريق الأحمر 1) ، من المحاليل المائية والتي تم ازلتها في هذه الدراسة.

أظهرت نتائج (AFM) أن معدل حجم الجسيمات للبوليمر المشترك النانوي كانت (74.39 نانومتر) تمت دراسة تأثير ثلاث درجات حرارية (298، 308 و K318) وأربعة تراكيز مختلفة (1 ، 3 ، 5 و 7 ppm) من البوليمر المشترك النانوي ومن الواضح أنها تلعب دورًا مهمًا جدًا في عملية الامتزاز،

وأظهرت النتائج التجريبية أن امتزاز الأصباغ (البرتقالي-G و تفريق الأحمر1) على سطح هذا البوليمر النانوي يزداد مع زيادة درجة الحرارة ، مما يعني أن العملية هي عملية ماصة للحرارة ، بينما أظهرت النتائج التي تم الحصول عليها من صبغة (الصفراء الفعالة 145) أن الامتزاز يتناقص مع زيادة درجة الحرارة ، مما يعني أن العملية عملية باعثة للحرارة ، والنتائج أظهر الحصول على فعالية عالية للبوليمر النانوي في التخلص من الملوثات (الصفراء الفعالة 145 ، البرتقالي-G و تفريق الأحمر1).



جمهورية العراق
وزارة التعليم العالي و البحث العلمي
جامعة كربلاء
كلية التربية للعلوم الصرفة
قسم الكيمياء

ازالة الأصباغ الملوثة للماء بأستخدام بوليمر نانوي جديد)

هذه الرسالة مقدمة إلى
مجلس كلية التربية للعلوم الصرفة - جامعة كربلاء ، كجزء من متطلبات نيل
درجة الماجستير في علوم الكيمياء

من قبل

علي فاضل عبدالله العامري

بكالوريوس كيمياء / جامعة القادسية (2014)

إشراف

**الأستاذ الدكتور
محمد ناظم بهجت**

2022A.D

1443A.H